AD-786 546

ADVANCED FEASIBILITY INVESTIGATION FOR DETERMINING ARMY HELICOPTER GAS TURBINE ENGINE MAXIMUM POWER AVAILABLE

Edward V. Fox, et al

Hamilton Standard

Prepared for:

Army Air Mobility Research and Development Laboratory

August 1974

Unclassified

SECURITY CLASSIFICATION OF THIS PAGE (When Data Entered)

REPORT DOCUMENTATION PAGE		READ INSTRUCTIONS BEFORE COMPLETING FORM
1. REPORT NUMBER USAAMRDL-TR-74-49	2. GOVT ACCESSION NO.	3. RECIPIENT'S CATALOG NUMBER AD-786546
4. TITLE (and Subtitle) ADVANCED FEASIBILITY INVESTIGATION FOR DETERMINING ARMY HELICOPTER GAS TURBINE ENGINE MAXIMUM POWER AVAILABLE		5. TYPE OF REPORT & PERIOD COVERED Final Report 6. PERFORMING ORG. REPORT NUMBER HSER 6392
7. AUTHOR(s) Edward V. Fox, Allen Rapp Salvador Ledesma, Roy W. Schneider Anthony J. Martin, Louis A. Urban John S. Williamson		8. CONTRACT OR GRANT NUMBER(s) DAAJ02-73-C-0047
9. PERFORMING ORGANIZATION NAME AND ADDRESS Hamilton Standard Division of United Aircraft Corporation Windsor Locks, Conn. 06096		10. PROGRAM ELEMENT, PROJECT, TASK AREA & WORK UNIT NUMBERS 1F162203AH8603
11. CONTROLLING OFFICE NAME AND ADDRESS Eustis Directorate U. S. Army Air Mobility R&D Laboratory Fort Eustis, Va. 23604		12. REPORT DATE August 1974 13. NUMBER OF PAGES 123
14. MONITORING AGENCY NAME & ADDRESS(if different from Controlling Office)		15. SECURITY CLASS. (of this report) Unclassified 15a. DECLASSIFICATION/DOWNGRADING SCHEDULE

16. DISTRIBUTION STATEMENT (of this Report)

Approved for public release; distribution unlimited.

17. DISTRIBUTION STATEMENT (of the abstract entered in Block 20, if different from Report)

18. SUPPLEMENTARY NOTES

19. KEY WORDS (Continue on reverse side if necessary and identify by block number)

Gas turbines
Power
Helicopters

20. ABSTRACT (Continue on reverse side if necessary and identify by block number)

An advanced investigation was conducted by Hamilton Standard Division of United Aircraft Corporation, Windsor Locks, Connecticut, to determine the feasibility of developing a method to predict the maximum power available (MPA) from a helicopter gas turbine engine at full power conditions. This study program was a follow-on of an earlier program under contract DAAJ02-72-C-0003.

DD FORM 1 JAN 73 1473 EDITION OF 1 NOV 65 IS OBSOLETE

Unclassified

SECURITY CLASSIFICATION OF THIS PAGE (When Data Entered)

20. Continued.

The objectives of this program were to improve the ± 3.5% accuracy determined feasible under the first study program toward the original ± 1% accuracy goal, to demonstrate the prediction system using actual engine data, and to define the system implementation in detail.

The Lycoming T53-L13 engine selected for the first investigation was also used under this program. Using the previously developed engine model, the mathematical prediction method was rigorously refined, resulting in the expectation that an MPA system accuracy of ± 2.8% appears feasible at a power level of 50% or greater.

The refined model was then evaluated using historical engine data for ten (10) Lycoming T53-L13 engines. The engine baselines were determined and the MPA's were predicted at periods of time ranging from 1200 hours to 4200 hours after baseline acquisition. The model was evaluated using two methods -- the first basing th prediction upon engine parameters sensed at one reduced power level, the second based upon sensing engine parameters at two different reduced power levels and extrapolating to the maximum power prediction.

The MPA system, consisting of an Electronic Unit (for computations), an Indicator/Control Unit and the necessary engine sensors are defined in detail. System hardware, software and engine sensor specifications (based upon best available sensors) were defined.

The results of this study indicate that attainment of ± 2.2 to ± 2.8% MPA prediction accuracies are feasible with present day sensors. The evaluation of the MPA prediction method using actual engine data provided encouraging results; however, present T53-L13 engine sensors in general are too inaccurate for a proper evaluation.

A further program using an engineering breadboard MPA system with engine (s) instrumented with the best available sensors and expanded engine operating ranges under test cell conditions would provide the information necessary to accurately determine the feasibility of the system.

EUSTIS DIRECTORATE POSITION STATEMENT

This report is considered to be a comprehensive investigation of all of the factors that affect the prediction of maximum power of Army helicopter gas turbine engines. It is considered to have met the objectives of the effort and serves to compliment the work performed previously by Hamilton Standard for the Eustis Directorate under Contract DAAJ02-72-C-0003.

The contents of the report have been reviewed by this Directorate and are considered to be a satisfactory report of the effort performed under the contract.

The results of the investigation show that development of a method to predict the maximum power available (MPA) of an Army helicopter gas turbine engine prior to lift-off is feasible; however, even with improvements in sensor accuracies, the development of an MPA prediction system with an accuracy of ± 1% is doubtful.

The technical monitor for this contract was Mr. G. William Hogg, Military Operations Technology Division.

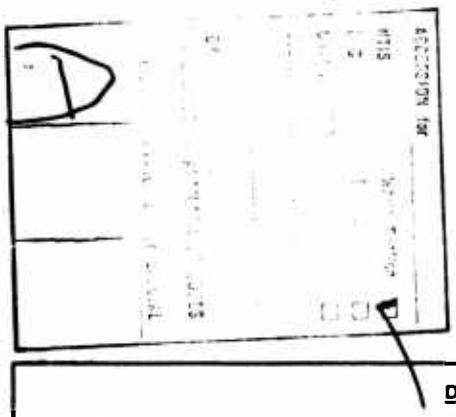

TABLE OF CONTENTS

LIST OF ILLUSTRATIONS

LIST OF TABLES

INTRODUCTION

The purpose of the first investigation was to determine the feasibility of developing a method to predict, with an accuracy of better than ± 1%, the maximum power which can be produced by a helicopter gas turbine engine at full-power conditions. The prediction was to be made using information obtained from the engine while the engine was operated prior to lift-off at a partial-power condition of no more than 30% of normal rated power. The prediction method was to be capable of identifying the changes in maximum engine power available due to all possible types of engine deterioration and all ambient conditions. The study was based on a Lycoming T53-L13 gas turbine engine currently being used in the Army UH-1 helicopter.

This is a follow-on program to determine the effects of higher power levels, a continuous update system, and improved sensor accuracies on the possible improvement of MPA prediction accuracy. This second program includes a more detailed system definition of MPA hardware requirements and implementation methods. In addition, an evaluation of the MPA prediction method using actual T53-L13 engine data was conducted. The availability of this T53-L13 engine data required that this follow-on program be based upon this engine.

The following tasks were undertaken:

TASK I Analytical Studies and System Definition

1. Modify and expand existing model to improve MPA prediction accuracy.
2. Evaluate model accuracy at power levels of 50% to 90% of normal rated power.
3. Evaluate use of continuously updating engine operating conditions.
4. Determine adaptability of MPA system for engine diagnostics.
5. Define MPA system operation.
6. Determine MPA hardware requirements.
7. Determine hardware availability.

TASK II Evaluation of MPA Prediction Method

1. Prepare test plan.

2. Procure engine data from AVCO Lycoming.

3. Evaluate model using the engine data at power levels of 60%, 70%, 80% and 90%.

TASK III Customer Demonstration

1. Provide a computer deck and user manual of the MPA prediction computer program.*

2. Demonstrate program capability on an IBM 360 at Fort Eustis.

---

*The user's manual is contained in HSER 6381 which is reproduced in Appendix I of this report.

MATHEMATICAL SYSTEM MODEL

A mathematical system model was constructed during Phase I of the MPA program under Contract DAAJ02-72-C0003 funded by the Eustis Directorate, U. S. Army Air Mobility Research and Development Laboratory, that included the basic power prediction concept plus additional features for computing the errors in power prediction. A prerequisite for constructing this prediction model involved a detailed knowledge of the engine characteristics on which the maximum power was to be predicted.

A mathematical model of a "typical" Lycoming T53-L13 engine was evolved on an IBM 370 computer, based on engine modeling concepts developed by Hamilton Standard. The so-called "typical" T53-L13 engine was actually the average characteristics of test-cell data from 75 engines. This test data provided the steady-state values for N_1, T_3, P_3, T_9, SHP, and W_f at standard-day conditions from idle to maximum power. The independent variables (such as component efficiencies and geometries) of the generic engine model were selected to duplicate the steady-state test data from the "typical" engine. The resulting computer model of the T53-L13 engine was then used to provide all required interrelationships. For example, changes in engine speed, temperature, pressure, or power resulting from changes in engine geometry, component efficiency, or air pumping capacity were computed. The engine model was used to compute the partial derivatives or influence of any engine parameter on any engine variable referred to in this report as the "B-matrix" and the "C-matrix."

The basic tool in developing the power prediction algorithm is Gas-Path Analysis developed by Hamilton Standard which quantitatively defines how the various engine performance parameters change with respect to each other or with changes in the environment or the engine fuel control. From a steady-state operating condition, a set of "influence coefficients" interrelating all the various engine performance parameters is determined. From this set of influence coefficients, the steady-state characteristics as well as the influence coefficients at any other power condition can be determined. The influence coefficients computed will ultimately be used in the power prediction scheme. Since the accuracy to which power can be predicted is affected by the accuracy of the influence coefficients, it is necessary that these coefficients be computed as precisely as possible.

The MPA algorithm requires engine data from an initial calibration to be used as a baseline from which all future MPA predictions are computed. This baseline data must encompass the entire range of engine operation at which the future MPA predictions will be performed. This baseline data relates future actual low power measurements to the actual engine high power characteristics including the effects of possible engine degradations and differences in ambient conditions.

The MPA mathematical system model consists of obtaining at low power a set of steady-state, low-power engine measurements, i.e., T_1, P_1, N_1, N_2, P_3, T_3, W_f, SHP and T_7. These low-power measurements are then referred to standard day conditions. The referred values of N_1, T_3, W_f, T_7 and SHP plotted as a function of P_{3C} are then compared to those stored baseline characteristics of these parameters at the same value of P_{3C}, i.e., power level. In addition, a correction factor (as a function of N_1 referred speed) is applied to the measured SHP to account for the possibility of the N_2 speed being different from the optimum N_2 speed. Similarly, a "B-matrix", developed for a particular engine model, is computed. Both the "baseline" values and the "B-matrix" are computed at the measured P_{3C} by use of linear interpolation of P_3. By computing the relative difference between the referred measurement data and the computed baseline data and using the computed "B-matrix", the variations in airflow pumping capacity, efficiencies and geometries at the low-power condition can be obtained from the following matrix equation:

$$\begin{bmatrix} \text{DWA} \\ \text{DETAC} \\ \text{DETAT} \\ \text{DETAPT} \\ \text{DA5} \\ \text{DAN} \end{bmatrix} = \begin{bmatrix} (W_a - W_{acB})/W_{acB} \\ (\eta_c - \eta_{cB})/\eta_{cB} \\ (\eta_t - \eta_{tB})/\eta_{tB} \\ (\eta_{PT} - \eta_{PTB})/\eta_{PTB} \\ (A_5 - A_{5B})/A_{5B} \\ (A_N - A_{NB})/A_{NB} \end{bmatrix} = B \begin{bmatrix} \text{DN1} \\ \text{DT3} \\ \text{DWF} \\ \text{DSHP} \\ \text{DT7} \end{bmatrix}$$

It is assumed in this algorithm that the relative variations in airflow pumping capacity, efficiencies, and geometries near maximum power are the same as occur at the measurement power (i.e., the percent-of-point engine degradation is essentially independent of power level). Therefore, the relative variations computed at measurement power are used for the relative variations at high power.

Maximum power at each of the three engine limits is then determined

From the following equations:

On the T_7 temperature limit

$$SHP\theta T = (SHPRFT7)\ \delta_1\ (1 + DWA)^{C11}\ (1 + DETAC)^{C12}\ (1 + DETAT)^{C13}$$
$$(1 + DETAPT)^{C14}\ (1 + DA5)^{C15}\ (1 + DAN)^{C16}\ FT\ (TAM)$$

On the N_1 speed limit

$$SHP\theta N = (SHPRFN1)\ \delta_1^{C27}\ (1 + DWA)^{C21}\ (1 + DETAC)^{C22}$$
$$(1 + DETAT)^{C23}$$
$$(1 + DETAPT)^{C24}\ (1 + DA5)^{C25}\ (1 + DAN)^{C26}\ F_N\ (TAM)$$

On the W_f fuel flow limit

$$SHP\theta W = (SHPRFWF)\ \delta_1^{C37}\ (1 + DWA)^{C31}\ (1 + DETAC)^{C32}$$
$$(1 + DETAT)^{C33}$$
$$(1 + DETAPT)^{C34}\ (1 + DA5)^{C35}\ (1 + DAN)^{C36}\ F_W\ (TAM)$$

The engine maximum power available prediction is the least of three computed engine powers when on the T_7, N_1 and W_f limits, i.e., SHPθ = MINIMUM (SHPθT, SHPθN, SHPθW). This resulting computed corrected SHP is then referred to measurement ambient conditions yielding the MPA predicted SHP.

A detailed description of this MPA prediction algorithm is included in USAAMRDL Technical Report 72-58 titled "Feasibility Investigation for Determining Army Helicopter Gas Turbine Engine Maximum Power Available" written under contract DAAJ02-72-C-0003.

MODEL ACCURACY

Efforts in Phase II were made toward improving the MPA model accuracy developed under Phase I. Areas studied were improved sensor accuracies, use of a continuous update system and use of power levels of 50% or higher. While improved sensor accuracies and higher power levels offered improved MPA prediction accuracy, the continuous update method offers an insignificant improvement in accuracy.

MPA prediction accuracy is affected by the power level at which the MPA prediction is made. Increasing the power at which MPA prediction is made tends to reduce prediction error, but as shown in Figures 1 and 2, additional significant improvements in accuracy are required if a prediction accuracy goal of $\pm$ 1% error is to be met.

One class of errors results from the MPA baseline engine model being different from the actual engine. This difference results from engine changes (degradation) occurring since engine installation and calibration. Any technique where the MPA baseline engine model is periodically modified to duplicate the actual engine would eliminate this class of MPA prediction errors. Figure 3 includes an error summary of such a technique incorporated into the MPA system having the errors shown in Figure 2. In other words, the errors in Figure 3 are a summary of the MPA error caused only by:(1) control errors at the power limit, (2) sensor errors at the MPA measurement and prediction power, and (3) the influence of nonstandard day. Elimination of the class of errors resulting from the MPA baseline engine model being different from the actual engine does provide some improvement in MPA accuracy. A comparison of Figure 2 with Figure 3 indicates that the major contribution to MPA errors is concentrated within the errors caused by:(1) control power limit errors, (2) sensor errors at the MPA prediction power, and (3) the influence of nonstandard day.

The control power limit errors are the same at all power levels and are for the N_1 limit, T_7 limit, and W_f limit $\pm$ .44%, $\pm$ 1.55%, and $\pm$ .74% max SHP respectively. The errors due to the influence of nonstandard day are also the same at all power levels and are for the N_1 limit, T_7 limit, and W_f limit $\pm$ 0.1, $\pm$ 0.23, and $\pm$ 0.21% max SHP respectively. Figure 4 shows how low power sensor errors vary as a function of power level. If a factor of two improvement in T_7 error from $\pm$ 6.3°F to $\pm$ 3.2°R could be obtained, the control power limit error when on T_7 limit would be reduced from $\pm$ 1.55% to $\pm$ 0.78% max SHP.

Figure 5 shows the total RSS error in predicted power as a function of power level if a factor of two improvement in T_7 sensor accuracy from $\pm$ 6.3°R to $\pm$ 3.2°R were obtained. In a similar manner Figure 6 shows the

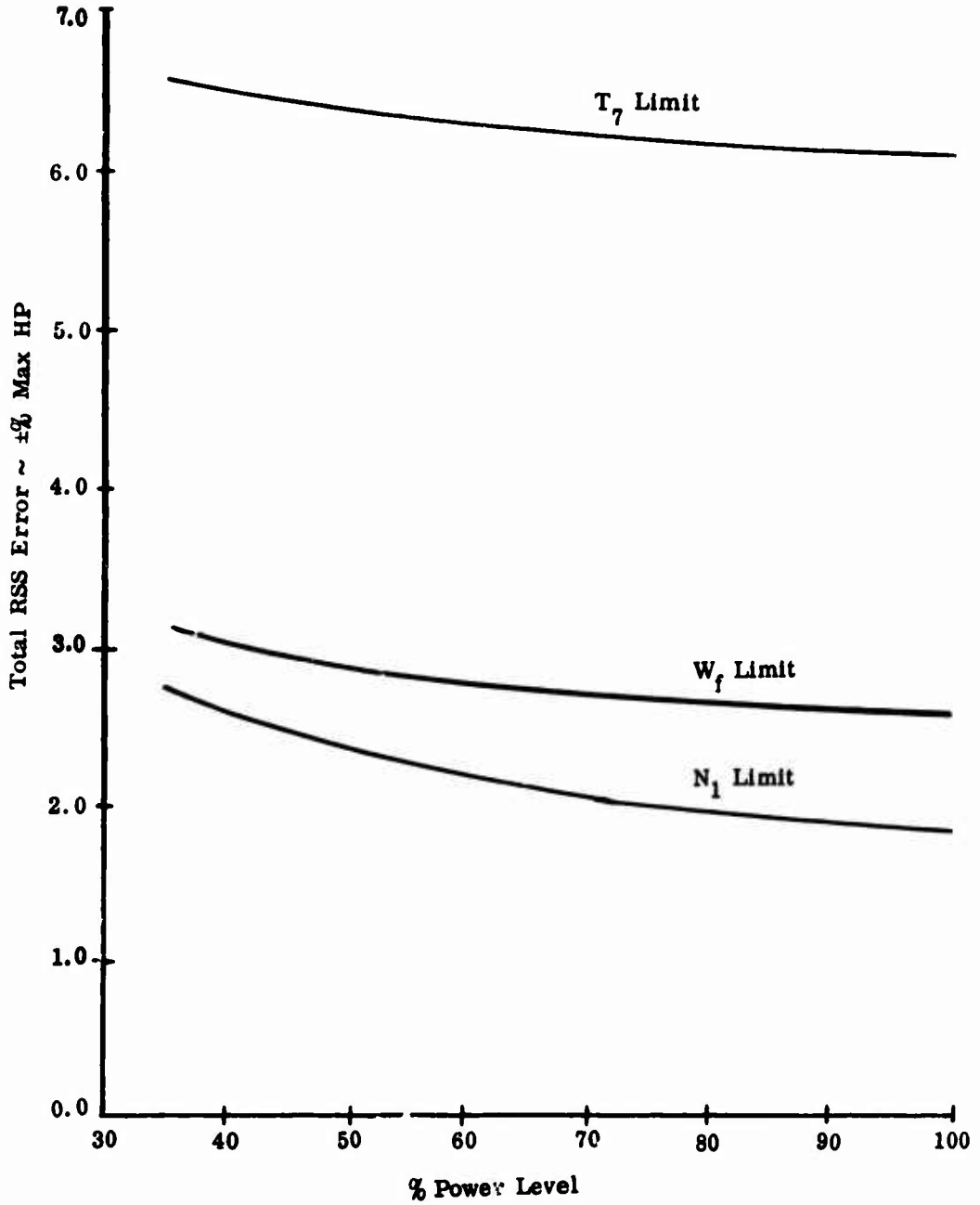

Figure 1. Total RSS Error in Predicted Power With Uncertainty in W_{BL} and SPE.

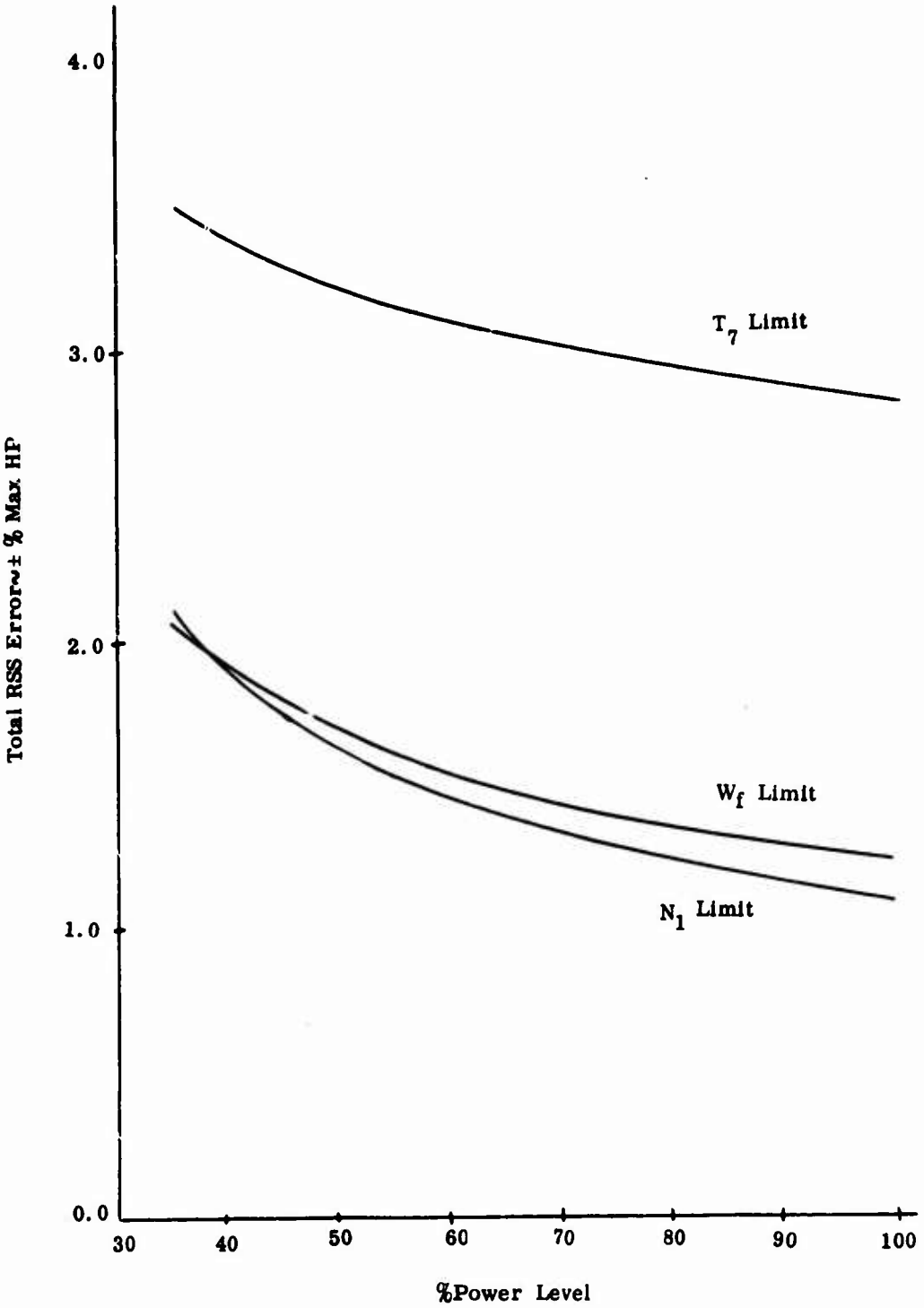

Figure 2. Total RSS Error in Predicted Power With no Uncertainty in W_{BL} and SPE.

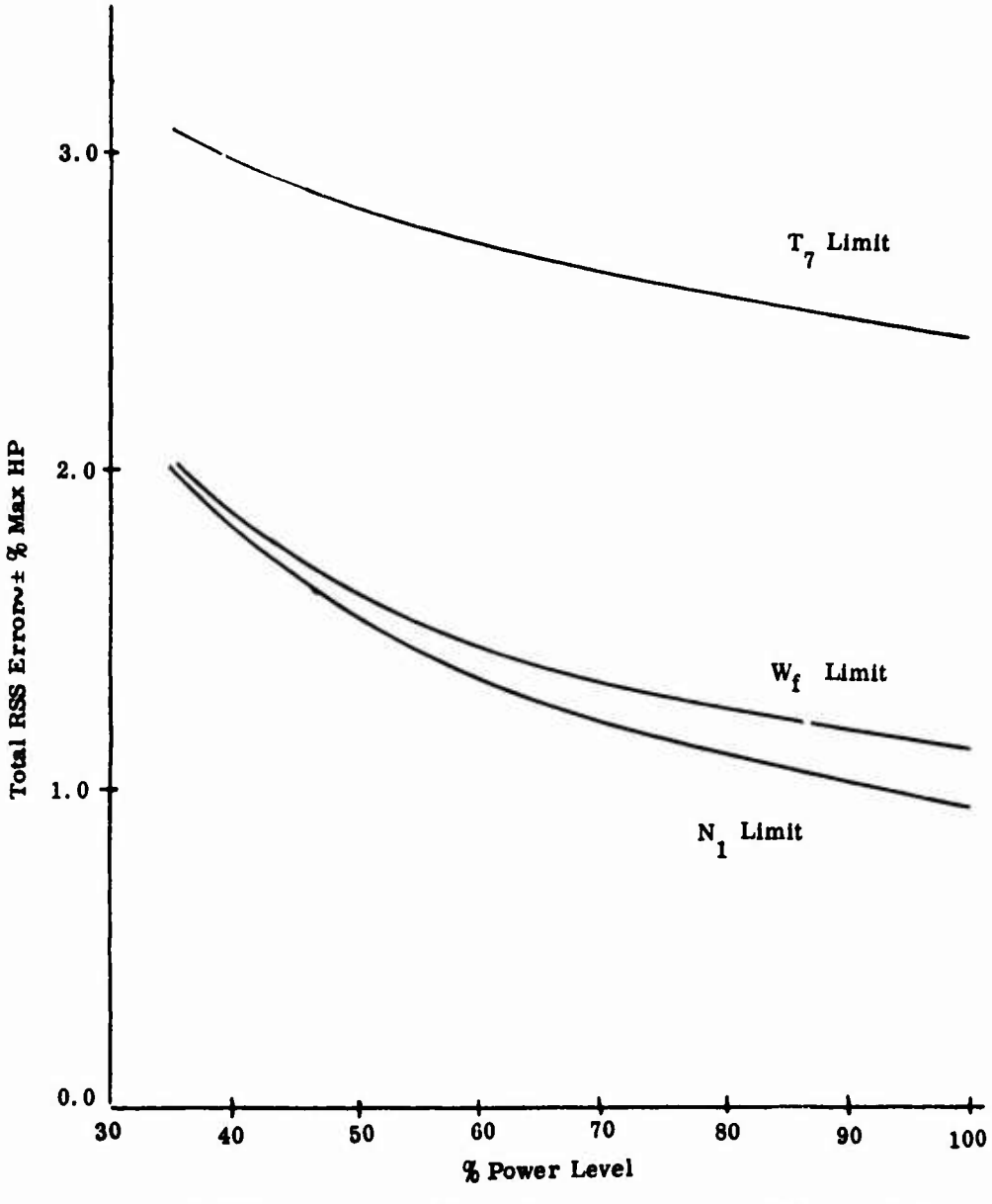

Figure 3. Total RSS Error in Predicted Power - Caused by Influence of Non-standard Day Continuous Update Method.

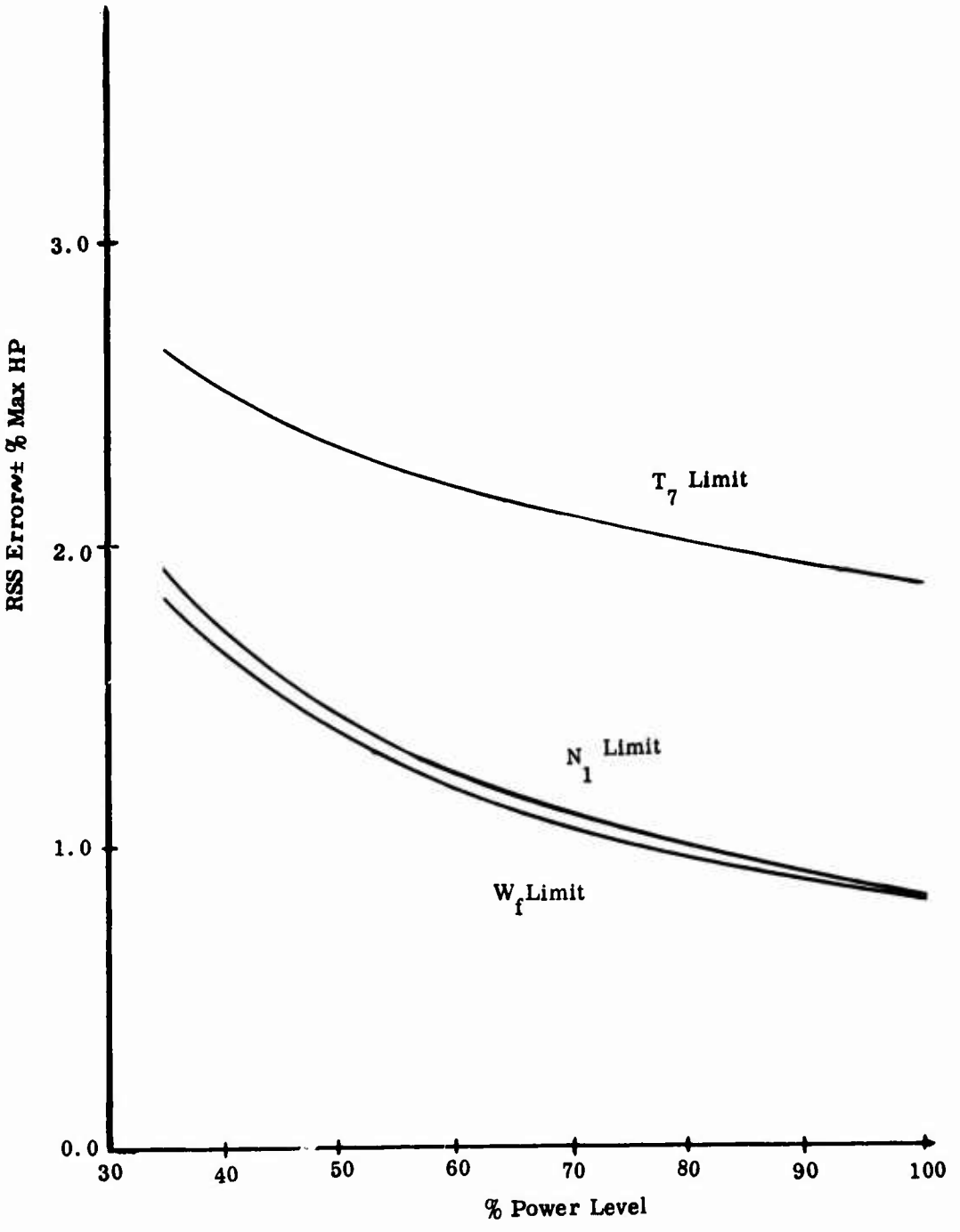

Figure 4. RSS Error in Predicted Power due to Only Low-Power Sensor Errors.

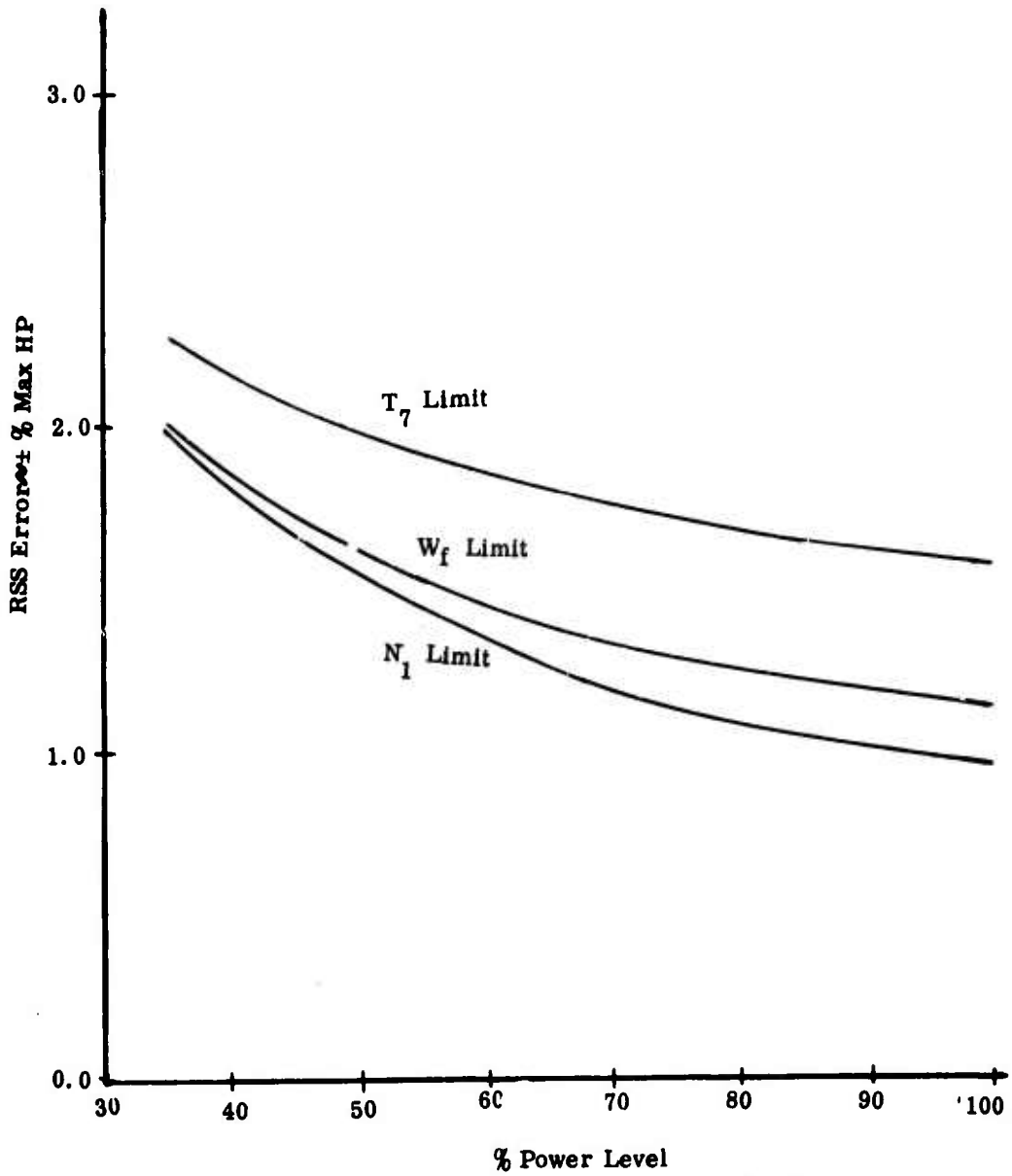

Figure 5. Total RSS Error in Predicted Power due to Errors in Sensors at Low and High Power, Control Limits, and Influence of Nonstandard Day.

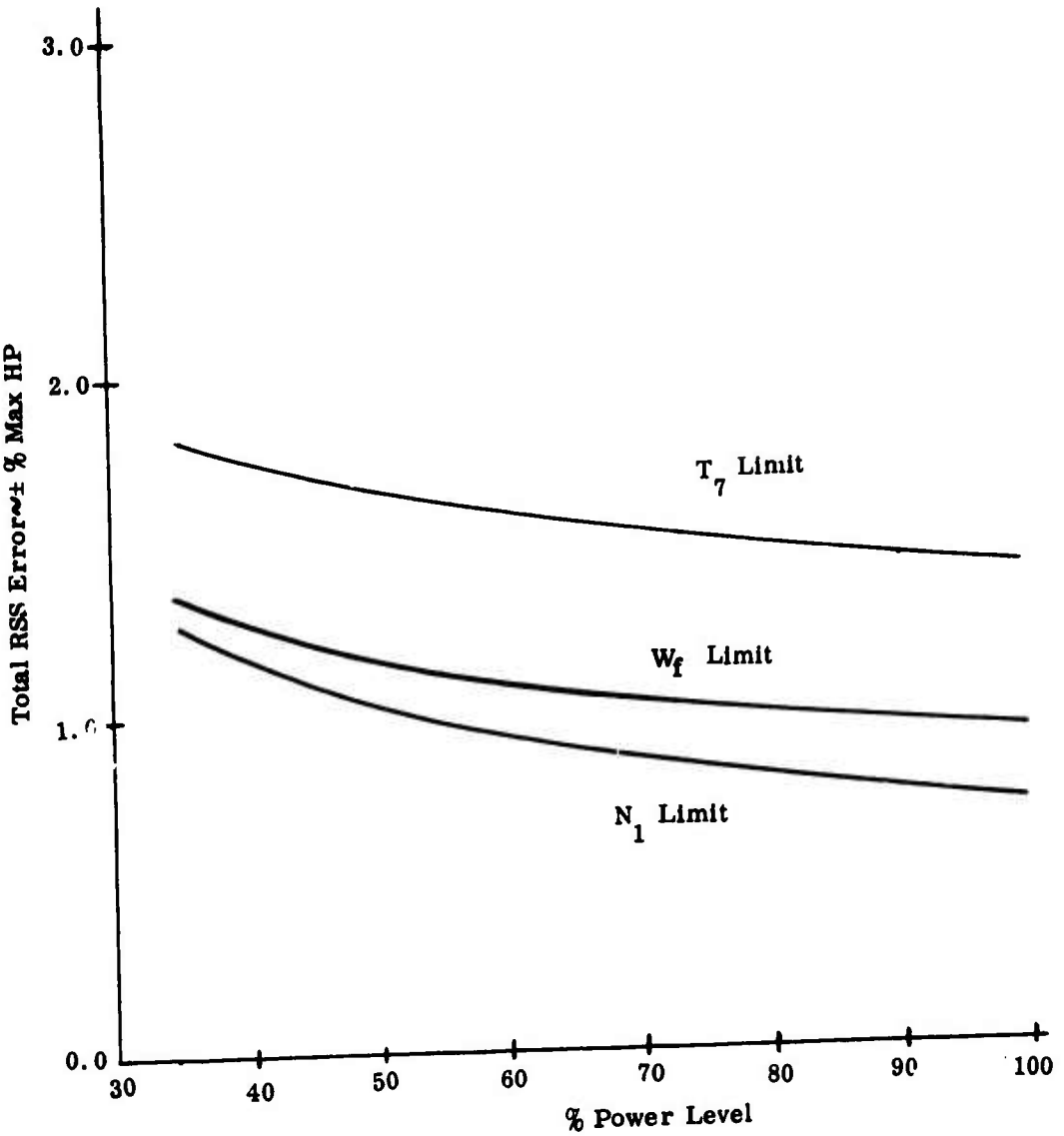

Figure 6. Total RSS Error in Predicted Power due to Errors in T_1, T_7, and SHP Sensors Reduced by 50%.

total RSS error in predicted power as a function of power level if an additional factor of two improvement in SHP sensor accuracy from ± 10 SHP to ± 5 SHP were obtained. The following table summarizes what effect improved sensor accuracy has in reducing total RSS error in predicting MPA at 50% power over a base system that includes only errors due to (1) control power limit errors, (2) sensor errors at 50% power, and (3) the influence of nonstandard day:

Total RSS Error in Predicted Power at 50% Power

	N_1 Limit	T_7 Limit	W_f Limit
Base System	± 1.54%	± 2.84%	± 1.60%
Improved T_7 Sensor (± 3.2°R)	± 1.54%	± 1.97%	± 1.60%
Improved SHP Sensor (±5 HP)	± 1.04%	± 2.65%	± 1.17%
Improved T_7 and SHP Sensors	± 1.04%	± 1.68%	± 1.17%

From these comparisons it is evident that the Phase II study must include an effort to improve sensor accuracies, in particular those of the T_7 and SHP sensors, whereas periodically updating the MPA baseline model does not yield a sufficient improvement in MPA accuracy.

ACCURACY BREAKDOWN

The total RSS error in predicting MPA has been broken down for a system using Set IV sensors which were selected in the Phase I study into the following error sources:

a. Use of base engine "C" for degraded engine

b. Nonstandard day

c. Linearization of nonlinear differential equations

d. High-power degradation being different from low-power degradation

e. $\partial A_N/A_N \neq -\partial \eta_{PT}/\eta_{PT}$

f. Sensor errors at low power

g. Control limit and sensor errors at high power

h. Change in actual power due to uncertainty in W_{BL} and SPE at high power

i. Uncertainty in W_{BL} and SPE at low power

The results of investigating the first five error sources for potential improvement are as follows:

Use of Base Engine "C" for Degraded Engine

Part of the MPA algorithm involves the use of base engine "C" coefficients to compute the variation in MPA caused by ambient conditions and engine degradation. In particular, the variation in MPA caused by engine degradation when on a limit is:

$$SHP_{DEGRADED} = SHP_{BASE} + C_1 \Delta W_A + C_2 \Delta \eta_c + C_3 \Delta \eta_T + C_4 \Delta \eta_{PT} + C_5 \Delta A_5 + C_6 \Delta A_N \quad (1)$$

where C_1 through C_6 relate the variations in horsepower resulting from the engine degradation (ΔW_A, $\Delta \eta_C$, $\Delta \eta_T$, $\Delta \eta_{PT}$, ΔA_5, ΔA_N). A separate set of "C" coefficients is needed for each limit, i.e., T_7 limit, W_f limit, and N_1 limit.

A more accurate form of the above equation is:

$$SHP_{DEGRADED} = SHP_{BASE} (1 + \Delta W_A)^{C_1} (1 + \Delta \eta_C)^{C_2} (1 + \Delta \eta_T)^{C_3} (1 + \Delta \eta_{PT})^{C_4} (1 + \Delta A_5)^{C_5} (1 + \Delta A_N)^{C_6} \quad (2)$$

Since the "C" coefficients somewhat depend on the engine operating conditions, degradations in engine performance may change the value of the "C" coefficient. The sensitivity to variations in "C" can be determined from the equation (2) above. For example, consider a degraded compressor efficiency (η_C) when on the T_7 limit.

$$SHP_{DEGRADED} = SHP_{BASE} \quad (1 + \Delta\eta_C)^{(C_2 + C_2 \text{ ERROR})} \qquad (3)$$

or

$$SHP_{DEGRADED} = SHP_{BASE} \quad (1 + \Delta\eta_C)^{C_2} \quad (1 + \Delta\eta_C)^{C_2 \text{ ERROR}} \qquad (4)$$

This shows that the MPA error results from the combination of a significant degradation and an error in C.

Studies have been conducted to determine how "C" should be varied as a result of each specific engine degradation when on each of the three limits. Results are listed in Table I and Table II. A review of this data indicates that variations in "C" caused by any degradation is very small when on either the fuel limit or the speed limit. However, a degradation in η_C, η_t, A_5, or A_N caused a significant variation in several "C" coefficients when on the temperature (T_7) limit. Modifying C_1 through C_6 (as defined in equation (2)) to account for engine degradation would significantly reduce MPA errors associated with engine degradation.

Using the terminology of the Phase I final report, the T_7 limit "C's" can be written as:

$C12 = C12_{BASE} + j\ (DETAC) + n\ (DETAT) + s\ (DA5) + w\ (DAN)$

$C13 = C13_{BASE} + k\ (DETAC) + p\ (DETAT) + t\ (DA5) + x\ (DAN)$

$C15 = C15_{BASE} + l\ (DETAC) + q\ (DETAT) + u\ (DA5) + y\ (DAN)$

$C16 = C16_{BASE} + m\ (DETAC) + r\ (DETAT) + v\ (DA5) + z\ (DAN)$

The computer model of the T53-L13 engine was used to compute the variations to the base "C" coefficients as follows:

j = -4.48	n = -5.91	s = +3.01	w = -3.91
k = -5.93	p = -7.07	t = +3.66	x = -4.89
l = +2.99	q = +3.59	u = -5.17	y = +5.74
m = -3.517	r = -4.33	v = +5.529	z = -6.55

TABLE I. C VARIATION FOR -1% DEGRADATION IN EFFICIENCIES

C Variation for -1% Degradation in η_C

	T_7			W_f			N_1		
Limit Value	1742.91 (base)	1742.91 (-1% η_C)	Delta C	793.07 (base)	793.07 (-1% η_C)	Delta C	24700 (base)	24605 (-1% η_C)	Delta C
η_C	2.94378	3.034253	.090473	.75845	.76394	.00549	-.577986	-.572816	-.00517
η_T	3.915878	4.035329	.119451	1.118029	1.126243	.008214	-.795747	-.789197	-.00655
η_{PT}	1.006409	1.006323	-.000086	1.005383	1.00534	-.000043	1.004693	1.00465	-.000046
A_5	-1.813379	-1.873981	.060602	-.568623	-.573674	.005051	.825495	.82626	.0007624
WA	.196527	.174245	-.022282	.050636	.047357	-.003279	1.249505	1.24534	-.00416
AN	2.431786	2.510726	.07894	-.033884	-.0353119	.0014279	-1.692862	-1.6952	.002334

C Variation for -1% Degradation in η_T

	T_7			W_f			N_1		
Limit Value	1742.91 (base)	1742.91 (-1% η_T)	Delta C	793.07 (base)	793.07 (-1% η_T)	Delta C	24700 (base)	24498 (-1% η_T)	Delta C
η_C	2.94378	3.063049	.119269	.756[illegible]	.779514	.021064	-.577986	-.563937	-.014
η_T	3.915878	4.058582	.142704	[illegible]	1.13942	.021391	-.795747	-.77496	-.02078
η_{PT}	1.006409	1.006292	-.000117	1.005383	1.005258	-.000125	1.004693	1.004573	-.000119
A_5	-1.813379	-1.886716	.073337	-.568623	-.579316	.010693	.825495	.82428	-.0012
WA	.196527	.166163	-.030364	.050636	.0437512	-.006885	1.249505	1.24201	-.00749
AN	2.431786	2.530752	.098966	-.033884	-.037038	.003154	-1.692862	-1.696934	.00407

TABLE I. CONTINUED

Limit Value	1742.91 (base)	1742.91 ($-1\%\eta_{PT}$)	Delta C	793.06 (base)	793.06 ($-1\%\eta_{PT}$)	Delta C	24700 (base)	24699.9 ($-1\%\eta_{PT}$)	Delta C
η_C	2.94378	2.943725	-.000055	.75845	.758418	-.000032	-.577986	-.577986	-.00004
η_T	3.915878	3.915806	-.000072	1.118029	1.117986	-.000043	-.795749	-.795741	-.000006
η_{PT}	1.006409	1.006350	-.000059	1.005383	1.005334	-.000049	1.004693	1.00465	-.00004
AS	-1.813379	-1.813378	.000001	-.568623	-.568611	-.000012	.825495	.825490	-.000005
WA	.196527	.196508	-.000019	.050636	.050629	-.000007	1.249505	1.249466	-.000039
AN	2.431786	2.431657	-.000129	-.033884	-.033983	-.000099	-1.692862	-1.692915	.000053

TABLE II. C VARIATION FOR +1% DEGRADATION IN A_5

Limit Value	T_7 1742.91 (base)	1742.91 (+1% A5)	Delta C	W_f 793.07 (base)	792.985 (+1% A5)	Delta C	N_1 24700 (base)	24605.6 (+1% A5)	Delta C
η_C	2.94378	3.004745	.060965	.75845	.764072	.005622	-.577986	-.571684	-.006
η_T	3.915878	3.990236	.074358	1.118029	1.121109	.00308	-.795747	-.786855	-.00889
η_{PT}	1.006409	1.006384	-.000025	1.005383	1.005360	-.000023	1.004693	1.004660	-.000033
A5	-1.813379	-1.915654	.102275	-.568623	-.587561	.018938	.825495	.836198	.010703
WA	.196527	.178078	-.018449	.050636	.047237	-.003399	1.249505	1.244	-.005809
AN	2.431786	2.547572	.115786	-.033884	-.018552	-.015332	-1.692862	-1.7027	.009877

Limit Value	T_7 1742.91 (base)	1742.91 (-1% WA)	Delta C	W_f 793.07 (base)	793.07 (-1% WA)	Delta C	N_1 24700 (base)	24731 (-1% WA)	Delta C
η_C	2.94378	2.922626	-.021154	.75845	.755267	-.003183	-.577986	-.5795	.001514
η_T	3.915878	3.887088	-.02879	1.118029	1.11353	-.004499	-.795747	-.79753	.001783
η_{PT}	1.006409	1.00639	-.000019	1.005383	1.005380	-.000003	1.004693	1.00465	-.000043
A5	-1.813379	-1.796209	-.01717	-.568623	-.56546	-.003163	.825495	.826783	.001288
WA	.196527	.206943	.010416	.050636	.053731	.003095	1.249505	1.2568	.007295
AN	2.431786	2.404925	-.026861	-.033884	-.038367	.004483	-1.692862	-1.70192	.009058

TABLE II. CONTINUED

LIMIT VALUE	T_7 1742.91 (base)	1742.91 (+1% AN)	Delta C	W_f 793.06 (base)	793.06 (+1% AN)	Delta C	N_1 24700 (base)	24741 (+1 % AN)	Delta C
n_C	2.943780	2.864941	-.078839	.75845	.759402	.000952	-.577986	-.578332	.000346
n_T	3.915878	3.816065	-.099813	1.118029	1.123294	.005265	-.795747	-.796213	.000466
n_{PT}	1.006409	1.006563	.000154	1.005383	1.005470	.000087	1.004693	1.004712	.000019
A_5	-1.813379	-1.700882	-.112497	-.568623	-.553689	-.014934	.825495	.814616	-.01886
WA	0.196527	0.225007	.02848	.050636	.0552206	.004585	1.249505	1.260219	.01074
AN	2.431786	2.292518	-.139268	-.033884	-.053118	.0192346	-1.692862	-1.695023	.002161

As a check on the improved accuracy due to modification of the base "C" coefficients, the following data was obtained:

1. For a 3% decrease in η_C, a 2% decrease in η_T and η_{PT}, a 2% increase in A_5 and A_N, and a 1% decrease in W_A, the degraded horsepower was obtained from the computer model of the engine by computing for 100 iterations; the predicted horsepower for each of the 6 engine parameters was 1158.85. Using the modified "C" coefficients, the predicted horsepower would have been 1156.42 for a prediction error of -.21%. Using unmodified "C" coefficients the predicted horsepower would have been 1171.16 for a prediction error of +1.06%.

2. Computing each of the degradations individually, the following prediction errors were obtained for T_7 limit:

Degradation	HP Actual	HP Predicted C Modified	% Error	HP Predicted C Unmodified	% Error
-3% η_C	1275.09	1275.17	+.006	1280.40	+.42
-2% η_T	1290.27	1290.29	+.002	1293.98	+.29
-2% η_{PT}	1372.31	NA	NA	1372.32	+.001
+2% A_5	1348.29	1348.35	+.005	1351.11	+.21
+2% A_N	1465.73	1465.80	-.005	1469.60	+.26
-1% W_A	1397.66	NA	NA	1397.75	+.006

These results show the improved horsepower prediction accuracy that can be obtained by modifying the base engine "C" as a function of the engine degradation. It is unrealistic to assume that maximum degradation in η_C, η_T η_{PT}, A_5, A_N and W_A will occur simultaneously; therefore the computed error - .21% is unrealistically large. Similarly, assuming that maximum degradation occurs in one parameter and no degradation occurs in any of the other parameters is unrealistic, so that the computed error of .002 to .006% is unrealistically small. The error resulting from estimated simultaneous realistic degradations in all parameters is estimated to be .06% . This modification has been incorporated into the MPA algorithm.

Nonstandard Day

It is noted that the interpolation of "C" coefficients (as defined in detail in the Phase I final report) adjusted all "C" coefficients as a function of T1 temperature. Thus, letting the "C" coefficients also be functions of η_C, η_T, A_5, and A_N is an extension of the same basic idea. The Phase I study showed that interpolation of "C" at a

nonstandard day in combination with a degraded engine would yield a prediction error of 0.1%, 0.23%, 0.1% when on the N_1, T_7, and W_f limits respectively due to errors in the "C" coefficients. There is no apparent rational interpolation of "C" in addition to those described earlier that would yield an additional accuracy improvement.

Linearization of Nonlinear Differential Equations

The error in linearization of the nonlinear differential equations is caused by errors in the "B" and "C" coefficients. It was estimated (in the Phase I study) that all "B" coefficients were uncertain by ± 5%, where the "B" coefficients provide the relation between engine parameter degradation and variations in engine measurements. In a similar manner, all "C" coefficients were estimated to be uncertain by ± 5%.

A more detailed study has been conducted to evaluate the errors introduced by linearization of the nonlinear differential equations and to show how the "B" and "C" coefficients influence MPA model accuracy. This study indicates that only a small portion of the "B" and "C" coefficients have a significant influence on MPA model accuracy.

Significant "B" coefficients were identified as follows. At an MPA power of 50%, ηc, ηT, ηPT and AN, A_5, and W_A were degraded one-at-a time. For example, ηc was degraded 3% by successively degrading ηc in .01% increments for 300 increments. The resultant variation in measurements could then be defined. These variations in measurements in combination with the "B" coefficients could be used to compute the degradation in ηc as follows:

$$\frac{\Delta \eta c}{\eta c} = \Sigma \left[\frac{\partial \eta c / \eta c}{\partial \text{Measurement}/\text{Measurement}} \right] \left[\frac{\Delta \text{Measurement}}{\text{Measurement}} \right] = \Sigma (B) \left[\frac{\Delta \text{ Measurement}}{\text{Measurement}} \right]$$

It is noted that the contribution to ($\Delta \eta c / \eta c$) is dependent on the product of a "B" coefficient and the corresponding measurement variation. The 3% degradation in ηc yields the numerical results shown below:

Measurement Name	$\frac{\Delta \text{ Measurement}}{\text{Measurement}}$	"B" Coefficient	$\frac{\Delta \text{ Measurement}}{\text{Measurement}}$ X "B"
N1	-.00319	-.0250	+.00008
T_3	+.01364	-2.2747	-.03098
W_f	+.03183	0.	0.
SHP	+.02634	0.	0.
T7	+.01827	0.	0.
	Computed ($\Delta \eta c / \eta_c$)		-.0309 = -3.09%

This example shows that the only "B" coefficient that must be accurate to compute the degradation in ηc is the "B" coefficient associated with the T3 measurement. The significant "B" coefficients for all engine degradations are listed in Table III. In addition, this study showed that "B" coefficients (as used at constant P3) do not vary significantly during engine degradation. Therefore, the use of the "B" coefficients computed from the nondegraded engine is nearly correct for the degraded engine. In summary, the accuracy of computing the engine degradations is primarily dependent on a few significant "B" coefficients and nearly independent of the accuracy of the remaining "B" coefficients.

Significant "C" coefficients were identified as follows. The maximum power degradation computation at each limit is dependent on both the engine degradation and the magnitude of the "C" coefficient associated with each engine degradation. The estimated maximum engine degradations are listed in Table IV. The MPA error at maximum degradation resulting from a $\pm$ 5% error in C is also listed in Table IV. This detailed error list shows that a few "C" coefficients are the most significant as identified in Table III.

TABLE III. "B" AND "C" COEFFICIENTS THAT HAVE A SIGNIFICANT INFLUENCE ON MPA ACCURACY

Degradation Parameter	Measurement That has a Significant "B" Coefficient Association
η_c	T3
η_T	W_f, T_7, SHP
$\eta_{PT \& An}$	W_f, T_7, SHP
A5	W_f, T_7
W_A	N_1

"C" Coefficients That Have A Significant Influence on MPA Accuracy

"C" Coefficient	Significant Degradation Parameter
C on N_1 Limit	A_N
C on T_7 Limit	η_c, η_T, A_5, A_N
C on W_f Limit	(None)

TABLE IV. DETAILED ERROR LIST - LINEARIZATION OF NONLINEAR DIFFERENTIAL EQUATIONS

Variable	Max. Variation %	Base Engine "C" N_1 Limit	T_7 Limit	W_f Limit	hp Error at ±5% "C" N_1 Limit % Power	T_7 Limit % Power	W_f Limit % Power
η_c	-3.5	-.5780	2.9438	.7584	.101	.515	.133
η_T	-2.5	-.7957	3.9159	1.1180	.100	.490	.140
η_{PT}	-2.5	1.0047	1.0064	1.0054	.126	.126	.126
A_5	2.2	0.8255	-1.8134	-.5686	.091	.200	.062
A_N	2.2	-1.6929	2.4318	-.0339	.186	.268	.004
W_A	-2.0	1.2495	0.1965	.0506	.125	.020	.005
				RSS Error	.308	.796	.239
					Hp Error at ±5% "B"		
η_c	-3.5	-.5780	2.9438	.7584	.101	.515	.133
η_T	-2.5	-.7957	3.9159	1.1180	.100	.490	.140
η_{PT}	-2.5	1.0047	1.0064	1.0054	.126	.126	.126
A_5	2.2	0.8255	-1.8134	-.5686	.091	.200	.062
A_N	2.2	-1.6929	2.4318	-.0339	.186	.268	.004
W_A	-2.0	1.2495	0.1965	.0506	.125	.020	.005
				RSS Error	.308	.796	.239
				RSS Error due to ±5% error in "C" and ± 5% Error in "B"	.436	1.126	.338

An improvement in the accuracy of the significant "B" and "C" coefficients would yield a reduction in the modeling error resulting from linearization of the nonlinear differential equations. The nonlinear engine model used in this study is based on successive iterations of the influence coefficients as described in detail in the Phase I study. It appears that such an engine model will not yield an accuracy better than ± 5% in the off-line computation of the "B" and "C" coefficients. However, more sophisticated nonlinear engine models are often made as an aid in engine and control development. Such an engine model could improve the accuracy of the off-line computation of the "B" and "C" coefficients. This engine model is typically developed by the engine manufacturer. The estimated accuracy in the significant "B" and "C" coefficients based on the more sophisticated engine model is ± 1.5%. Table V is a detailed error list based on "B" and "C" accuracies of ± 1.5%.

High-Power Degradation Being Different From Low-Power Degradation

The MPA algorithm computes the variation in engine degradation parameters (geometries and efficiencies) at part power and assumes that these parameters degrade the same percent-of-point at maximum power as occurred at part power. It is possible that increasing the part power at which MPA measurements are made would result in less uncertainty in the degradation parameters, hence reduce this error. However, the uncertainty in the degradation parameters (as defined in the Phase I study) has also been used in this study. The detailed error list is shown in Table VI.

Assumption that $(\partial AN/AN) = -(\partial \eta PT/ \eta PT)$

The Phase I Study recommended the use of Set IV sensors, which used the approximation that $(\partial AN/AN) = - (\partial \eta PT/ \eta PT)$, such that the P_7 sensor could be deleted. The degradations where $(\partial AN/_{AN})$ is not equal to $- (\partial \eta PT/ \eta PT)$ yield an error in the MPA computation. This error was small relative to total system MPA error in the Phase I Study. However, the present studies have reduced other error sources so that this error now becomes one of the major modeling errors. This error source could be eliminated by the addition of a P_7 sensor (i.e., use of Set I sensors). This would result in a change in the "B" coefficients, which would influence part power error sources. Although use of Set I sensors eliminates the error due to the assumption that $(\partial A_N/A_N) = - (\partial \eta PT/ \eta PT)$, the error summary is slightly worse than error summary using Set IV sensors because other sensor errors now become more significant. The error summary using Set I sensors is shown in Table VII, and a detailed error list is shown in Table VIII. The error summary using Set IV sensors is shown in Table IX, and a detailed

TABLE V. DETAILED ERROR LIST - LINEARIZATION OF NONLINEAR DIFFERENTIAL EQUATIONS

Variable	Maximum Variation %	Base Engine "C" N_1 Limit	T_7 Limit	W_f Limit	hp Error at ± 1.5% "C" N_1 Limit % Power	T_7 Limit % Power	W_f Limit % Power
η_c	-3.5	-.5780	2.9438	.7584	.030	.155	.040
η_T	-2.5	-.7957	3.9159	1.1180	.030	.147	.042
η_{PT}	-2.5	1.0047	1.0064	1.0054	.038	.038	.038
A5	2.2	0.8255	-1.8134	-.5686	.027	.060	.019
AN	2.2	-1.6929	2.4318	-.0339	.056	.080	.001
WA	-2.0	1.2495	0.1965	.0506	.038	.006	.002
			RSS Error		.092	.239	.072
					hp Error at ± 1.5% "B"		
η_c	-3.5	-.5780	2.9438	.7584	.030	.155	.040
η_T	-2.5	-.7957	3.9159	1.1180	.030	.147	.042
η_{PT}	-2.5	1.0047	1.0064	1.0054	.038	.038	.038
A5	2.2	0.8255	-1.8134	-.5686	.027	.060	.019
A_N	2.2	-1.6929	2.4318	-.0339	.056	.080	.001
W_A	-2.0	1.2495	0.1965	.0506	.038	.006	.002
			RSS Error		.092	.239	.072
			RSS Error due to ± 1.5% error in "C" and ± 1.5% error in "B"		.13	.34	.10

TABLE VI. DETAILED ERROR LIST-HIGH-POWER DEGRADATION DIFFERENT FROM LOW-POWER DEGRADATION

Limit	Variable	Base Engine "C"	Estimated Difference Between Low and High Power Degradation (% of Point)		Horsepower Error
N_1	Nc	-.5780	±0.15		.0867
	n_T	-.7957	±0.10		.0796
	n_{PT}	1.0047	±0.10		.1005
	Wa	1.2495	±0.10		.1250
	A5	0.8255	0.		0.
	A_N	-1.6929	0.		0.
				RSS Error	0.20%
T_7	n_c	2.9438	±0.15		.4416
	n_T	3.9159	±0.10		.3916
	n_{PT}	1.0064	±0.10		.1006
	Wa	0.1965	±0.10		.0196
	A5	-1.8134	0.		0.
	A_N	2.4318	0.		0.
				RSS Error	0.60%
W_f	n_c	.7584	±0.15		.1138
	n_T	1.1180	±0.10		.1118
	n_{PT}	1.0054	±0.10		.1005
	Wa	.0506	±0.10		.0051
	A5	-.5685	0.		0.
	A_N	-.0339	0.		0.
				RSS Error	0.19%

TABLE VII. ERROR SUMMARY SHEET - PREDICTION AT 50.2% POWER AT N2 = 100%, USING INTERPOLATED "C" IN PREDICTION ALGORITHM SET I SENSORS

Error Source	N_1 Limit % Power	T_7 Limit % Power	W_f Limit % Power
Linearization of Nonlinear Differential Equations	.13	.34	.10
Nonstandard Day	.10	.23	.21
Use of Base Engine "C" For Degraded Engine With Degradation Correction Factor Applied	.03	.06	.03
High-Power Degradation Different from Low-Power Degradation	.20	.60	.19
Sensor Errors at Low Power	1.48	1.95	1.61
Control Limit and Sensor Errors at High Power	.42	1.21	.74
Total RSS Error	1.56	2.41	1.80
Change in actual power due to uncertainty in W_{BL} and SPE at high power	1.37	4.63	2.16
Uncertainty in W_{BL} and SPE at Low Power	.46	1.68	.77
Total RSS Error Including W_{BL} and SPE Uncertainty	2.13	5.48	2.92

TABLE VIII. DETAILED ERROR LIST - SENSOR ERRORS AT 50.2% POWER AND AT MAXIMUM POWER, USING SENSORS AT LOW POWER AS TABULATED

Best Available Set I Sensors

Sensor	Error	Error in % of Point	(Low Power) Sensitivity N_1 Limit	T_7 Limit	W_f Limit	HP Prediction Error N_1 Limit	T_7 Limit	W_f Limit
N_1	±2.5RPM	±.011	-5.954	-1.973	-1.369	.0655	.0217	.0151
T_3	±0.5°R	±.0541	.009	-.036	.015	.0005	.0020	.0008
W_f	±2.65 pph	±.500	-.575	.014	-1.453	.2875	.007	.7265
SHP	±10HP	±1.422	1.002	1.001	1.002	1.4248	1.4234	1.4248
T_7	±4.5°R	±.294	.066	-4.259	.134	.0194	1.2522	.0394
N_2	±2.5RPM	±.0128	.539	.539	.539	.0069	.0069	.0069
T_1	±0.5°R	±.0964	2.694	4.502	0.896	.2597	.4340	.0864
P_1	±.01psi	±.068	-.075	-.424	.987	.0051	.0288	.0671
P_3	±.05 psi	±.063	.134	.032	.005	.0084	.0020	.0003
P_7	±.05 psi	±.175	-.472	-.687	-.559	.0826	.1202	.0978
				RSS Error		1.482	1.950	1.608

Variable	Uncertainty	(Low Power) Sensitivity N_1 Limit	T_7 Limit	W_f Limit	HP Variation N_1 Limit	T_7 Limit	W_f Limit
W_{bz}	±.5%	-.912	-3.183	-1.459	.456	1.592	.730
SPR	±.3%	-.203	1.770	.838	.0609	.531	.2514
			RSS Error		.46	1.678	.772

TABLE IX. ERROR SUMMARY SHEET - PREDICTION AT 50.2% POWER AT N_2 = 100%, USING INTERPOLATED "C" IN PREDICTION ALGORITHM SET IV SENSORS

Error Source	N_1 Limit % Power	T_7 Limit % Power	W_f Limit % Power
Linearization of Nonlinear Differential Equations	.13	.34	.10
$\partial AN/AN \neq$ to $- \frac{\partial \eta_{PT}}{\eta_{PT}}$	.30	.54	.40
Nonstandard Day	.10	.23	.21
Use of base engine "C" for degraded engine with degradation correction factor applied	.03	.06	.03
High power degradation being different from low power degradation	.20	.60	.19
Sensor errors at low power	1.22	1.66	1.38
Control limit and sensor errors at high power	.41	1.20	.77
Total RSS Error	1.35	2.24	1.66
Change in actual power due to uncertainty in W_{BL} and SPE at high power	1.38	4.74	2.17
Uncertainty in W_{BL} and SPE at low power	0.41	1.20	.77
Total RSS Error including W_{BL} and SPE uncertainty	1.98	5.50	2.84

error list is shown in Table X. As in the Phase I study, the Set IV sensors are recommended to be used in power prediction.

A review of Table IX indicates that the major MPA prediction errors are associated with uncertainty in bleed air and shaft power extraction, and the sensor and engine-control errors. Since uncertainty in bleed air and shaft power extraction may be minimized by procedural techniques during MPA prediction, the remaining major MPA error is caused by sensor errors. In particular, the MPA error is primarily determined by the T_7 and SHP sensor errors.

TABLE X. DETAILED ERROR LIST - SENSOR ERRORS AT 50.2% POWER AND AT MAXIMUM POWER, USING SENSORS AT LOW POWER AS TABULATED BEST AVAILABLE SET IV SENSORS

Sensor	Error	Error In % of Point	(Low Power) Sensitivity N_1 Limit	T_7 Limit	W_f Limit	HP Prediction Error N_1 Limit	T_7 Limit	W_f Limit
N_1	±2.5 RPM	±.011	-6.039	-1.862	-1.308	.0664	.0205	.0144
T_3	±0.5 °R	±.0541	-.03103	.1613	.0680	.00168	.00873	.00368
W_f	±2.65 pph	±.500	-.5751	.0142	-1.484	.2876	.0071	.742
SHP	±10 HP	±1.422	.8323	.7833	.8124	1.1835	1.1138	1.1552
T_7	±4.5°R	±.294	.2077	-4.1814	.2796	.0611	1.229	.0822
N_2	±2.5 RPM	±.0128	.4517	.4194	.4386	.00576	.00537	.00561
T_1	±0.5 °R	±.0964	2.596	4.380	.791	.2503	.4222	.0763
P_1	±0.01 psi	±.068	-.401	-.840	.656	.0273	.0571	.0446
P_3	±0.05 psi	±.063	.1334	.047	.0059	.0084	.00296	.00037
					RSS Error	1.247	1.713	1.378
			(High Power)					
N_1	±2.5 RPM	±.01	-3.715	0	0	.0372	0	0
W_f	±4 pph	±.50	-.563	0	+1.469	.2815	0	.7345
T_7	±4.8 °R	±.28	0	-4.314	0	0	1.2079	0
T_1	±0.5 °R	±.10	-.756	0	0	.0756	0	0
P_1	±.01 psi	±.068	0	0	-.435	0	0	.0296
N_1 Set	+21 RPM	+.08	3.715	0	0	.2972	0	0
T_7 Set	0	0	0	4.314	0	0	0	0
W_f Set	± .27 pph	± .034	0	0	-1.469	0	0	.2155
					RSS Error	.4179	1.2079	.7350

Variable	Uncertainty	N_1 Limit	(Low Power) Sensitivity T_7 Limit	W_f Limit	N_1 Limit	HP Variation T_7 Limit	W_f Limit
W_{BL}	±.5%	-.915	-3.184	-1.464	.458	1.592	.732
SPE	±.3 hp/pps	-.2	1.775	.841	.06	.532	.252
			RSS Error		0.462	1.678	0.774
			(High Power)				
WBL	±1.5%	-.915	-3.078	-1.433	1.372	4.617	2.150
SPE	±.3 hp/pps	-.156	1.343	.641	.0468	.4029	.1923
			RSS Error		1.373	4.634	2.159

RESULTS OF EVALUATION OF MPA ACCURACY BASED ON ENGINE TEST DATA

Actual engine test data from ten T53-L13 engines was provided by Lycoming. This test data included both calibration data when the engine was new and calibration data after extensive field use in the range of 60 to 100% SHP. The field use for the ten engines was in the range of 1192 to 4217 hours.

The actual T53 controls (and maximum power limits) are different from the engine control used in the MPA study activity. The actual engine maximum power was defined for this study to be the actual SHP that occurred at the following limits:

$$N_1 = 25400 \quad \text{RPM}$$

$$T_7 = 1840 \quad {}^{\circ}\text{R}$$

$$W_f = 820 \quad \text{PPH}$$

Therefore, the ten engines were defined to have identical N_1, T_7 and W_f limits, but different maximum power when "new".

All tabulated data as received from Lycoming was already referred to one ambient temperature ($T_1 = 32^{\circ}F$). Also the measured engine power was corrected to optimum SHP (i.e., SHP at optimum N_2 speed). The MPA algorithm was modified to account for these test data characteristics. The predicted MPA using the MPA algorithm and resulting MPA algorithm errors were computed as follows:

1. Change engine test referred curve fit data ($T_1 = 32^{\circ}$) to 59° standard day.
2. Obtain baselines ($N_1/\sqrt{\theta_1}$, $SHP/\delta_1\sqrt{\theta_1}$, $T3/\theta_1$, $WF/\delta_1\theta_1^{Y}$, and T_7/θ_1 vs. P_3/δ_1) from "new" engine calibration data. SHP is optimum SHP for baseline.
3. Compute SHP reference when on each limit (T_7, W_f, or N_1) based on defined limit in T_7, W_f, or N_1 droop for "new" engine.
4. Load data from items 2 and 3 above into MPA model in preparation for MPA prediction on this specific engine.
5. Select "degraded" data from same engine. At the part power points to be evaluated, determine T_1, P_1, N_1, N_2, SHP, T_3, W_F, T_7 and P_3 to be used as "measurements".

6. Load "measurements" from Item 5 above into MPA model and let MPA model compute maximum corrected SHP when on each of the three limits (T_7, W_F, or N_1). These SHP's are the predicted corrected SHP's. Select the least corrected SHP and uncorrect it to obtain the actual SHP limit.

7. To compute MPA prediction error, determine MPA when on each limit (T_7, W_F or N_1) from "degraded" engine data. These MPA's are actual corrected SHP's.

8. Compute % error between corrected SHP in Item 6 and Item 7.

The above procedure was used to determine MPA prediction accuracy for "measurements" at 60%, 70%, 80%, and 90% SHP for the ten engines. Results are tabulated in Table XI and include "engine age" between "new" calibration and "degraded engine" measurements. The maximum SHP when "new" for each of the three defined limits is also listed. A brief review of MPA prediction accuracy indicates excellent prediction accuracy for some engines and poor prediction accuracy on other engines; i.e., engine-to-engine prediction accuracy is not consistent.

First let us look at the expected errors if the best available sensors were used or, in our case, the present T53-L13 engine sensors. Figure 2 shows that the expected RSS error in predicted power using the best available sensors and with no uncertainty in bleed airflow and shaft power extraction is 3.10% on the T_7 limit, 1.54% on the W_f limit and 1.48% on the N_1 limit when at the 60% power level. The Lycoming engine test data was acquired utilizing the present T53-L13 engine test cell sensors which do not in general meet the MPA sensor accuracy requirements. Therefore, the criteria for evaluating the relative merit of the MPA predictions based on the Lycoming engine data must be based upon an MPA error analysis incorporating the present T53-L13 sensors. Table XII includes a detailed listing of the horsepower prediction error at 50% power level based on sensor accuracies only. The most significant measurement error on Table XII is caused by the T_1 measurement. However, a T_1 error would cause an MPA prediction error in one direction only and the data of Table XI indicates that the error pattern is random. Therefore, disregarding the influence of T_1 on the prediction accuracy, the anticipated MPA prediction accuracies with the T43-L13 engine sensors are 2.10% on the N_1 limit, 7.96% on the T_7 limit, and 2.88% on the W_f limit. This is the criterion upon which the MPA predictions using Lycoming engine data shall be judged.

A comparison of Tables XI and XII indicates that the MPA prediction error exceeded the analytical error for some engines. Studies were directed at determining the cause of the inconsistency in MPA prediction accuracy and associated excessive errors for some engines.

TABLE XI. MPA PREDICTION ERROR SUMMARY - ONE POINT METHOD

S/N LE-14016 (4217 HOURS)

POWER	LIMIT	MAX HP	MPA MAX HP	% ERROR	
90%	N_1	1390	1386	-0.3	
	T_7	1411	1438	+1.9	
	W_f	1422	1438	+1.1	
80%	N_1	1390	1381	-0.6	
	T_7	1411	1410	-0.1	
	W_f	1422	1435	+0.9	Max HP "new"
70%	N_1	1390	1375	-1.1	N_1 1461
	T_7	1411	1377	-2.4	T_7 1425
	W_f	1422	1433	+0.8	W_f 1447
60%	N_1	1390	1367	-1.6	
	T_7	1411	1344	-4.8	
	W_f	1422	1428	+0.4	

S/N LE-21304 (2381 HOURS)

POWER	LIMIT	MAX HP	MPA MAX HP	% ERROR	
90%	N_1	1296	1297	+0.1	
	T_7	1296	1275	-1.6	
	W_f	1355	1353	-0.2	
80%	N_1	1296	1304	+0.6	
	T_7	1296	1280	-1.2	
	W_f	1355	1354	-0.1	Max HP "new"
70%	N_1	1296	1319	+1.8	N_1 1387
	T_7	1296	1287	-0.7	T_7 1416
	W_f	1355	1355	+0.0	W_f 1410
60%	N_1	1296	1340	+3.4	
	T_7	1296	1301	+0.4	
	W_f	1355	1363	+0.6	

TABLE XI. CONTINUED

S/N K-125 (2464 HOURS)

Power	Limit	Max HP	MPA Max HP	% Error	
90%	N_1	1303	1300	-0.2	
	T_7	1198	1193	-0.4	
	W_f	1314	1311	-0.2	
80%	N_1	1303	1305	+0.2	
	T_7	1198	1196	-0.2	
	W_f	1314	1316	+0.2	Max HP "new"
70%	N_1	1303	1301	-0.2	N_1 1391
	T_7	1198	1192	-0.5	T_7 1278
	W_f	1314	1313	-0.1	W_f 1351
60%	N_1	1303	1291	-0.9	
	T_7	1198	1189	-0.8	
	W_f	1314	1307	-0.5	

S/N K-117 (1192 HOURS)

Power	Limit	Max HP	MPA Max HP	% Error	
90%	N_1	1282	1251	-2.4	
	T_7	1100	1081	-1.7	
	W_f	1248	1236	-1.0	
80%	N_1	1282	1244	-3.0	
	T_7	1100	1076	-2.2	
	W_f	1248	1218	-2.4	Max HP "new"
70%	N_1	1282	1232	-3.9	N_1 1377
	T_7	1100	1066	-3.1	T_7 1312
	W_f	1248	1202	-3.7	W_f 1332
60%	N_1	1282	1214	-5.3	
	T_7	1100	1051	-4.4	
	W_f	1248	1176	-5.8	

TABLE XI. CONTINUED

S/N K-116 (1249 HOURS)

Power	Limit	Max HP	MPA Max HP	% Error	
90%	N_1	1342	1346	+0.3	
	T_7	1438	1476	+2.6	
	W_f	1395	1412	+1.2	
80%	N_1	1342	1343	+0.1	
	T_7	1438	1493	+3.8	
	W_f	1395	1418	+1.6	Max HP "new"
70%	N_1	1342	1335	-0.5	N_1 1385
	T_7	1438	1503	+4.5	T_7 1440
	W_f	1395	1421	+1.9	W_f 1380
60%	N_1	1342	1324	-1.3	
	T_7	1438	1515	+5.4	
	W_f	1395	1427	+2.3	

S/N LE 21404 (3002 HOURS)

Power	Limit	Max HP	MPA Max HP	% Error	
90%	N_1	1280	1283	+0.2	
	T_7	1392	1393	+0.1	
	W_f	1394	1401	+0.5	
80%	N_1	1280	1290	+0.8	
	T_7	1392	1422	+2.2	
	W_f	1394	1413	+1.4	Max HP "new"
70%	N_1	1280	1298	+1.4	N_1 1386
	T_7	1392	1451	+4.2	T_7 1500
	W_f	1394	1428	+2.4	W_f 1435
60%	N_1	1280	1308	+2.2	
	T_7	1392	1487	+6.8	
	W_f	1394	1445	+3.7	

TABLE XI. CONTINUED

S/N K-124 (2458 HOURS)

Power	Limit	Max HP	MPA Max HP	% Error	
90%	N_1	1258	1248	-0.8	
	T_7	1175	1129	-3.9	
	W_f	1290	1291	+0.1	
80%	N_1	1258	1239	-1.5	
	T_7	1175	1146	-2.5	
	W_f	1290	1299	+0.7	Max HP "new"
70%	N_1	1258	1231	-2.2	N_1 1395
	T_7	1175	1166	-0.8	T_7 1355
	W_f	1290	1313	+1.8	W_f 1387
60%	N_1	1258	1217	-3.3	
	T_7	1175	1180	+0.4	
	W_f	1290	1325	+2.7	

S/N LE-14083 (1200 HOURS)

Power	Limit	Max HP	MPA Max HP	% Error	
90%	N_1	1311	1320	+0.7	
	T_7	1247	1203	-3.5	
	W_f	1345	1367	+1.6	
80%	N_1	1311	1352	+3.1	
	T_7	1247	1215	-2.6	
	W_f	1345	1403	+4.3	Max HP "new"
70%	N_1	1311	1388	+5.9	N_1 1466
	T_7	1247	1223	-1.9	T_7 1446
	W_f	1345	1447	+7.6	W_f 1461
60%	N_1	1311	1437	+9.6	
	T_7	1247	1236	-0.9	
	W_f	1345	1496	+11.2	

TABLE XI. CONTINUED

S/N LE-14018 (1200 HOURS)

Power	Limit	Max HP	MPA Max HP	% Error	
90%	N_1	1294	1281	-1.0	
	T_7	1478	1473	-0.3	
	W_f	1361	1354	-0.5	
80%	N_1	1294	1264	-2.3	
	T_7	1478	1442	-2.4	
	W_f	1361	1336	-1.8	Max HP "new"
70%	N_1	1294	1242	-4.0	N_1 1436
	T_7	1478	1410	-4.6	T_7 1336
	W_f	1361	1315	-3.4	W_f 1402
60%	N_1	1294	1218	-5.9	
	T_7	1478	1373	-7.1	
	W_f	1361	1287	-5.4	

S/N K-144 (1507 HOURS)

Power	Limit	Max HP	MPA Max HP	% Error	
90%	N_1	1502	1490	-0.8	
	T_7	1445	1450	+0.3	
	W_f	1530	1506	-1.6	
80%	N_1	1502	1473	-1.9	
	T_7	1445	1456	+0.8	
	W_f	1530	1495	-2.3	Max HP "new"
70%	N_1	1502	1450	-3.5	N_1 1328
	T_7	1445	1459	+1.0	T_7 1397
	W_f	1530	1477	-3.5	W_f 1420
60%	N_1	1502	1425	-5.1	
	T_7	1445	1466	1.4	
	W_f	1530	1454	-5.0	

TABLE XII. MPA ERROR ANALYSIS AT 50% POWER WHEN USING LYCOMING TEST CELL SENSORS

Sensor	Error	% of Point	Sensitivities			HP Prediction Error (%)		
			N_1 Limit	T_7 Limit	W_f Limit	N_1 Limit	T_7 Limit	W_f Limit
N_1	± 49.4 rpm	.22	-6.039	-1.862	-1.308	1.33	.41	.29
T_3	± 16.2 °R	1.76	-.03103	.1613	.0680	.05	.28	.12
W_f	± 7.9 pph	1.53	-.5751	.0142	-1.484	.88	.02	2.27
SHP	± 7.56 hp	1.07	.8323	.7833	.8124	.89	.84	.87
T_7	± 28 °R	1.84	.2077	-4.1814	.2796	.38	7.69	.51
N_2	± 42.2 rpm	0.2	.4517	.4194	.4386	.09	.08	.09
P_1	± .32 psi	2.18	-.401	-.840	.656	.87	1.83	1.43
P_3	± 2.2 psi	2.82	.1334	.047	.0059	.38	.13	.02
			RSS Error With T_1 Error Excluded			2.10	7.96	2.88
T_1	± 9.6°R	1.85	2.296	2.380	.791	4.80	8.10	1.46
			RSS Error With T_1 Error Included			5.24	11.36	3.23

An initial attempt was made to correlate the degradations DWA, DETAC, DETAT, DETAPT, DA5 and DAN of the "good" engines (engines with low errors in MPA prediction) with the degradations of the "bad" engines (engines with high MPA prediction errors). The "bad" engines were serial numbers K117, LE14083, LE14018, LE14018 and K144. Degradations that were small in the "good" engines were both small and large in the "bad" engines and, similarly, degradations that were large in the "good" engines were both large and small in the "bad" engines.

Another attempt was made to correlate excessive MPA prediction errors to specific engine measurements. Table XIII contains a tabulation of the percent difference between baseline and degraded-engine measurements (i.e., measurement difference caused by degradation). The change in measurement-delta when decreasing part power from 90% to 60% may be observed and has been listed in Table XIV. Between 90% power and 60% power there is a significant change of the measurement delta for shaft horsepower, SHP, and fuel flow, W_f, in those engines with excessive power prediction error at low power, i.e., the baseline and degraded engine corrected measurement were not parallel. To check the importance of this observation, the measurements of SHP and W_f for all engines at power levels of 60%, 70% and 80% were arbitrarily revised to give the same measurement difference as was obtained at 90% power (i.e., corrected SHP and W_f measurement were nearly parallel to baseline). Table XV includes a summary of prediction errors comparing normal measurements with the arbitrarily revised SHP and W_f measurements. The underlined errors are those which exceed the expected MPA prediction accuracies with T-53 engine sensors. Table XV under the column headed "with normal measurements" displays the errors for each limit and power level for all ten (10) engines. The columns headed "with revised SHP and W_f measurements" display the improvement in MPA accuracy if SHP and W_f measurements at 60%, 70%, and 80% are arbitrarily revised to have the same percent difference (from the baseline) as occurred at 90% power. This arbitrarily revised measurement shows that the MPA error for "bad engines" generally improved on the N_1 and W_f limits, but T_7 limit accuracy degraded. The column headed "revised SHP, W_f, and T_7 measurements" displays the improvement in T_7 limit MPA accuracy if T_7 as well as SHP and W_f are arbitrarily revised. Table XV suggests that the engines having excessive MPA prediction errors are related to engine characteristics as measured by SHP and W_f when on the N_1 and W_f limits and SHP, W_f, and T_7 when on the T_7 limit. There was no apparent trend in ΔSHP, ΔW_f, and Δ T, as engine power at MPA measurement was reduced from 90% to 60% power.

The best correlation between excessive MPA prediction errors and engine characteristics is obtained by observing the trend of the computed engine degradation as engine power is changed between 60% and 90% power. These

TABLE XIII. INFLUENCE OF REAL ENGINE DEGRADATION ON MEASUREMENTS

% Power	% Difference Between Baseline and Degraded Engine Measurement				
	N_1	T_3	W_F	SHP	T_7
S/N LE-14016					
90	-0.5	0.9	-7.0	11.1	-2.9
80	-0.2	1.0	-6.1	-10.2	-2.1
70	0.1	1.1	-5.3	- 9.4	-1.3
60	0.4	1.3	-3.9	- 8.0	-0.4
S/N 21304					
90	0.9	-0.8	0.9	- 2.7	1.6
80	1.2	-0.6	2.8	0	2.2
70	1.3	-0.4	5.1	3.6	2.8
60	1.6	0	8.0	9.1	3.5
S/N K-125					
90	1.0	-0.5	-0.1	-3.1	0.8
80	0.8	-0.4	-0.7	-3.8	0.6
70	0.6	-0.4	-1.3	-5.1	0.4
60	0.5	-0.4	-2.0	-6.9	0.1
S/N K-117*					
90	1.4	1.4	9.7	6.9	5.6
80	1.4	1.4	8.9	4.2	5.1
70	1.2	1.2	7.9	1.0	4.6
60	1.2	1.2	7.2	-2.8	4.1
S/N K-116					
90	-1.1	-0.9	-9.8	-12.1	-3.7
80	-0.7	-1.0	-9.4	-11.3	-3.6
70	-0.3	-1.1	-8.7	-10.3	-3.4
60	0.2	-1.2	-8.0	- 8.9	-3.2
S/N LE 21404					
90	-0.1	-1.2	-6.6	-11.8	-1.5
80	0	-1.2	-6.3	-11.0	-1.6
70	0.2	-1.3	-6.1	- 9.8	-1.6
60	0.3	-1.3	-5.7	- 8.2	-1.7

TABLE XIII. CONTINUED

% Power	% Difference Between Baseline and Degraded Engine Measurement				
	N_1	T_3	W_f	SHP	T_7
S/N K-124					
90	1.6	1.4	2.5	-3.5	3.1
80	1.5	1.3	1.0	-5.4	2.3
70	1.4	1.2	-0.9	-7.5	1.5
60	1.3	1.2	3.2	-10.4	0.7
S/N LE-14083*					
90	1.7	-0.1	3.5	-1.6	3.5
80	1.6	0.2	3.5	1.0	3.8
70	1.6	0.5	3.6	4.3	4.3
60	1.6	0.7	3.9	8.8	4.8
S/N LE-14018*					
90	1.3	0.5	-3.8	-8.9	-4.8
80	1.1	0.4	-4.2	-11.0	-4.8
70	1.0	0.3	-4.6	-13.5	-4.8
60	0.9	0.2	-4.9	-16.4	-4.8
S/N K-144*					
90	-2.0	-2.2	-2.3	2.7	-0.3
80	-1.7	-2.1	-2.1	2.4	-0.5
70	-1.4	-2.1	-1.6	1.8	-0.6
60	-1.2	-2.1	-1.0	1.3	-0.9

* Engines with large MPA prediction errors.

TABLE XIV. INFLUENCE OF ENGINE POWER LEVEL ON MEASUREMENT - DELTA

	CHANGE IN % MEASUREMENT - DELTA DUE TO A CHANGE IN ENGINE POWER FROM 90% TO 60%				
	N_1	T_3	W_F	SHP	T_7
S/N LE-14016	0.9	0.4	3.1	3.1	2.5
S/N LE-21304	0.7	0.8	7.1	11.8	1.9
S/N K-125	-0.5	0.1	-1.9	-3.8	-0.7
S/N K-117	-1.2	-0.2	-2.5	9.7	-1.5
S/N K-116	1.3	-0.3	1.8	3.2	0.5
S/N LE-21404	0.4	-0.1	0.9	3.6	-0.2
S/N K-124	-0.3	-0.2	-5.7	-6.9	-2.4
S/N LE-14083	-0.1	0.8	0.4	10.4	1.3
S/N LE-14018	-0.4	-0.3	-1.1	-7.5	0
S/N K-144	0.8	0.1	1.3	-1.4	-0.6

TABLE XV. COMPARISON OF POWER PREDICTION ERRORS

S/N LE-14016	With Normal Measurements			With Revised SHP And W_f Measurements			With Revised SHP, W_f, & T_7 Measurements
% Power	N_1	T_7	W_f	N_1	T_7	W_f	T_7
90	-0.3	1.9	1.1	-0.3	1.9	1.1	1.9
80	-0.6	-0.1	0.9	-1.	-0.9	1.5	2.4
70	-1.1	-2.4	0.6	-1.7	-4.0	2.0	2.9
60	-1.6	-4.8	0.4	-2.9	-7.5	2.5	3.2
S/N LE-21304							
90	0.1	-1.6	-0.2	0.1	-1.6	-0.2	-1.6
80	0.6	-1.2	-0.1	-1.1	-4.3	0	-1.6
70	1.8	-0.7	0.0	-1.9	-7.2	0.3	-1.6
60	3.4	0.4	0.6	-3.5	-10.7	0.6	-1.8
S/N K-125							
90	-0.2	-0.4	-0.2	-0.2	-0.4	-0.2	-0.4
80	0.2	-0.2	0.2	0.5	0.5	-0.1	-0.3
70	-0.2	-0.5	-0.1	1.1	1.6	0	-0.1
60	-0.9	-0.8	-0.5	1.5	3.2	0.1	-0.1
S/N K-117*							
90	-2.4	-1.7	-1.0	-2.4	-1.7	-1.0	-1.7
80	-3.0	-2.2	-2.4	-1.0	0.5	-1.0	-2.1
70	-3.9	-3.1	-3.7	0.3	2.7	-1.1	-2.4
60	-5.3	-4.4	-5.8	1.5	5.0	-1.2	-2.6
S/N K-116							
90	0.3	2.6	1.2	0.3	2.6	1.2	2.6
80	0.1	3.8	1.6	-0.5	3.9	1.5	3.3
70	-0.5	4.5	1.9	-1.6	2.6	1.8	3.7
60	-1.3	5.4	2.3	-3.4	2.2	2.1	4.0
S/N LE-21404							
90	0.2	0.1	0.5	0.2	0.1	0.5	0.1
80	0.8	2.2	1.4	0.1	1.2	1.0	0.1
70	1.4	4.2	2.4	-0.2	1.9	1.4	1.3
60	2.2	6.8	3.7	-0.5	2.9	1.7	1.8
S/N K-124							
90	-0.8	-3.9	0.1	-0.3	-3.9	0.1	-3.9
80	-1.5	-2.5	0.7	-0.5	-0.2	0.2	-3.9
70	-2.2	-0.6	1.8	-0.2	3.7	0.3	-3.8
60	-3.3	0.4	2.7	0	7.7	0.4	-3.7

TABLE XV. CONTINUED

S/N LE-14083*	With Normal Measurements			With Revised SHP And W_f Measurements			With Revised SHP, W_f, & T_7 Measurements
% Power	N_1	T_7	W_f	N_1	T_7	W_f	T_7
S/N LE-14083*							
90	0.7	-3.5	1.6	0.7	-3.5	1.6	-3.5
80	3.1	-2.6	4.3	0.7	-5.3	1.9	-3.4
70	5.6	-1.9	7.6	0.5	-7.6	2.2	-3.5
60	9.6	0.9	11.2	0.5	-9.8	2.4	-3.5
S/N LE-14018*							
90	-1.0	-0.3	-0.5	-1.0	-0.3	-0.5	-0.3
80	-2.3	-2.4	-1.8	-0.6	-0.4	-0.4	-0.2
70	-4.0	-4.6	-3.4	-0.4	-0.3	-0.4	-0.1
60	-5.9	-7.1	-5.4	0.1	0	-0.4	0.1
S/N K-144*							
90	-0.8	0.3	-1.6	-0.8	0.3	-1.6	0.3
80	-1.9	0.8	-2.3	-1.5	1.0	-1.5	0.4
70	-3.5	1.0	-3.5	-2.3	1.7	-1.8	0.4
60	-5.1	1.4	-5.0	-3.2	2.6	-2.0	0.3

*Bad Engines.

computed degradations for the ten engines are plotted in Figures 7 through 16. Note that essentially all computed engine degradations display a significant change as measurement power is changed from 60% to 90%. There is a consistent trend in the degradation within any one engine as power is changed. This consistency adds credibility to the indication that engine degradation is changing as a function of power level.

It is evident that the basic algorithm assumption of percent-of-point engine degradation being essentially independent of power level is suspect and can potentially introduce significant MPA prediction errors. The engine data indicates that it is desirable to modify the MPA prediction algorithm to include the effect of engine degradation at high power being different from engine degradation at low (measurement) power. One such modification has been partially evaluated. Figures7 through 16 indicate a reasonably consistent trend in engine degradation versus P3 as power is varied from 60% to 90% (i.e., locus of points form an essentially straight line). Unfortunately there is no actual engine test data available at low engine power (below 60%), so it is not known if the locus of points down to 20% or 30% power would remain essentially a straight line. The algorithm modification consists of two sets of steady-state engine measurements at low power (separated by 10% to 20% in power) and degradation is computed for both sets of low power measurements. The trend of each computed engine degradation is established and the change in degradation with power can be determined (i.e., slopes of lines in Figures 7 through 15). The degradation at 100% power may then be determined by extrapolating the trend of degradation determined from the two low-power measurement sets. This algorithm modification was evaluated using the actual engine test data at engine data measurement sets of 60% and 70% power; the results are tabulated in Table XVI. Similarly, the measurement sets at 60% and 80% were used and results are tabulated in Table XVII. Results from Tables XI, XVI, and XVII are summarized in Table XVIII, comparing the MPA prediction accuracy of the two-measurement (with degradation extrapolation) to single-measurement algorithm. The MPA prediction accuracy using this degradation extrapolation algorithm is better than computing MPA at 60%. It is not certain whether the improved accuracy resulted from the extrapolation concept or from the use of an extra measurement above 60% power. Unfortunately this uncertainty cannot be resolved without actual engine data at lower power levels.

In summary, the MPA prediction algorithm recommended in this Phase II Study is based on the assumption that engine degradation is essentially independent of engine power. There is no known proven method to remove this assumption with the use of actual engine degradation data at low power. Evaluation of the MPA prediction accuracy using actual engine test data shows that the MPA accuracy is usually within the accuracy determined by the analytical error analysis.

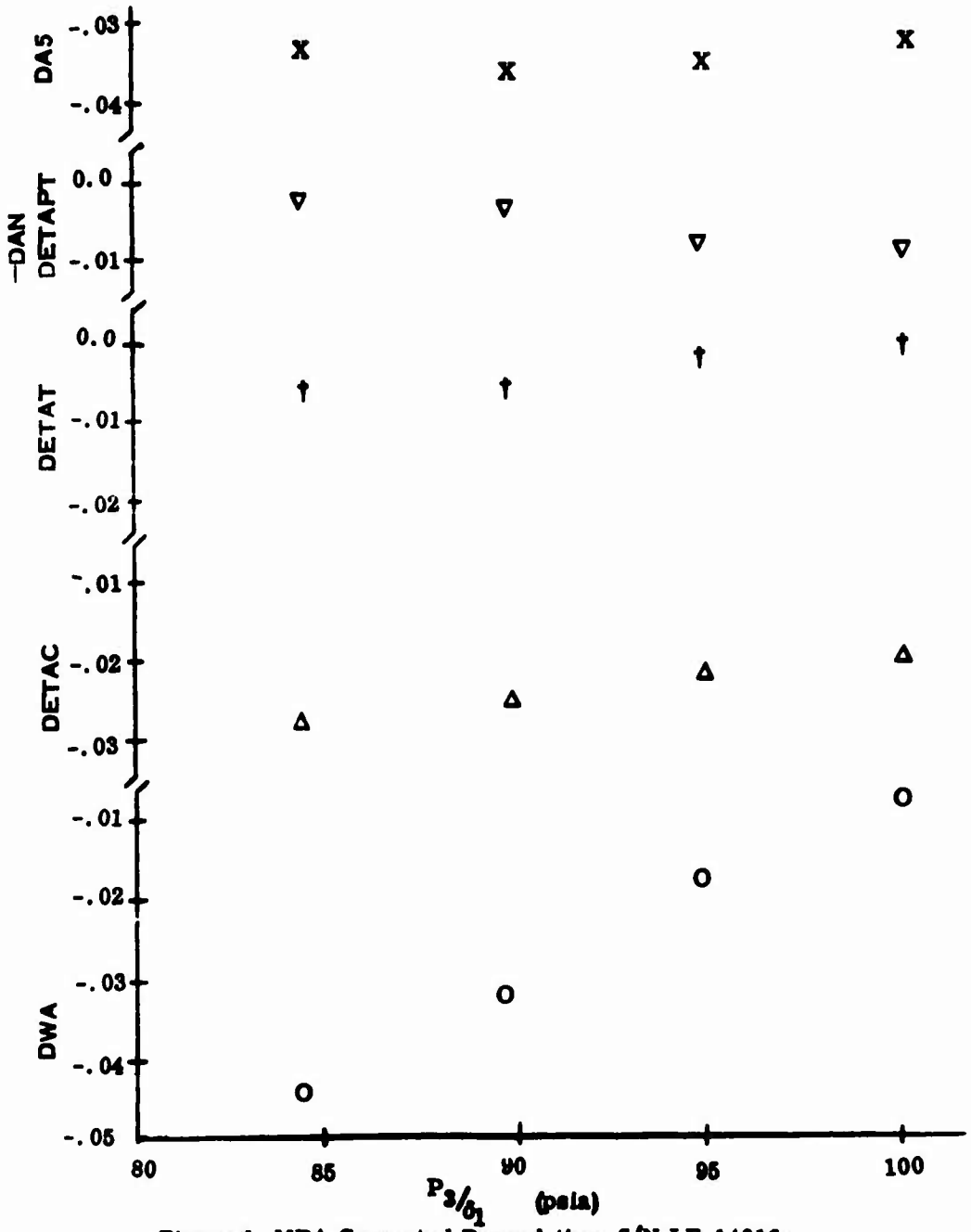

Figure 7. MPA Computed Degradations S/N LE-14016.

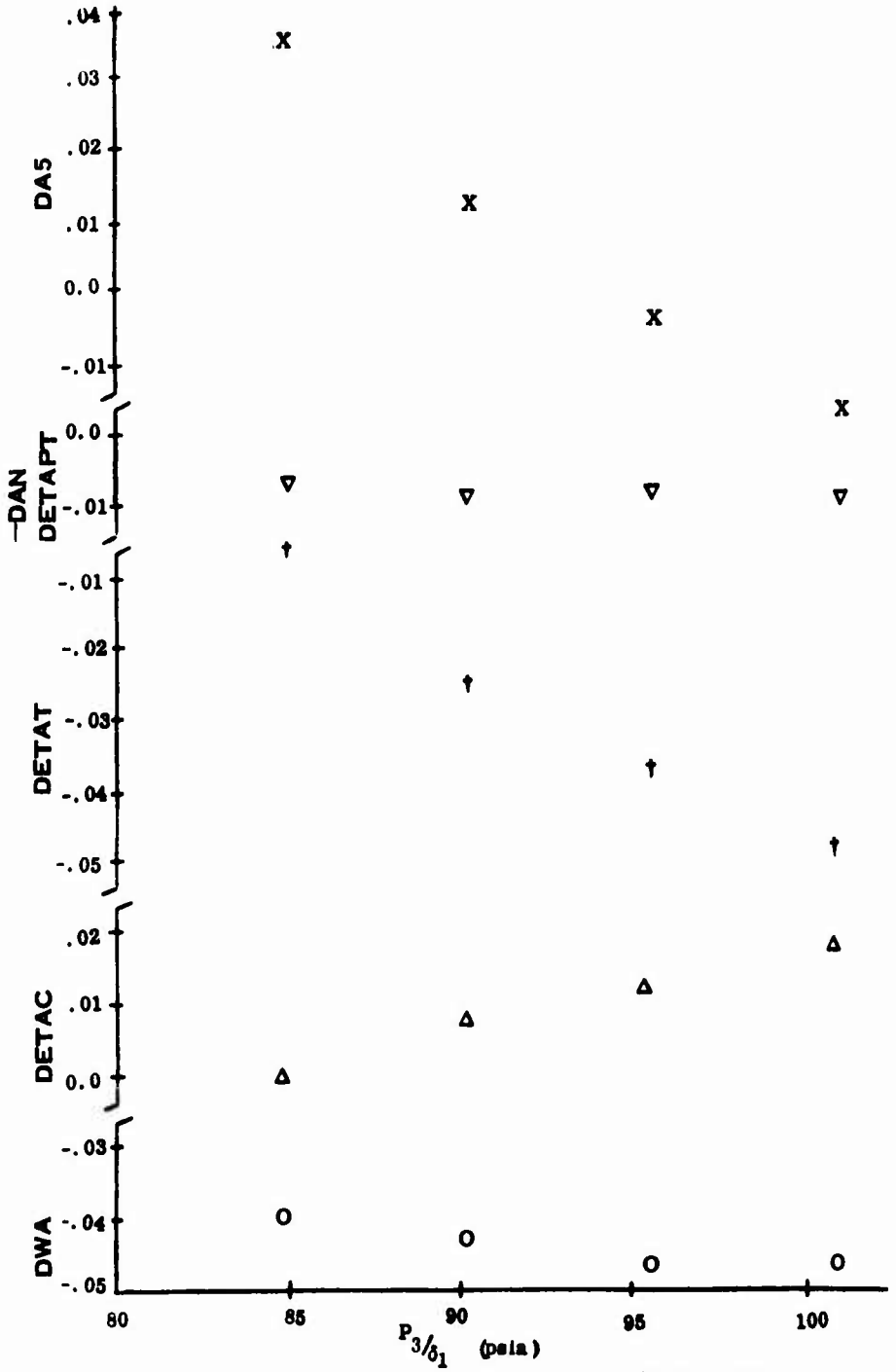

Figure 8. MPA Computed Degradations S/N LE-21304.

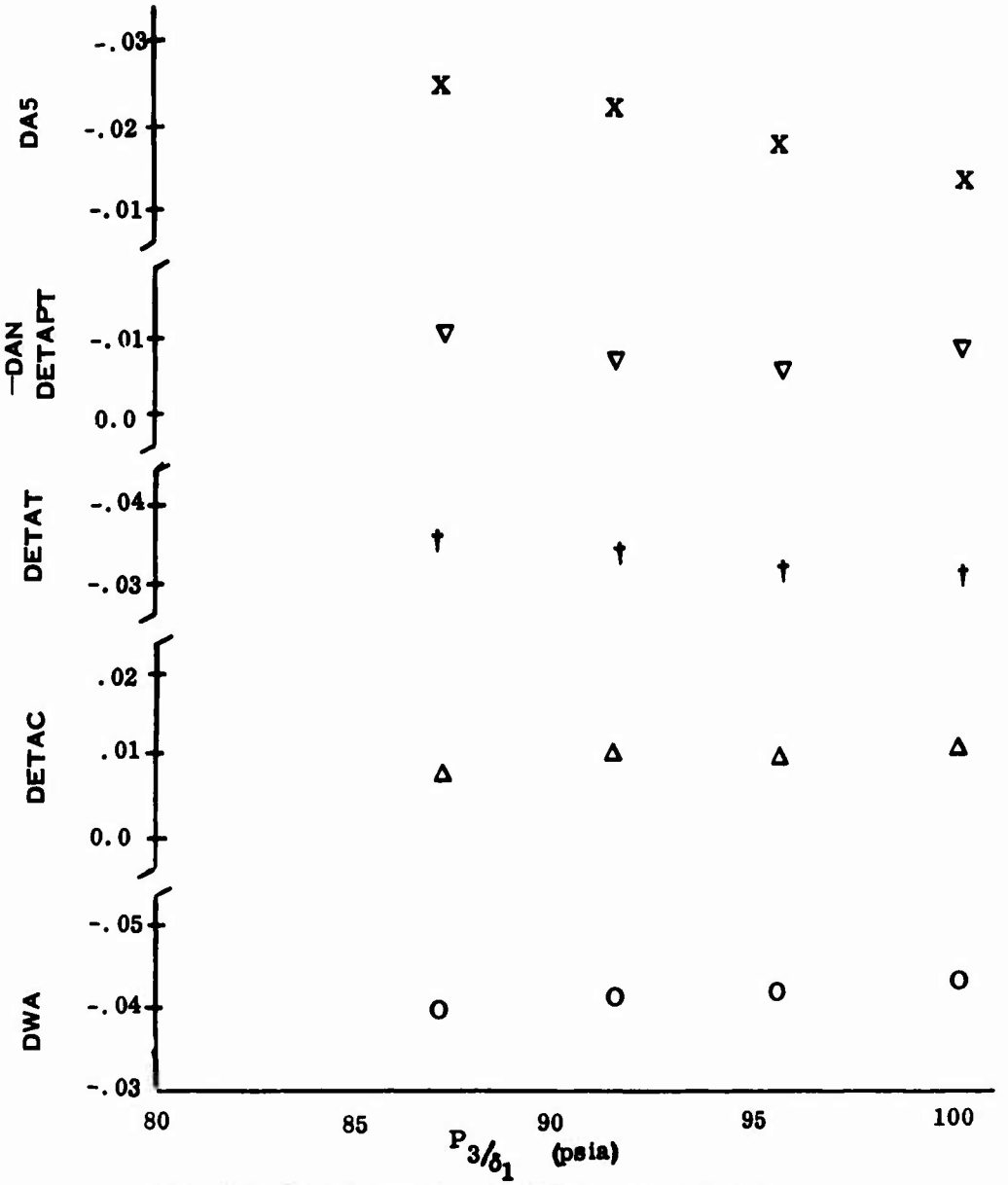

Figure 9. MPA Computed Degradations S/N K-125.

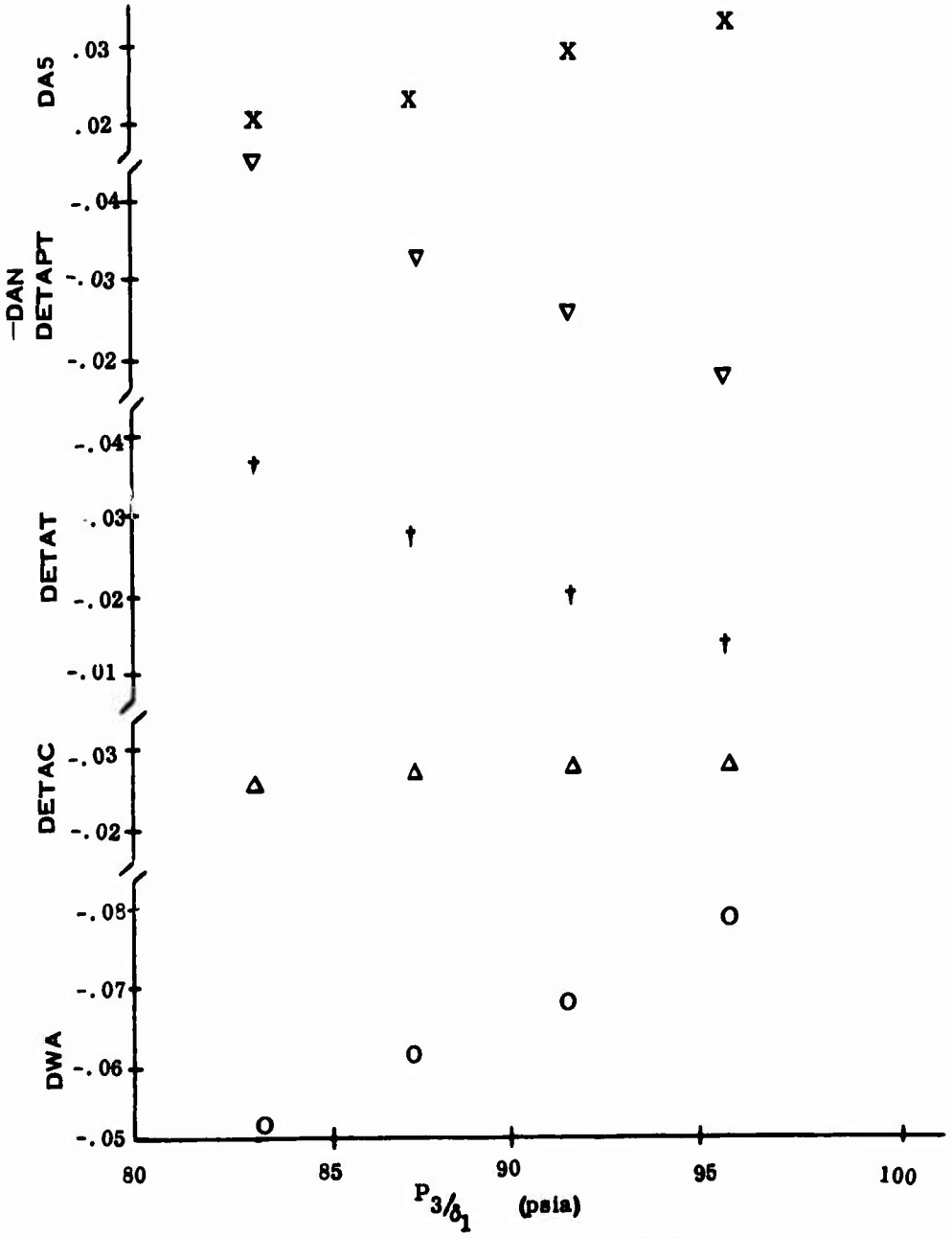

Figure 10. MPA Computed Degradations S/N K-117.

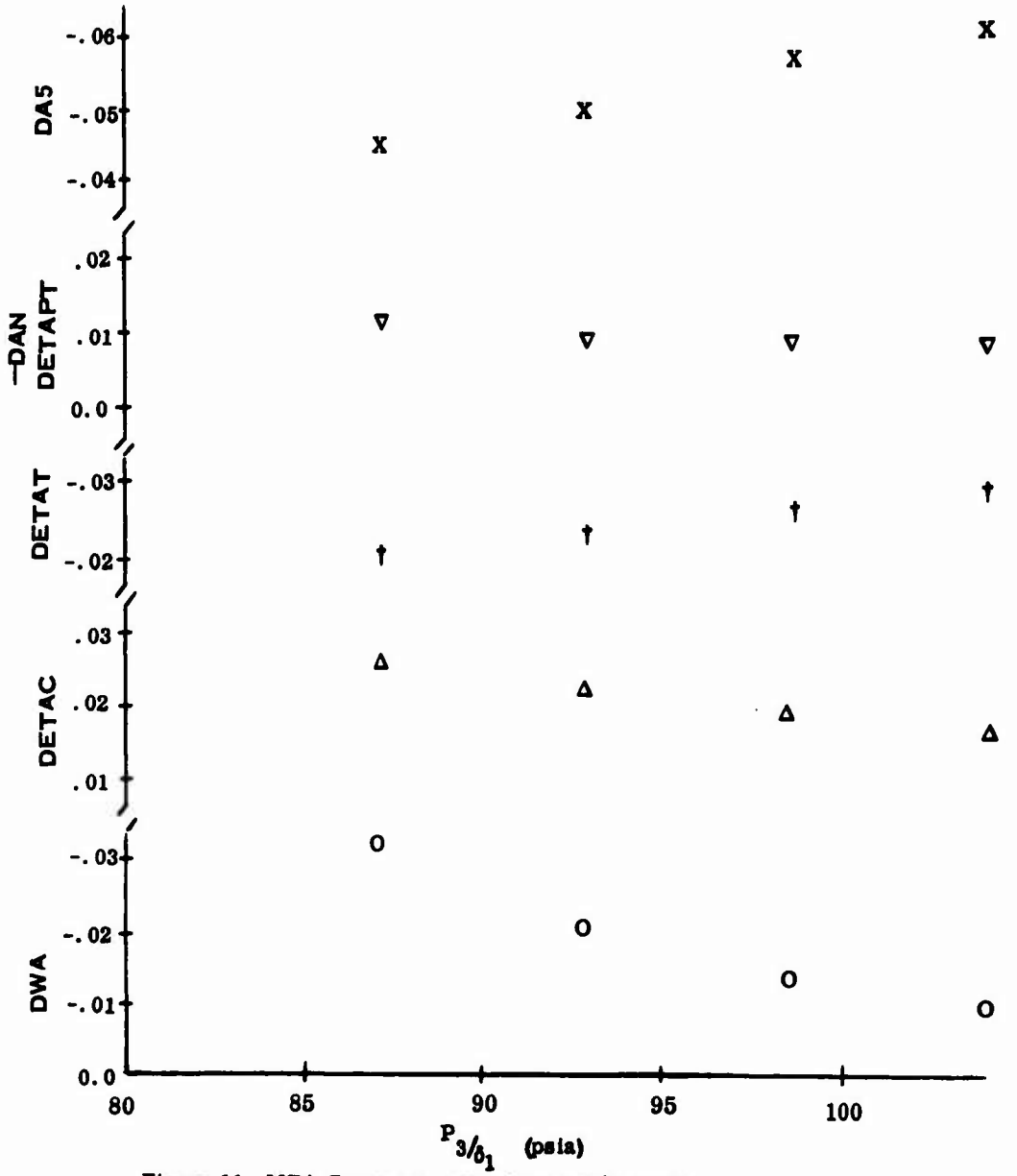

Figure 11. MPA Computed Degradations S/N K-116.

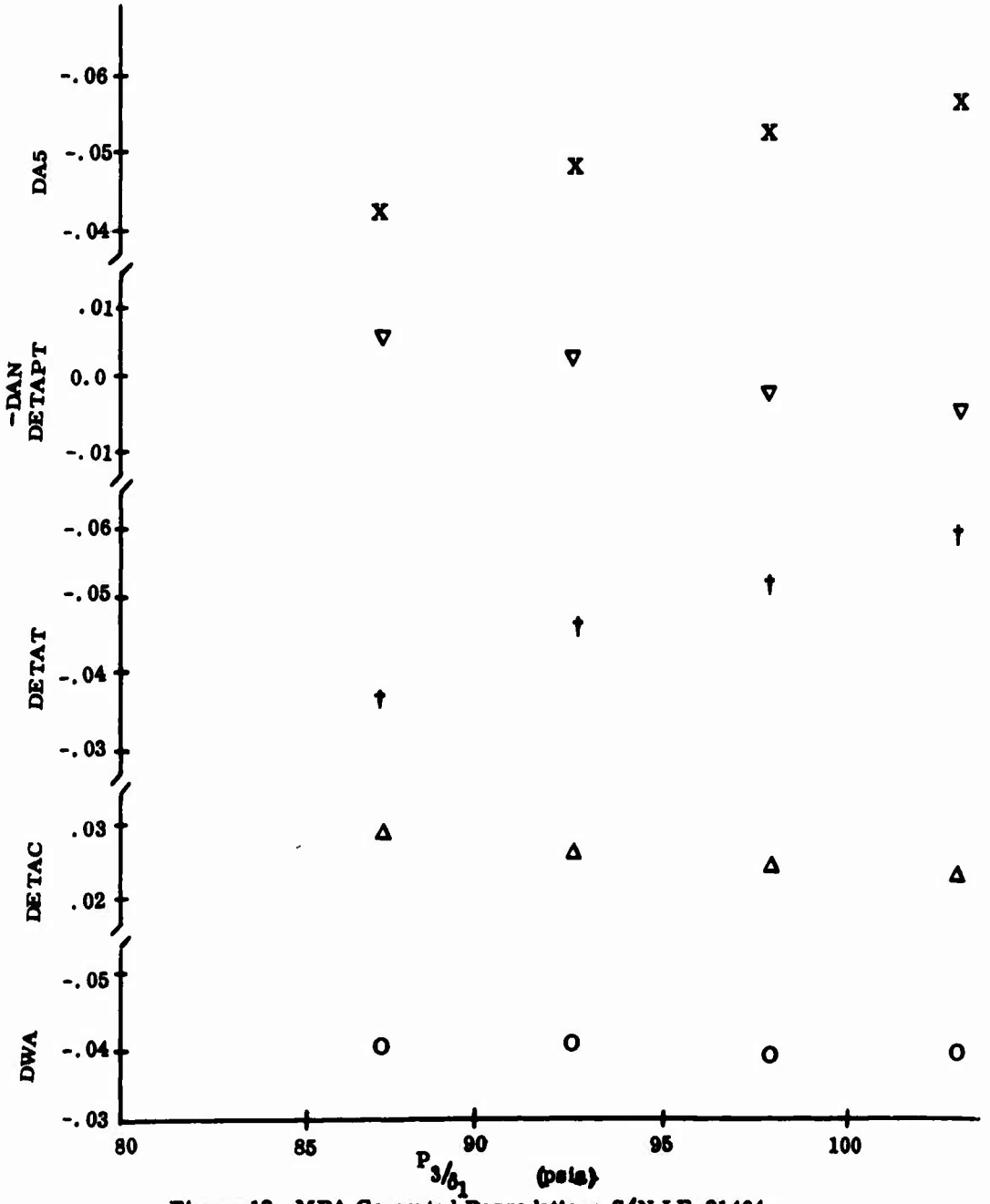

Figure 12. MPA Computed Degradations S/N LE-21404.

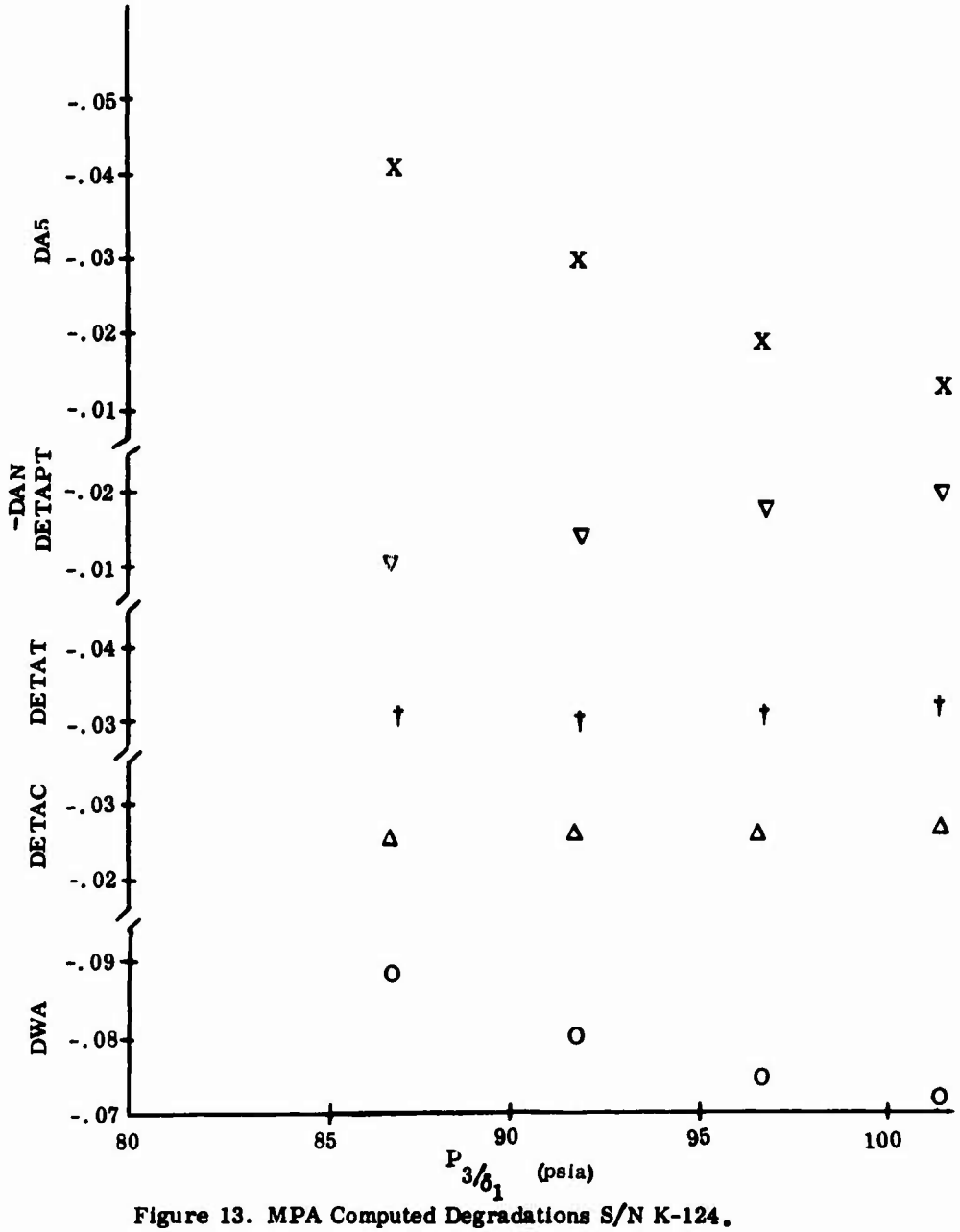

Figure 13. MPA Computed Degradations S/N K-124.

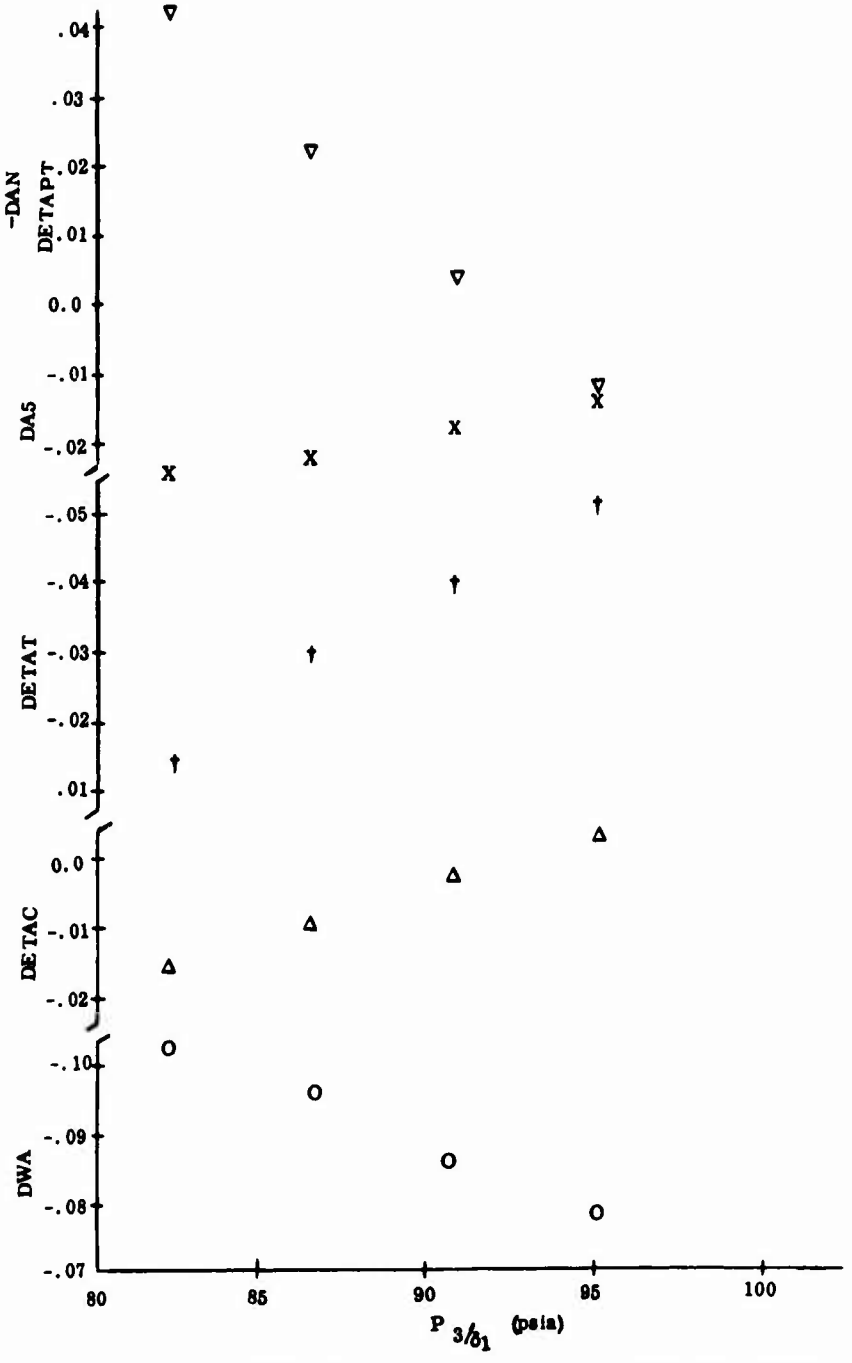

Figure 14. MPA Computed Degradations S/N LE-14083.

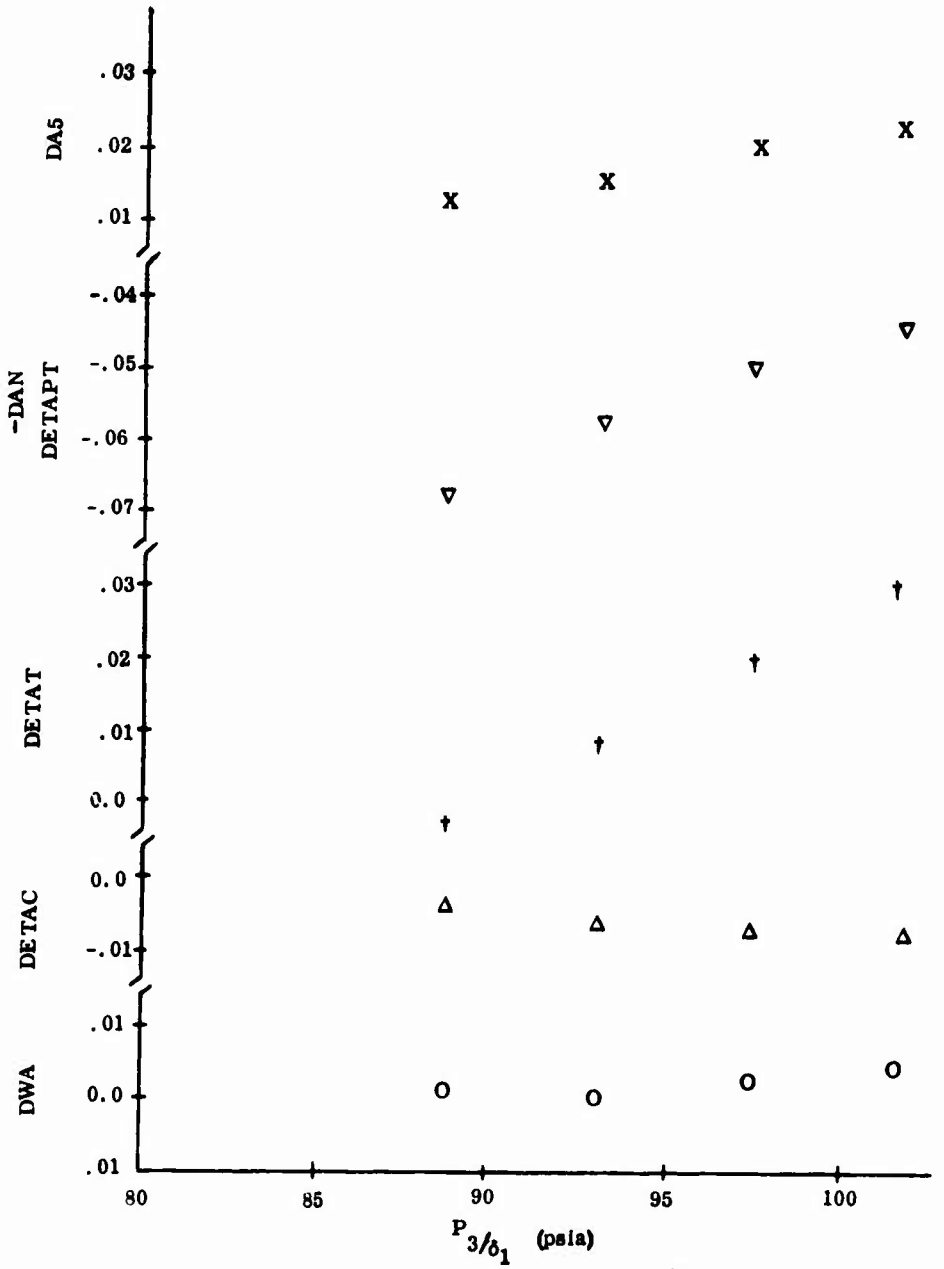

Figure 15. MPA Computed Degradations S/N LE-14018.

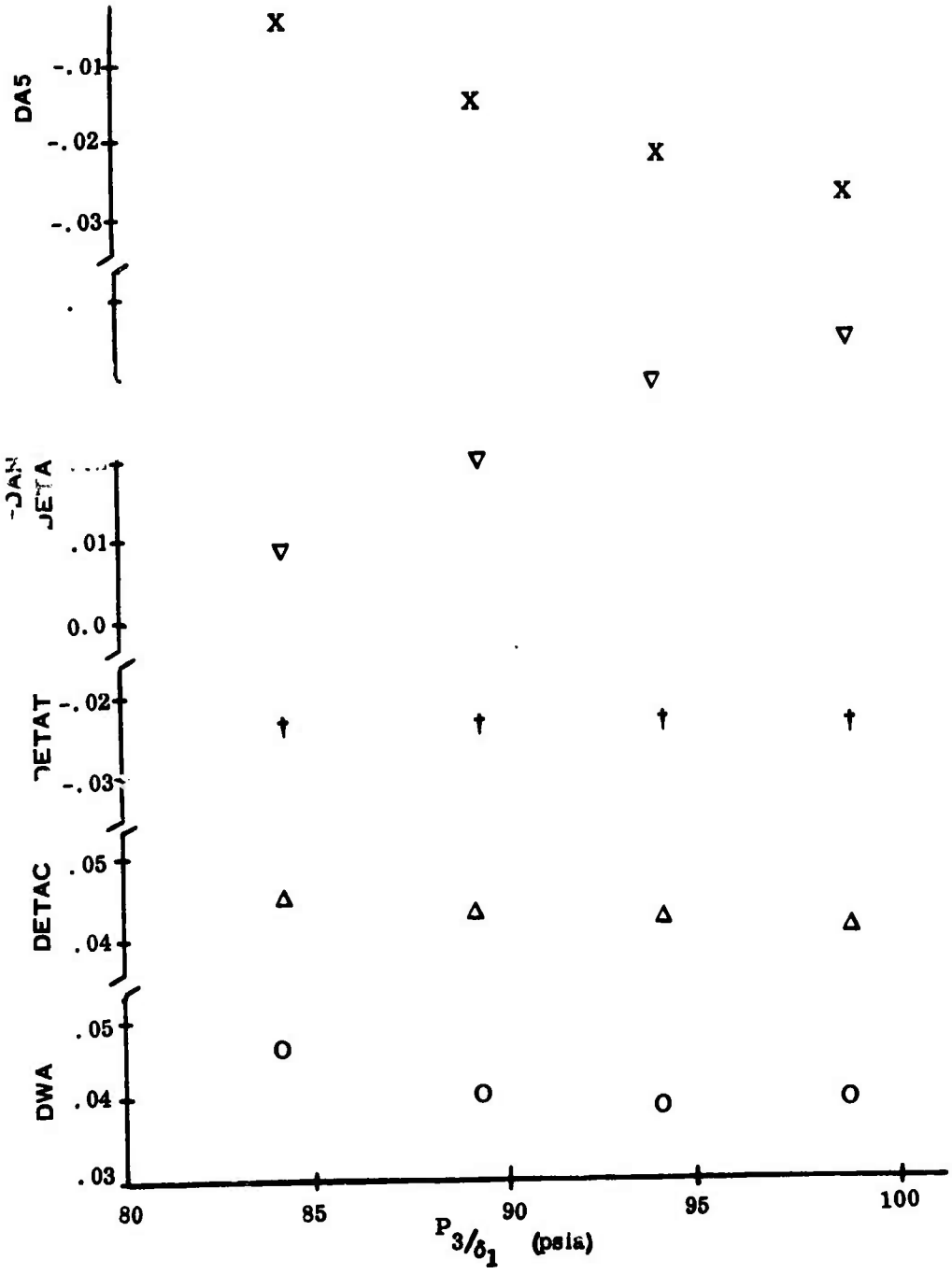

Figure 16. MPA Computed Degradations S/N K-144.

TABLE XVI. ALL ENGINES EVALUATED USING MEASUREMENT SETS AT 60% AND 70% POWER

S/N	Limit	Max HP	MPA Max HP	% Error
LE-14016	N_1	1390	1380	-0.7
	T_7	1411	1393	-1.3
	W_f	1422	1438	+1.0
LE-21304	N_1	1296	1304	+0.6
	T_7	1296	1271	-1.9
	W_f	1355	1348	-0.5
K-125	N_1	1303	1312	+0.7
	T_7	1198	1193	-0.4
	W_f	1314	1318	+0.3
K-117	N_1	1282	1262	-1.6
	T_7	1100	1080	-1.8
	W_f	1248	1234	-1.1
K-116	N_1	1342	1339	-0.2
	T_7	1438	1497	+4.1
	W_f	1395	1419	+1.7
LE-21404	N_1	1280	1295	+1.2
	T_7	1392	1425	+2.4
	W_f	1394	1419	+1.8
K-124	N_1	1258	1243	-1.2
	T_7	1175	1155	-1.7
	W_f	1290	1302	+0.9
LE-14083	N_1	1311	1339	+2.1
	T_7	1247	1204	-3.5
	W_f	1345	1393	+3.8

TABLE XVI. CONTINUED

S/N	Limit	Max HP	MPA MAX HP	% Error
LE-14018	N_1	1294	1262	-2.5
	T_7	1478	1421	-3.9
	W_f	1361	1331	-2.2
K-144	N_1	1502	1466	-2.4
	T_7	1445	1450	+0.4
	W_f	1530	1505	-1.6

TABLE XVII. ALL ENGINES EVALUATED USING MEASUREMENT SETS AT 60% AND 80% POWER

S/N	Limit	Max HP	MPA Max HP	% Error
	N_1	1390	1390	0.0
LE-14016	T_7	1411	1444	2.3
	W_f	1422	1439	1.2
	N_1	1296	1279	-1.3
LE-21304	T_7	1296	1250	-3.6
	W_f	1355	1347	-0.6
	N_1	1303	1319	1.2
K-125	T_7	1198	1198	0.0
	W_f	1314	1322	0.6
	N_1	1282	1293	0.9
K-117	T_7	1100	1094	-0.6
	W_f	1248	1271	1.8
	N_1	1342	1249	0.5
K-116	T_7	1438	1480	2.9
	W_f	1395	1415	1.4
	N_1	1280	1285	0.4
LE-21404	T_7	1392	1374	-1.3
	W_f	1394	1397	0.2
	N_1	1258	1258	0.0
K-124	T_7	1175	1122	-4.5
	W_f	1290	1277	-1.0

TABLE XVII. CONTINUED

S/N	Limit	Max HP	MPA Max HP	% Error
LE-14083	N_1	1311	1267	-3.4
	T_7	1247	1175	-5.8
	W_f	1345	1309	-2.7
LE-14018	N_1	1294	1303	0.7
	T_7	1478	1462	-1.1
	W_f	1361	1364	0.2
K-144	N_1	1502	1505	0.2
	T_7	1445	1441	-0.3
	W_f	1530	1547	1.1

TABLE XVIII. COMPARISON OF MPA ERRORS USING ACTUAL ENGINE DATA

S/N	Limit	MPA PREDICTION ERROR (%) Measurement at 60%	Measurement at 80%	Measurement at 60% & 70%	Measurement at 60% & 80%
	N_1	-1.6	-0.6	-0.7	0.0
LE-14016	T_7	-4.8	-0.1	-1.3	2.3
	W_f	0.4	0.9	+1.0	1.2
	N_1	3.4	0.6	+0.6	-1.3
LE-21304	T_7	0.4	-1.2	-1.9	-3.6
	W_f	0.6	-0.1	-0.5	-0.6
	N_1	-0.9	0.2	+0.7	1.2
K-125	T_7	-0.8	-0.2	-0.4	0.0
	W_f	-0.5	0.2	+0.3	0.6
	N_1	-5.3	-3.0	-1.6	0.9
K-117	T_7	-4.4	-2.2	-1.8	-0.6
	W_f	-5.8	-2.4	-1.1	1.8
	N_1	-1.3	0.1	-0.2	0.5
K-116	T_7	5.4	3.8	4.1	2.9
	W_f	2.3	1.6	1.7	1.4
	N_1	2.2	0.8	1.2	0.4
LE-21404	T_7	6.8	2.2	2.4	-1.3
	W_f	3.7	1.4	1.8	0.2

TABLE XVIII. CONTINUED

S/N	Limit	Measurement at 60%	Measurement at 80%	Measurement at 60% & 70%	Measurement at 60% & 80%
	N_1	-3.3	-1.5	-1.2	0.0
K-124	T_7	0.4	-2.5	-1.7	-4.5
	W_f	2.7	0.7	+0.9	-1.0
	N_1	9.6	3.1	+2.1	-3.4
LE-14083	T_7	-0.9	-2.6	-3.5	-5.8
	W_f	11.2	4.3	+3.8	-2.7
	N_1	-5.9	-2.3	-2.5	0.7
LE-14018	T_7	-7.1	-2.4	-3.9	-1.1
	W_f	-5.4	-1.8	-2.2	0.2
	N_1	-5.1	-1.9	-2.4	0.2
K-144	T_7	1.4	0.8	+0.4	-0.3
	W_f	-5.0	-2.3	-1.6	1.1

SYSTEM OPERATION

GENERAL

The MPA system hardware, consisting of an Electronic Unit (EU) and an Indicator Control Unit (I/CU), is designed to provide an accurate prediction of an engine's maximum power capability under its present deteriorated condition and under all ambient conditions. This objective is accomplished by utilizing engine sensor signals already provided by engine accessories or added specifically for this purpose, while the engine is operated on the ground at 50% or greater partial power. The MPAS will provide predicted engine maximum horsepower performance. The performance prediction utilizes a baseline engine performance characteristic preset into the EU at the time of installation of the new or overhauled engine.

Maximum power prediction will be available over a range of power lever angles of 50% to 100% coupled with an ambient temperature range of -60°F to 140°F, and ambient pressure range of 11 psia to 16 psia.

The MPA is specifically designed to accept ten Lycoming T53-L13 engine parameters ready for signal conditioning in the EU. These parameters are as follows:

1. Compressor Inlet Total Pressure (P_1)
2. Compressor Discharge Total Pressure (P_3)
3. Compressor Inlet Total Temperature (T_1)
4. Compressor Discharge Total Temperature (T_3)
5. Turbine Inlet Total Temperature (T_7)
6. Compressor Speed (N_1)
7. Turbine Speed (N_2)
8. Turbine Shaft Horsepower (SHP)
9. Fuel Mass Flow (Wf)
10. Fuel Temperature (Tf)

The ranges of measurement characteristics of the T53 engine are:

1. P_1: 11 psia to 16 psia
2. P_3: 50 psia to 110 psia
3. T_1: -60°F to 140°F
4. T_3: 210°F to 590°F
5. T_7: 640°F to 1340°F
6. N_1: 20K RPM to 25K RPM
7. N_2: 13K RPM to 22K RPM
8. SHP: 300 SHP to 1500 SHP

9. Wf: 350 pph to 800 pph
10. Tf: 40°F to 160°F

Capability to cover the characteristics of T53 engines out of this range exists, but at reduced system prediction accuracy.

To eliminate the need for retesting an engine to reestablish its baseline in the event of a removal of an EU, capability is included to permit the baseline characteristics of the engines to be transferred from the removed unit to the replacement unit without further engine testing. Similarly, engine sensors where practical are designed to be interchangeable to eliminate the need for retesting an engine to reestablish its baseline in the event of sensor failure. Calibration adjustment for the torque meter is provided to permit its replacement without further engine testing.

The MPA system also includes self-test capability. MPA built-in tests consist of continuous and pilot initiated checking of the sensor and EU functions. Readout of the self-test features is obtained by means of fault indicators (flags and lights) located on the EU and I/CU and a zeroed I/CU display.

OPERATION ON AIRCRAFT

Operation of the MPA system on the aircraft is controlled by the pilot through use of the Indicator/Control Unit (I/CU) switches: On/Off, Reset, and Mode Switch. Positions of the mode switch are identified as Test, Engine #1, Engine #2, and Total.

Depressing the power-on switch causes power to be applied to the I/CU and EU, resulting in all signal inputs being connected within the EU. Prior to engine startup, the display is blank at all mode positions except test. Rotating the mode switch to the test position causes an MPA value to appear in the digital display, which the pilot checks to verify the MPA program operation. The momentary operation of the digital display and fault light when switching into the test position checks the operation of the lights.

Following engine turn-on, with the engine at idle, the pilot must verify that engine power and bleed take-off are at known fixed settings.

To obtain an engine MPA, one frame of engine measurements is required from each engine at a 50% or greater PLA. Engines may be run simultaneously or individually. When engine steady-state conditions are reached, the engine frame indicator light on the I/CU will light to inform the pilot that the frame data has been obtained and that an MPA prediction for the engine is available.

The time required to achieve this steady-state, in fact, could be as long as 5 minutes if it were considered necessary to establish the most accurate long-term maximum power available. It is more likely, however, to be considered that the purpose of the MPA prediction is to inform the pilot of the short-term power availability for an emergency situation, and this time would be a matter of seconds. Some degradation in prediction accuracy would thus also be expected. The selection of either of these prediction criteria is preset into the EU and becomes an automatic process.

The mode switch position, Eng. #1, Eng. #2, and Total, causes the display to output the engine MPA's. The mode switch activates the Total display only if a prediction exists for both engines; otherwise it remains blank.

The display holds the MPA values, once obtained, and is not updated. To cancel an MPA for an engine, the mode switch is set to the engine number and the reset switch depressed. The MPA engine operating procedure described earlier must again be carried out to get the new MPA.

The off-switch is used to turn the system power off and clear the MPA display.

If during MPA operation, the fault light illuminates steadily, this indicates that either the EU or sensors or their wiring is defective. The cause of the malfunction is also indicated: An all zero MPA for all engines indicates an EU failure; a zero engine MPA indicates a failure of an engine sensor.

In the event of a loss of an engine MPA prediction, the pilot can estimate total helicopter MPA simply by doubling the MPA of the other engine. This technique would ensure continued MPA system operation although at reduced accuracy.

A back up baseline is provided within the EU to insure continued MPA operation, if a custom baseline could not be acquired because of, for example, helicopter operational problems.

BASELINE ACQUISITION

Engine baseline characteristics must be preset into the EU at the time of installation of a new or overhauled engine on the aircraft. For this purpose, the EU output provides the control and sensor digital data for the baseline acquisition equipment. The baseline acquisition and processing system block diagram shown in Figure 17 illustrates the major elements of this system. The EU interfaces directly with a magazine tape recorder which is used to store corrected engine run or with an MTU for manual recording of the engine data. In either case, the data is used in

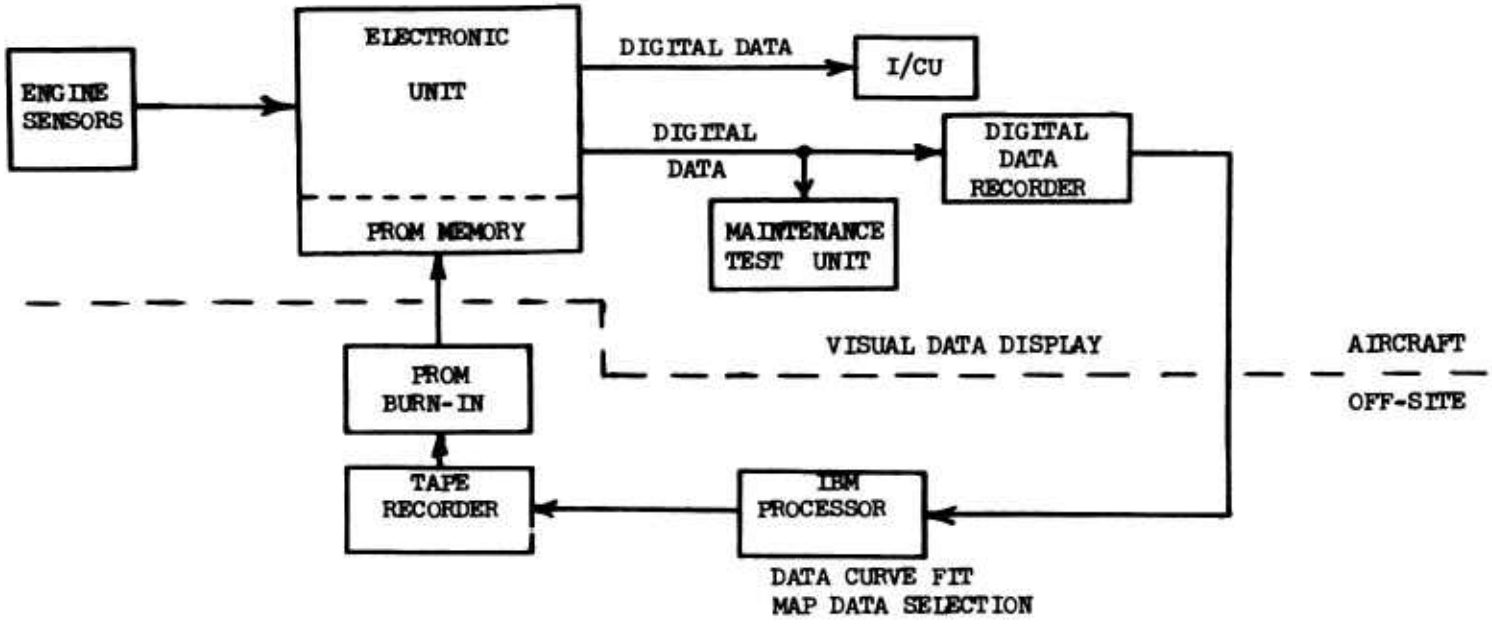

Figure 17. MPA Engine Custom Baseline Acquisition Block Diagram .

an off-site processor to manipulate the data to baseline requirements. The processor tape output is used to store the baseline data in PROM memory for eventual insertion into the EU. This tape may be preserved to permit data programming the PROM memory in the event of a malfunction of the baseline PROM memory.

BASELINE TRANSFER

From a system feasibility standpoint, it is highly desirable that the validity of the store engine baseline be independent of any malfunction that may occur in the MPA hardware.

In the event of engine sensor failures, the continuing validity of the baseline data depends upon the unit-to-unit repeatability between the replaced and replacing sensors. All MPA sensors are designed to be interchangeable. This permits sensor replacement without engine retesting for a new baseline. In the event of a replacement of a mass flow meter, the PROM chip storing temperature compensation must also be replaced in order to preserve the mass flow baseline. In the event of a replacement of the torque sensor, provisions are made in the EU to adjust the new sensor output to the stored torque sensor calibration curve in the EU memory. Discussion of the torque sensor calibration technique is presented in the next section of this report.

In the event of a replacement of an EU, the stored baseline and mass flow temperature compensation PROMs must be removed and placed in the new unit. In addition, calibration of the torque sensor output in the new unit must be done.

CALIBRATION

There are two distinct situations that require that the MPA system be subjected to some type of calibration procedure to provide assurance that the system will function in the intended manner. These situations are: (1) bench testing, either at the completion of the manufacturing cycle or following repairs, and (2) on the aircraft, following repair of the EU or torque sensor.

1. Calibration During Bench Testing

   During bench test, the EU can be tested to provide assurance that the EU signal conditioning accuracy is as specified. To accomplish this, a maintenance test unit (MTU) is used to provide variable resistances, millivolt signals and frequency signals simulating the normal input extremes of the sensors.

1. (continued)

   At this time the torque sensor and EU combination can also be checked for calibration. To accomplish this calibration, the strain gauged shaft is subjected to deadweight testing and the EU output is adjusted so that the digital output load agrees with the test load torque input.

2. Calibration on the Aircraft

   Calibration of the torque sensor on the aircraft, following a replacement of an EU or a torque sensor, can be accomplished accurately and routinely with engines nonoperating, using calibration shunts or strain gauges located on the torque shaft.

   In these techniques the calibration circuit is set up during the initial deadweight calibration of the torque sensor shaft. When the test signal from the torque sensor's calibration circuits is connected to the EU, the zero and gain of the signal amplifier are adjusted to obtain the full load torque reading on the MTU. The torque sensor is then ready for use, and has the required accuracy. Using this method, the torque sensor shaft and rotating transformer may be replaced with no requirement for load test equipment. Deadweight calibration during overhaul can check the accuracy of the test signal.

IMPLEMENTATION REQUIREMENTS

Implementation of an MPA system within the operating structure of a helicopter requires six major steps:

1. Application Study
2. Hardware and Software Specifications
3. Hardware Selection/Sensor Development Testing
4. Engine Performance and Control Data Program
5. Hardware Maintenance Support Program
6. Design, Development, Fabrication and System Evaluation

APPLICATION STUDY

The application study defines the scope of the application. It involves a joint effort of the procuring agency, engine manufacturer, and selected system contractor to determine or define the integration problems, the on-board sensors, the ability to share sensors, the modification, and additional MPA sensor which must be provided. The application study must also be extended to consider other uses for MPA, such as hover lift computer, to allow for building in the capacity to later add or extend to this capability.

HARDWARE AND SOFTWARE SPECIFICATIONS

Responsibility for each system sensor must first be defined. The MPA system vendor must be allowed to write MPA sensor specifications in order to meet MPA system requirements. Should the responsibility for multi-use MPA sensors be placed with another vendor (e.g., engine manufacturer), the MPA vendor should be allowed to assist in the sensor definition.

The MPA system vendor must write the EU and the I/CU detailed specifications based upon the procurement agency specification. These detailed specifications are required to insure that the accuracy, reliability, interchangeability, and maintainability requirements are met.

HARDWARE SELECTION/SENSOR DEVELOPMENT

Upon completion of the sensor specifications and submittal of these specifications to prospective vendors, the MPA system vendor must then review the various sensor proposals and select the best sensor in terms of accuracy, cost, reliability, etc. This sensor selection process may require the MPA system vendor to procure sample sensors and perform an evaluation test.

If the proposed MPA system installation utilizes an advanced engine fuel control system with state-of-the-art sensors, these sensors may meet the MPA sensor accuracy requirements. Therefore, further sensor development may not be necessary.

The MPA electronic system configuration and component selection will be predicated by the MPA system procurement and the detailed system specifications. Established design concepts and production components will be utilized wherever possible to minimize program cost.

ENGINE PERFORMANCE AND ENGINE CONTROL DATA PROGRAM

The MPA system is characterized to a particular engine type through the MPA power algorithm firmware. To generate this algorithm, the engine manufacturer must provide a complete set of engine internal performance data and the engine control characteristics, including droop line and engine performance limits. The data for the algorithm is based on an average performance of many engines over the idle to 100% engine PLA.

HARDWARE MAINTENANCE SUPPORT PROGRAM

A major implementation step for MPA includes the development of a maintenance test unit (MTU) to provide for maintenance support of MPA electronics and for baseline data acquisition. As MPA may well be a future dispatch and landing requirement for helicopter safe flight, maintenance support for MPA will receive top priority.

DESIGN, DEVELOPMENT, FABRICATION, SYSTEM TEST EVALUATION

The above functions combine several major implementation steps performed by the system vendor with the end result being demonstration of system design and performance compliance. Operations performed by the vendor include:

1. Design and checkout of signal conditioning hardware.

2. Integration and checkout of sensors with signal condition hardware.

3. Prepare software including:

   a. Storage of standardized sensor calibration and systematic error compensation curves in computer memory.

   b. Development and storage in computer memory of MPA engine power algorithm.

   c. Curve fitting and storage in computer memory of baseline engine data and backup baseline.

   d. Self-test.

4. Fabricate Demonstration System.

5. Engine Demonstration Test Program.

6. Qualification Testing.

SYSTEM EQUIPMENT DESCRIPTION

SYSTEM COMPONENTS

A maximum power available system suitable for helicopter operation, consists of three major components:

1. Engine Sensing Instrumentation
2. Electronic Unit (EU)
3. Indicator and Control Unit (I/CU)

ENGINE SENSING INSTRUMENTATION

Ten sensors per engine are required to monitor the engine parameters (pressures, temperatures, engine speeds and horsepower) to enable the objectives of the MPA to be achieved. The sensor outputs must be stable with respect to environmental variations such as temperature, vibration and shock over protracted periods between calibration. Sensor outputs are channeled via wire harnesses directly to the Electronic Unit. The characteristics of the sensor/EU interfaces are summarized in Figure 18.

Table XIX summarizes the required ten MPA sensors and their accuracies for the T53 engine measurement range. Except for the torque sensor, these accuracies are the best obtainable from sensors which are interchangeable without further calibration. The accuracies are achieved through computer compensation to eliminate all systematic (fixed) errors associated with each sensor type. Custom temperature compensation is provided for the pressure and mass flow measurements. Custom compensation for unit-to-unit variation is provided for the torque sensor.

ELECTRONIC UNIT (EU)

The primary functions of the EU for the MPA are:

1. Provide calibration standardization of the engine sensing instrumentation output scale factors (electrical output versus electrical input).

2. Provide calculation of the MPA from the engine sensor outputs according to the Gas Path Analysis Technique and output digital MPA to the I/CU display.

The secondary functions performed by the EU are system self-check and signal conditioning for baseline acquisition.

TABLE XIX. T53 ENGINE MPA INSTRUMENTATION ACCURACY REQUIREMENTS

Sensor	Span of Measure Min	Max	Sensor Type	Sensor Accuracy	Conditioning Accuracy	Total Accuracy
N_1	20 K rpm	25 K rpm	Pulse Pickup[1]	± .000	± 1.8 rpm	± 1.8 rpm
N_2	13 K rpm	22 K rpm	Pulse Pickup[1]	± .000	± 1.52 rpm	± 1.52 rpm
T_1	-60°F	140°F	Plat. Resistance[3]	± .74°F	± .99°F	± 1.73°F
T_3	210°F	590°F	Plat. Resistance	± .64°F	± 1.9°F	± 2.00°F
T_7	640°F	1340°F	Thermocouple 2)	± 3.9°F @ 640°F	± 2.4°F	± 4.6°F
				± 5.9°F @ 1340°F		± 6.4°F
P_1	11 psia	16 psia	Vibr. Cylinder[1]	± .009 psia	± .006 psia	± .011 psia
P_3	50 psia	110 psia	Vibr. Cylinder[1]	± .01 psia	± .059 psia	± .06 psia
SHP	300 shp	1500 shp	Strain Gauge[4] Torque Meter	± 11.7 shp	± 7.95 shp	± 14.1 shp
Wf	350 pph	800 pph	Mass Flow 1) Transmitter	± 7.3 pph @ 800 pph	± .5 pph	± 7.31 pph
				± 3.2 @ 350 pph	± .2 pph	± 3.21 pph
T_f	40°F	160°F	PLATINUM RESISTANCE	± 4.0°F	± .99°F	± 4.1°F

NOTES: 1) Based on 2 Mhz clock, 50 PPM accuracy, 120 period counter, 60 gear teeth
2) Special Grade Thermocouple
3) With De-icing Capability
4) With Custom Calibration; After Gear Reduction

1. PULSE PICKOFF

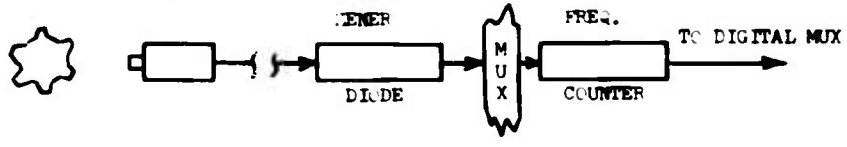

2. PLAT RESIS.

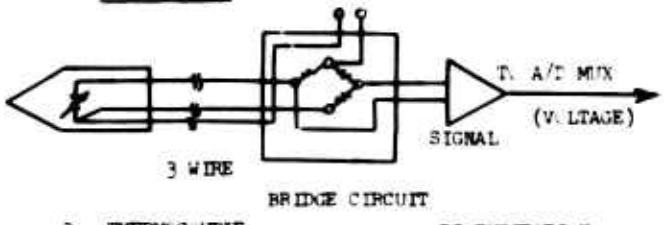

3. THERMOCOUPLE

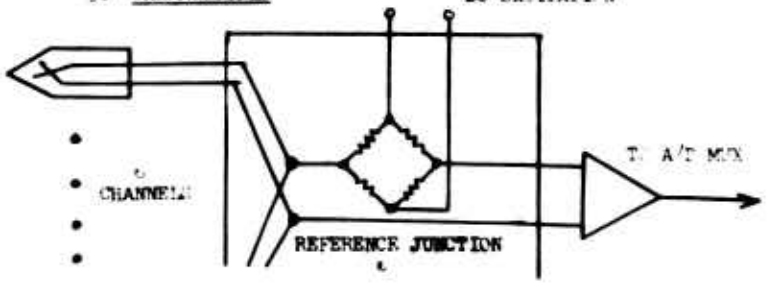

4. PRESSURE

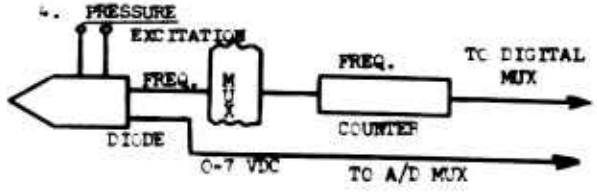

5. TORQUE

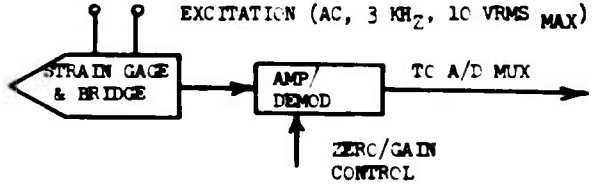

6. MASS FUEL FLOW TRANSMITTER

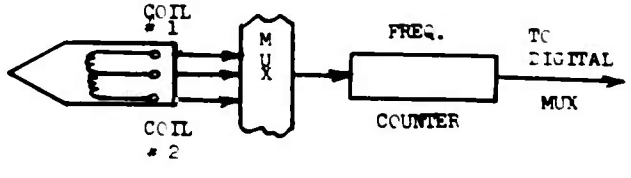

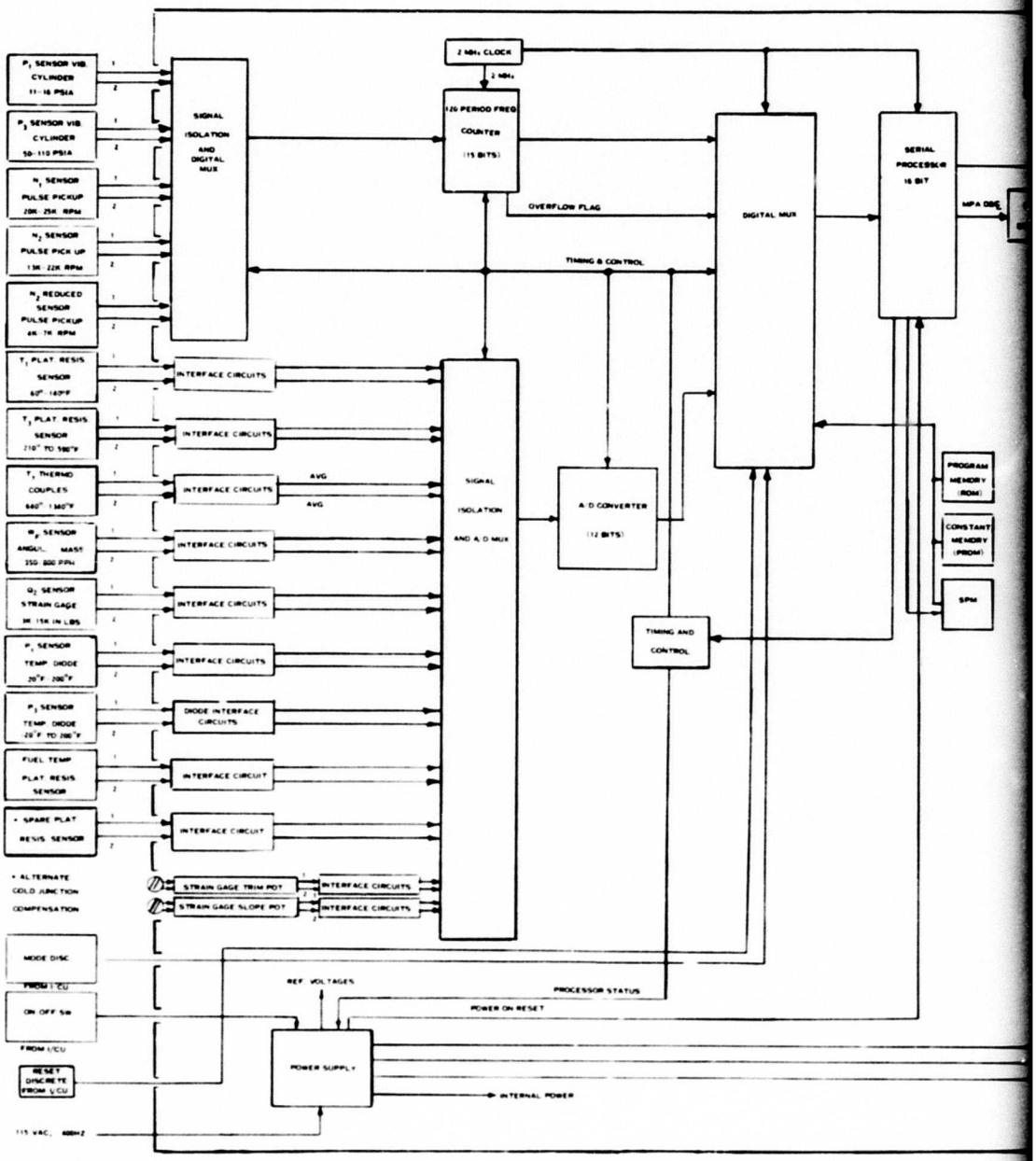

Figure 19. MPA EU Block Diagram (Twin Engine)

B

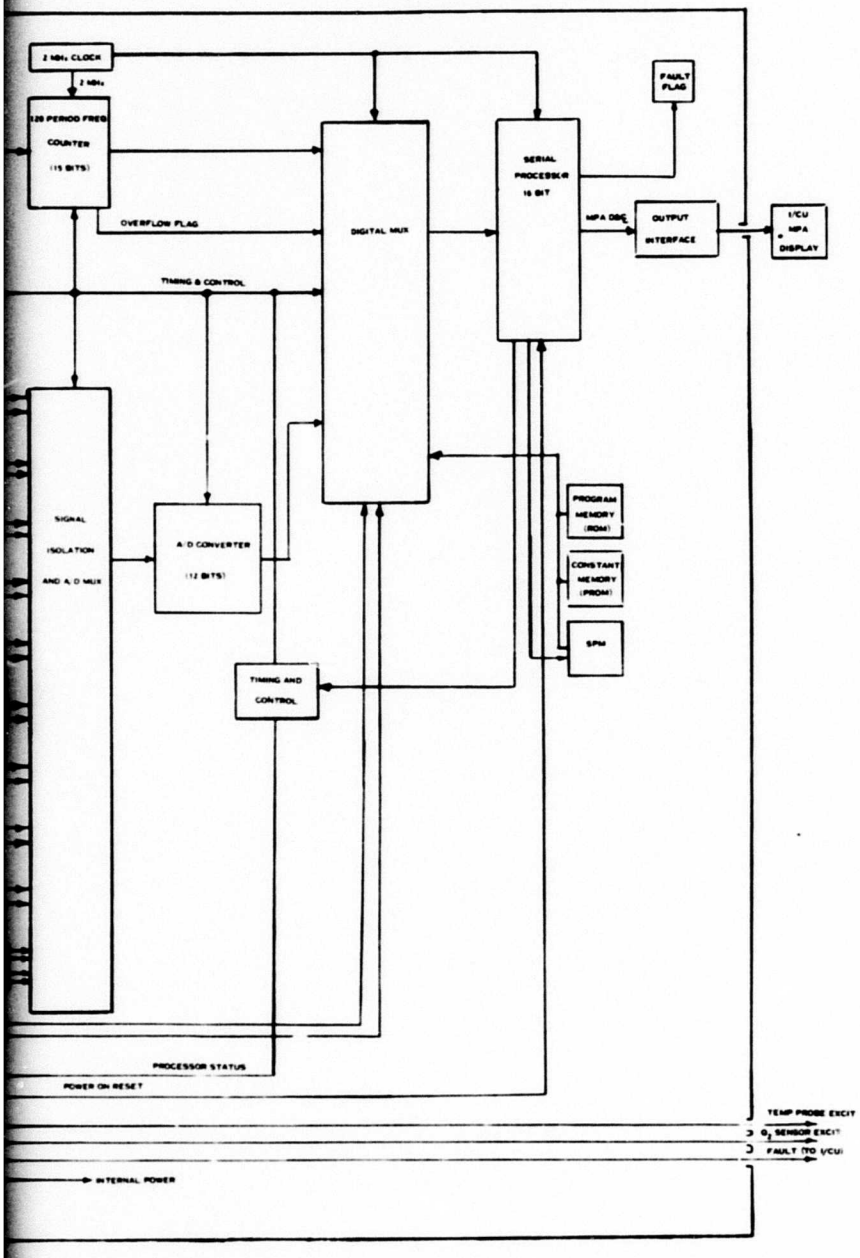
2 MHz CLOCK
2 MHz
320 PERIOD FREQ COUNTER (15 BITS)
OVERFLOW FLAG
TIMING & CONTROL
DIGITAL MUX
SERIAL PROCESSOR 16 BIT
FAULT FLAG
MPA DRC
OUTPUT INTERFACE
I/CU MPA DISPLAY
SIGNAL ISOLATION AND A/D MUX
A/D CONVERTER (12 BITS)
PROGRAM MEMORY (ROM)
CONSTANT MEMORY (PROM)
SPM
TIMING AND CONTROL
PROCESSOR STATUS
POWER ON RESET
TEMP PROBE EXCIT
O_2 SENSOR EXCIT
FAULT (TO I/CU
INTERNAL POWER

The functional modules of the EU are:

1. Signal Isolation and Selection Section
2. Signal Conditioning and Digitizing Circuit
3. Processor I/O
4. Processor Memory
5. Sensor Section
6. Power Supply

The signal isolation and selection section is responsible for ensuring that sensor signals are monitored on a noninterference basis and to allow signal selection at prescribed times, thus enabling time/sharing of the signal conditioning and digitized circuits.

The signal conditioning section is responsible for conditioning the generic types of signals to some common form to enable digitization.

The processor I/O section is responsible for the transfer of data into and out of the processor, typically digitized signal inputs and digital data outputs to the MPA display.

The processor and memory section are responsible for control of the data collection and analysis of this data. Based on this analysis, it provides relevant outputs to the Indicator/Control Unit (I/CU). The EU Sensor Section is responsible for housing the pressure sensor and thermocouple cold junction references.

The power supply provides all circuit voltages, excitation for strain gauges and temperature sensors, and an accurate reference voltage for the A/D Converter.

As shown in Figure 19, the EU hardware block diagram, the EU is broken down into several subfunctions which consist of the following.

Input Circuits

Various circuits and converters are required in order to properly manipulate the raw engine measurements to a form that the processor can properly act upon.

Signal Conditioning Interface Circuits

Figure 18 details the six basic sensor interface circuits which are signal conditioned within the EU. These circuits are:

Magnetic Speed Sensing Interface Circuit

The magnetic pickup speed sensor converts engine shaft speed into a single electrical pulse train signal. This is accomplished by using the motion of shaft-mounted magnetic gear teeth to generate a voltage pulse in the pole piece at the end of the pickup. The voltage generated is limited by the zener diode to a level compatible with the frequency input counter. The frequency input counter counts 120 pulses of input and outputs a digital count inversely proportional to the angular shaft speed.

Platinum RTP Interface Circuit

The platinum resistance temperature probe converts gas temperature into a precise resistance change causing an unbalance in the bridge circuit and a voltage output in proportion to the temperature. A three-wire bridge is used to compensate for resistance changes of the long connecting wires between the probe and bridge.

Thermocouple Interface Circuit

The six parallel thermocouple outputs through the engine harness are joined at the reference junction to provide an average T_7 measurement. By integrating copper leads with the reference junction, the thermocouple material is not connected to the input terminal of the amplifier, thereby eliminating secondary errors. An electrical bridge network is used for reference junction temperature change compensation to within $\pm$ 1.0^{o}F.

Pressure Sensor Interface Circuit

The frequency interface circuit used to condition the speed sensor and the fuel flow sensor is used also for the vibrating cylinder type pressure sensor. In addition to its digital pressure output, the vibrating cylinder outputs a 0-7 V signal depending on the pressure sensor temperature from a temperature sensing diode imbedded in its base. The digital computer uses the temperature sensor output to compensate the pressure sensor digital pressure output for the effect of temperature over a range of -65^{o}F to +265^{o}F. The pressure and pressure temperature characteristics are incorporated on a memory chip mounted with each pressure transducer. The transducer required excitations are +15 VDC, -15 VDC, and +7 VDC.

Torque Sensor

The torque sensor is of the integral strain gauge transformer type.

The strain gauge signal is passed from the torsion shaft, through the rotating transformer to a signal amplifier. It is then demodulated to obtain a DC signal directly proportional to the shaft torque. The torque sensor excitation is 10 VRMS, maximum; its nominal full scale output is 0.75 mv/volt of excitation.

Mass Fuel Flow Transmitter Interface Circuit

The transmitter converts fuel flow into two electrical signals. This is achieved by using the mass of the flowing fuel to create proportional angular displacement between two continuously rotating magnets. These magnets, which are driven by a fuel driven motor, induce pulses in two stationary coils. The time differences between the pulse induced in coil number 1 by magnet number 1 and the pulse induced in coil number 2 by magnet number 2 is a measure of the mass flow. The signal conditioner converts the two phased displaced signals into a digital signal proportional to the time separation between the two output signals from the transmitter.

Table XX summarizes the characteristics of the sensor signals provided by these circuits.

Frequency to Digital Converter Inputs

There are 12 separate frequency signals which are converted directly to digital information with a frequency to digital converter. This consists of a 2 MHz clock, a 15 bit counter, and a zero detector. The counter is enabled for 120 periods of the signal. The counter signals represent all the engine speeds, pressures, and engine fuel mass flow measurements.

Analog to Digital Converter Inputs

There are 14 separate analog inputs which are conditioned and transmitted to the analog multiplexer ready to be sampled by the analog to digital converter. The signals include all the engine temperatures, pressure sensor temperator, fuel temperature and torque. The A/D converter uses the successive approximation approach with 12 bits of conversion accuracy. The digital information from the A/D, together with the counter data, overflow memory, and discrete information, is fed into the digital multiplexer.

Multiplexer Inputs

A 12- and 14-channel multiplexer under control by the processor is

TABLE XX. MPA INTERFACES WITH SENSOR - QUANTITIES INDICATED ARE PER ENGINE

1. Variable Frequency Pressure Sensor Inputs (2)

Signal Source: Electronic Unit (EU) excited
Ranges: 0-20 psia; 0-250 psia
Excitation: 12 VDC provided by EU.
Configuration: Sensor location to be within EU.

2. Parallel Thermocouple Temperature Sensor Input (1)

Signal Source: Chromel-Alumel Thermocouple Probe
Range: 27 MVDC - 54 MVDC (640°F to 1340°F)
Scaling: Approximately 0.04 mv/°C (reference NBS thermocouple tables for actual calibration)
Configuration: 6 Parallel Thermocouples
Chromel-Alumel extension leads incorporated as part of installation.
Cold junctions and cold junction compensation to be provided by EU.

3. Resistance Temperature Sensor Inputs (3)

Signal Source: Platinum Resistance Probe
Signal Range: 396Ω to 620Ω (400°R to 600°R)
695Ω to 1090Ω (670°R to 1050°R)
509Ω to 640Ω (500°R to 620°R)
Excitation: Regulated voltage source provided by EU
Configuration: 3 wire probe installations

4. Magnetic Speed Sensor Inputs (3)

Signal Source: Electromagnetic tooth-rotor tachometer
Signal Range: 0-45V P-P
N_1 20K rpm to 25 K rpm
N_2 13K rpm to 22 K rpm
N_2 red 4 K rpm to 7 K rpm
Excitation: none, self-generating
Output Impedance: 144Ω

5. Mass Flow Sensor Input (1)

Signal Source: Flow Rate Transmitter, pulse difference
Signal Range: 0-5V
Excitation: None, self-generating

TABLE XX. CONTINUED

6. Torque Sensor Input (1)

Signal Source: Strain Gauge Torquemeter
Signal Range: 98,000 - 480,000 lb - in.
Excitation: 28 VDC

7. Pressure Sensor Correction Temperature Sensors (2)*

Signal Source - Diode
Signal Range - 0 - 7V (-65°F to 265°F)
Excitation - Constant Current
Configuration - Sensor location to be base of temperature sensor

*Non-engine sensor

used to channel the frequency and analog signals respectively into the single input counter and A/D converter. The multiplex switches interrogate the frequency inputs at typically 33 channels per second with a 30 millisecond per channel dwell; the analog signals are typically interrogated at the rate of 200 samples per second with a dwell of 5 milliseconds per channel.

The six-channel multiplexer also is controlled by the processor and is implemented with a series of digital switches. The digital multiplexer is necessary to channel the six-channel inputs into the single processor channel.

Discrete Inputs

Three discrete inputs representing I/CU mode and reset and MTU installed are channel led directly to the digital multiplexer.

Processor

The processor is a 16-bit serial computer in which the program instruction set is contained in 384 words of ROM. The remainder of the processor is comprised of three 16-bit serial-in, serial-out registers, a bit counter, a 16-bit inverted shift register for I/O, memory and logic. The processor has 16 arithmetic and logic instructions and will address directly any memory location or I/O required. The computations performed by the processor are summarized in the software block diagrams.

Output Interface

The output interface receives data words from the processor and encodes them in a form suitable for serial transmission to the indicator/control unit (I/CU) and/or the maintenance test unit (MTU).

The data transmitted is the MPA of each engine frame light bits, or total MPA to the I/CU and the sensor outputs for each engine in serial digital data form to the MTU. If the engine is not in steady state so that an MPA is unavailable, a code is sent blanking the I/CU display. Once an engine MPA is obtained, it is held in display until a reset discrete commands a new MPA calculation.

When in test mode, the data sent is the result of the program self-test dummy calculation, except for one frame which, when changing mode into or out of test, causes an all eights lamp test and fault light test data signal to be transmitted.

The output interface also receives data as a result of BITE self-test. If a failure occurs, the MPA displays are set to zero and the fault of flag is displayed.

Power Supply

One power supply is used to furnish the required power at the proper voltage levels to the engine monitoring circuits and processor. Separate circuitry is provided for each engine.

INDICATOR/CONTROL UNIT (I/CU)

The primary function of the I/CU is to provide the interface between the MPA equipment and the flight crew and relate the MPA and fault information to these personnel.

The I/CU contains the required input devices and indicators to adequately inform, and allow control inputs from, the flight crew. The I/CU provides front panel mounted displays of:

1. MPA Display - Maximum power available for two engines and total MPA for all engines combined and selected by a rotary switch used for a four-position mode control.

2. Mode Control - A rotary switch having provision for test, MPA for each of two engines and total MPA. In the test position, the processor performs a dummy MPA calculation using simulated sensor inputs. A light test (both digital and fault lights) shall be commanded by the computer when the mode switch is switched into or out of test.

3. On-Off Switch - An on/off push-button switch shall be used to turn off the I/CU readout display and EU.

4. Fault Light - A fault light connected to fail-safe circuits shall be provided to continually monitor power circuits and processor capability. The drive transistor for the fault indicator is activated by a power supply fault or by a processor fault, which is a signal resulting from a routine check of processor instruction, addressing and memory.

5. Reset Button - The reset button is provided so that the pilot can cancel a readout and initiate a new MPA calculation for the engine designated by the mode switch.

6. Frame Lights - Green annunciator lights, two for each engine, are provided on the I/CU to inform the flight crew that an engine MPA is available.

The I/CU hardware block diagram, illustrated in Figure 20, emphasizes the major interface connections between the I/CU and the EU. The major informational transfer between the units consists of two data words, a continuous 16-bit built-in test and frame/engine number serial data stream, and a 16-bit Binary Coded Decimal (BCD) MPA data stream for the digital display selected by the mode switch discretes. The BCD signal drives four BCD to seven segment decoder/drivers within the I/CU. The I/CU contains its own power supply to provide the low voltages for the data display and for the fault lamp.

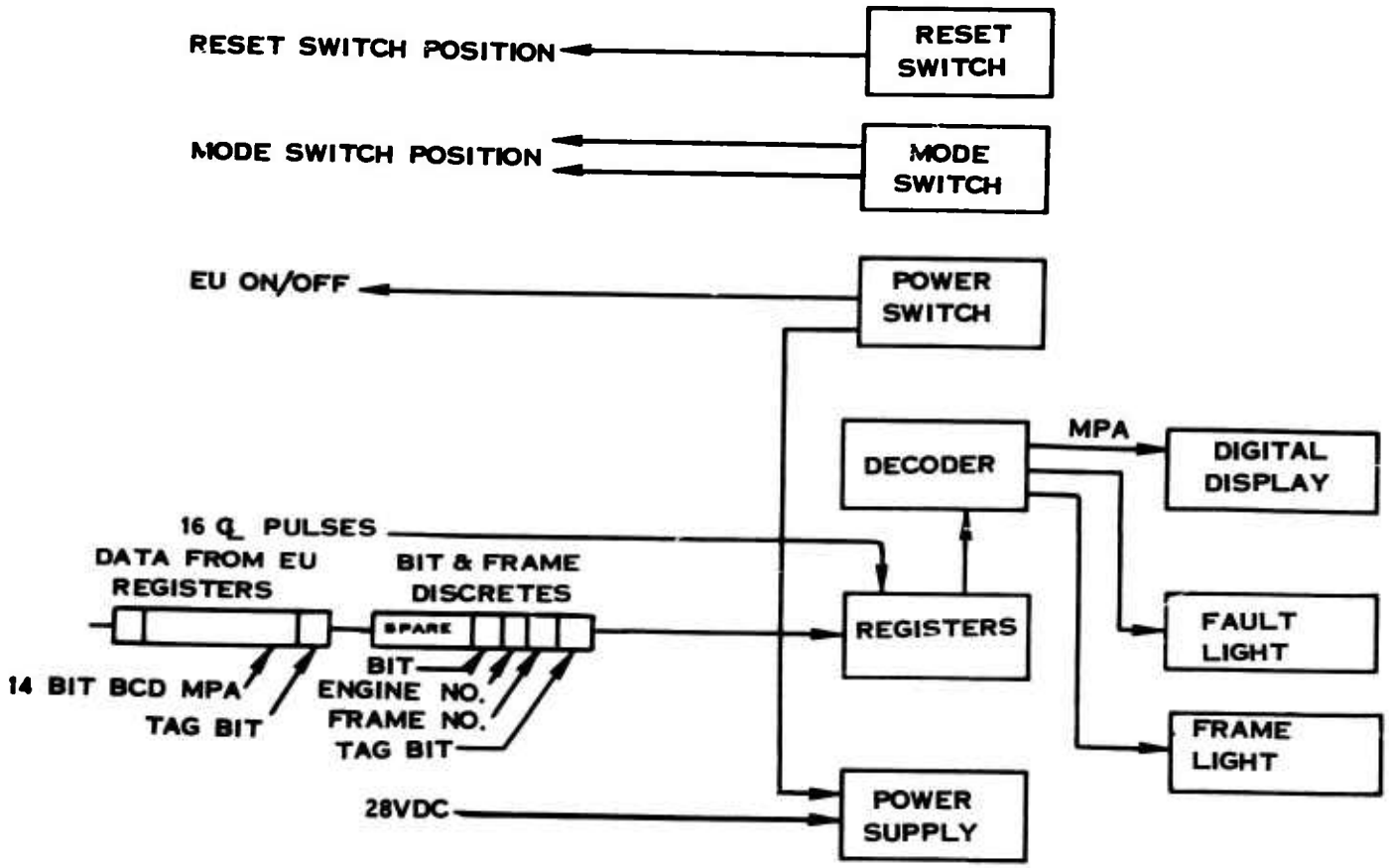

Figure 20. I/CU Hardware Block Diagram.

SYSTEM CONFIGURATION

ELECTRONIC UNIT (EU)

Figures 21 and 22 illustrate the electronic unit configuration. The front panel provides fault indicators, a test connector, and torque sensor calibration adjustment trimmers. An elapsed time indicator is installed for service/reliability purposes. The top panel provides the pressure ports. The pressure ports are foolproofed by size and orientation. Ports of the same boss size cannot be interchanged because of location limitations of the mating pressure lines. The rear panel provides the two engine connectors and the I/CU connector. The chassis is of aluminum sheet-metal construction. Removable side covers allow access to the electrical motherboard on one side and printed circuit board removal on the other.

The unit contains fourteen plug-in printed circuit boards, four vibrating pressure transducers and a power supply.

The printed circuit boards engage laterally into receptacles which are flow-soldered to the motherboard. The motherboard is mounted vertically to provide the most efficient cooling air circulation possible. Keying provisions insure proper printed circuit board alignment and orientation when installed in the unit. The boards are equipped with latches which aid board removal; when the latch is raised it provides a mechanical advantage to separate the mating connector halves. The board is also equipped with a handle which prevents damage to components when pulling the card from the support guides, as well as offering protection to card edge test connector pads. Mechanical retention is afforded by the unit cover panel.

The vibrating pressure transducers are mounted on a casting which provides standard MS 33649 bosses for fluid connections, internal drilled passages to the transducers, a printed circuit board and electrical input/output data connections. The entire transducer subassembly is easily removed for service and test. The individual transducer subassemblies are, in turn, readily removable.

The EU dissipates approximately 90 watts of electrical power, which is removed by a small propeller fan located in the bottom of the chassis. Slots between the card guides in the chassis bottom allocate cooling air to the individual cards in proportion to board power dissipations. The air exits through perforations in the chassis top.

The EU is capable of functioning within the Class 2 requirements of MIL-E-5400 for the temperature altitude condition up to an altitude of 10,000 feet.

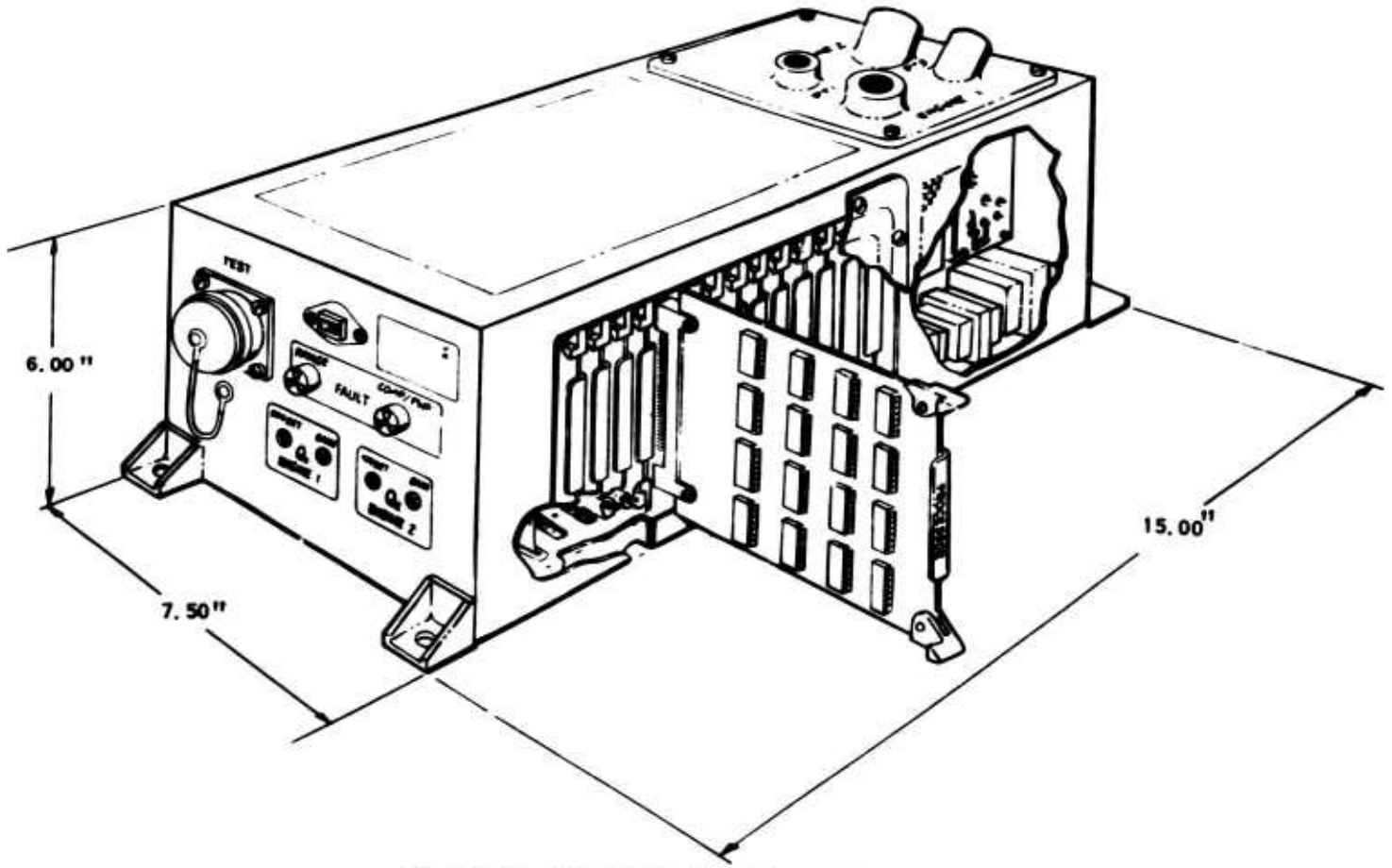

Figure 21. Electronic Unit Front View.

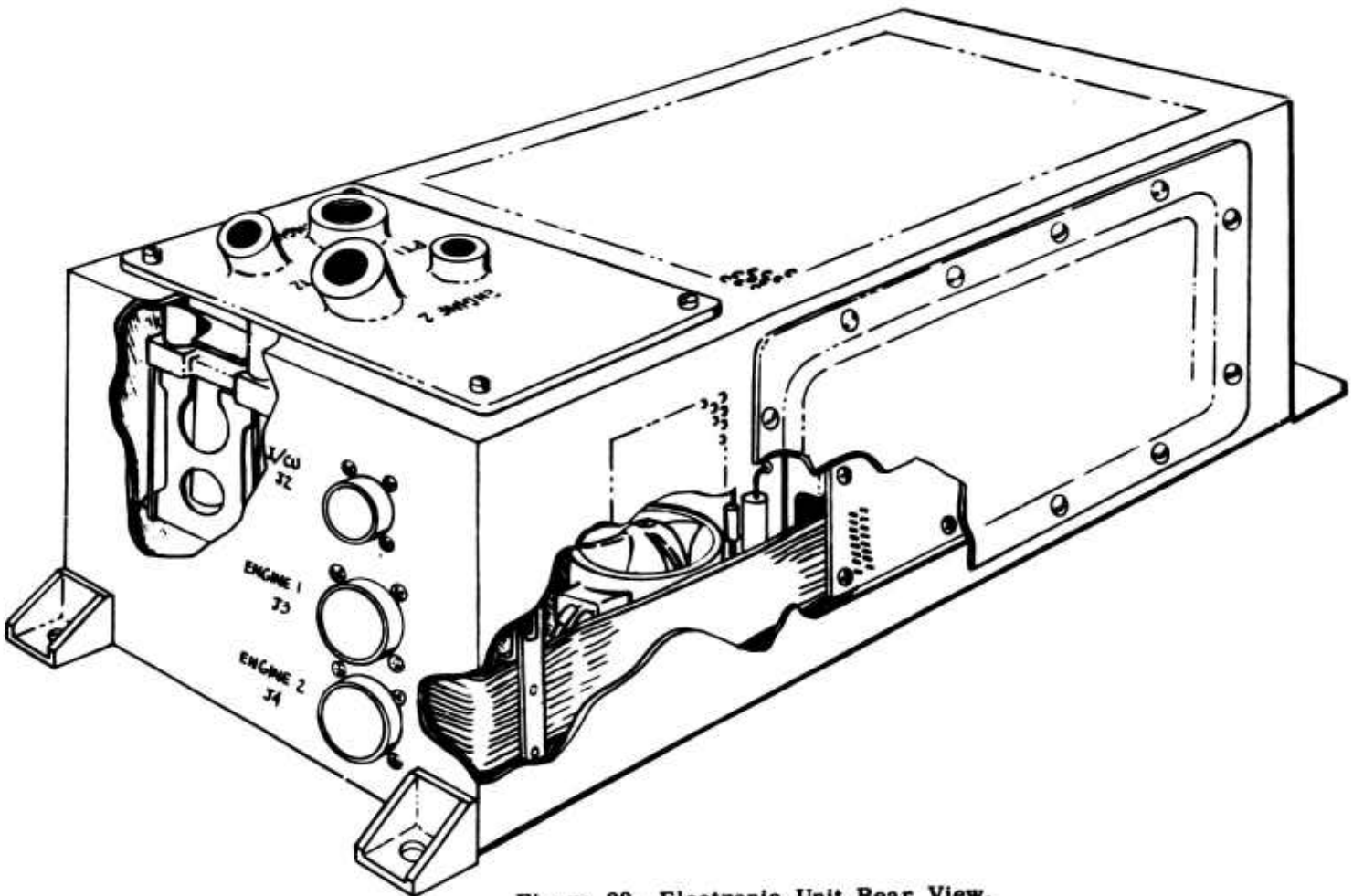

Figure 22. Electronic Unit Rear View.

The unit can be mounted directly to the airframe without resilient mounts to meet the requirements of vibration testing per MIL-E-5400 Curve III for helicopters (i.e., ±5 g sinusoidal waveform, 5 to 500 cps).

The weight of the electronic unit is 15 pounds.

INDICATOR/CONTROL UNIT

Figure 23 illustrates the indicator/control unit configuration. The I/CU is configured in accordance with MS 25212, "Control Panel, Console Type." It has an edge-lighted panel containing the four-digit incandescent lighted display providing the MPA to one horsepower resolution, the reset switch, a power on/off switch, a system fault light, a four-position mode switch, and a frame light at each engine position of the mode switch.

The unit contains two printed circuit boards, one for the light display drives and the second for the 5 VDC power supply powered by the aircraft 28 VDC.

Interconnection with the I/CU is made through the circular connector at the rear. The I/CU is removed by raising the unit from its mounts, requiring cable slack, and unplugging the connector.

The weight of the control panel is 1.5 pounds. The unit power consumption is 5 watts for circuit power and display lighting.

SYSTEM SOFTWARE

The digital program stored within the EU digital computer basically commands the computer to perform the following functions:

1. Manipulate steady-state engine measurement data to computer requirements.

2. Compute from the measured and stored baseline engine data and Gas Path Analysis (GPA) program the engine MPA prediction.

3. Output Digital MPA and/or measured data.

4. Self-test EU program and output fault indication.

5. Receive control inputs from the indicator/control unit of display and test.

The MPA software accomplishing these tasks are detailed in block diagrams, Figures 24 through 26.

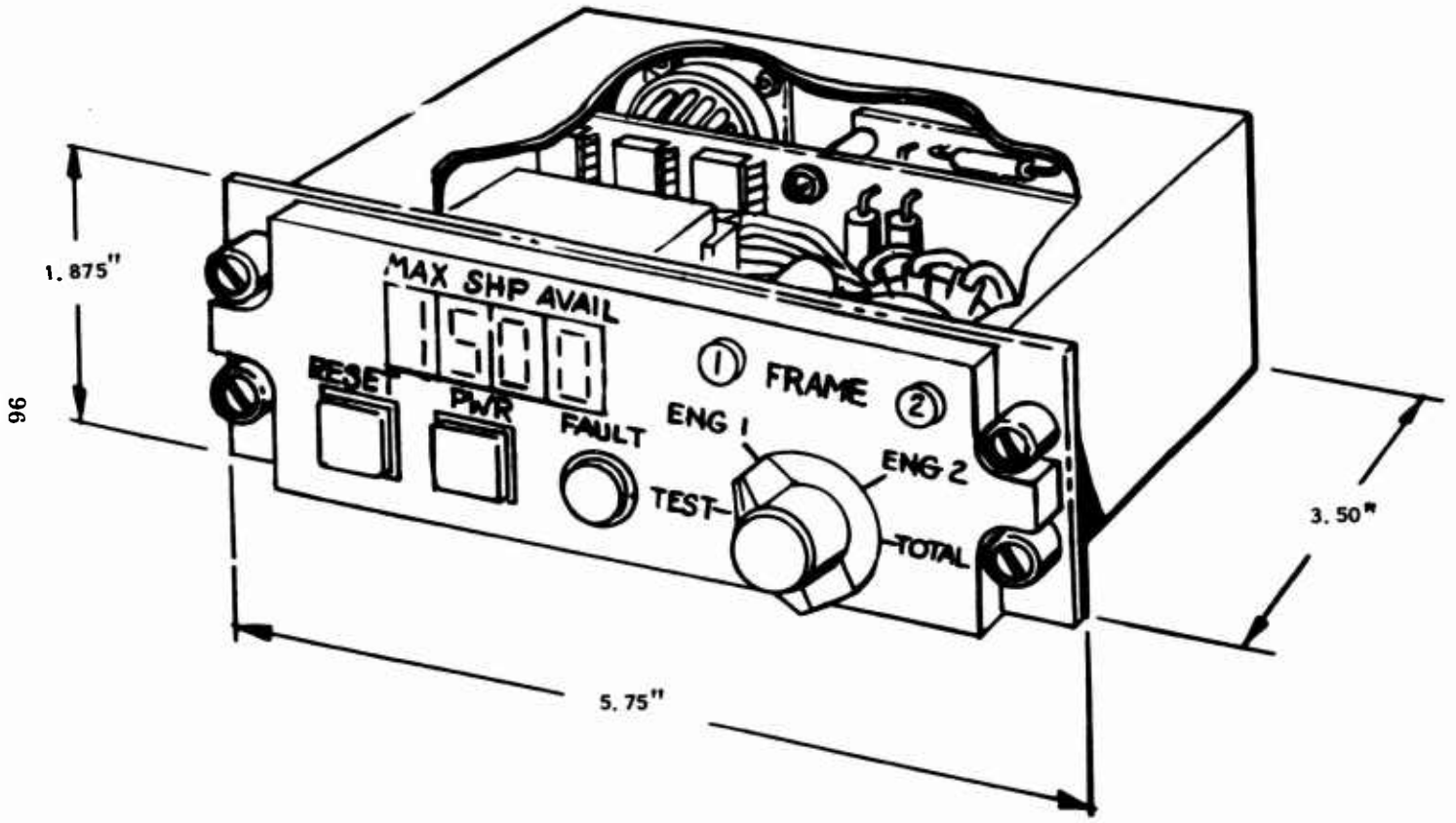

Figure 23. Indicator/Control Unit.

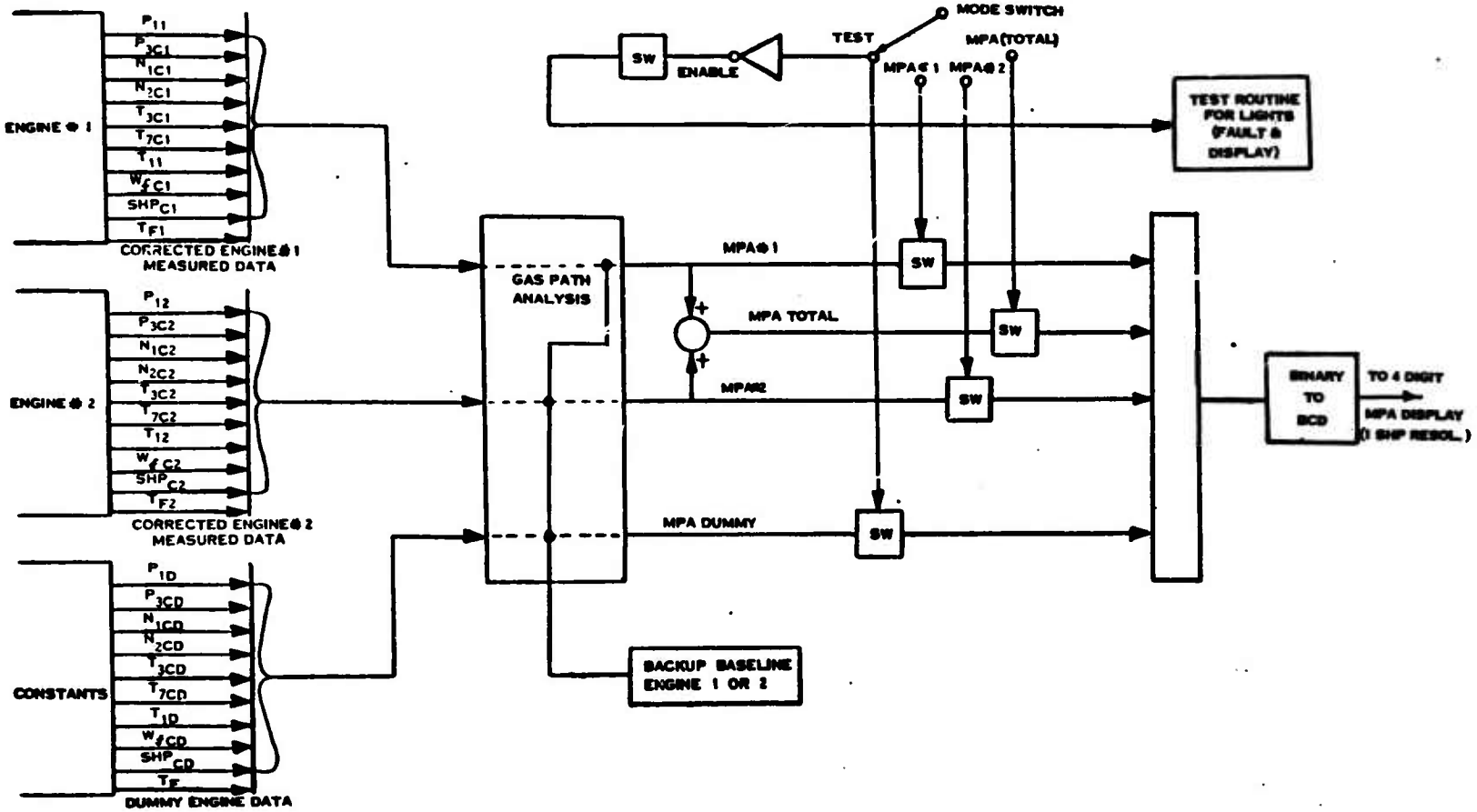

Figure 24. MPA System-Software Block Diagram (Twin Engine).

A

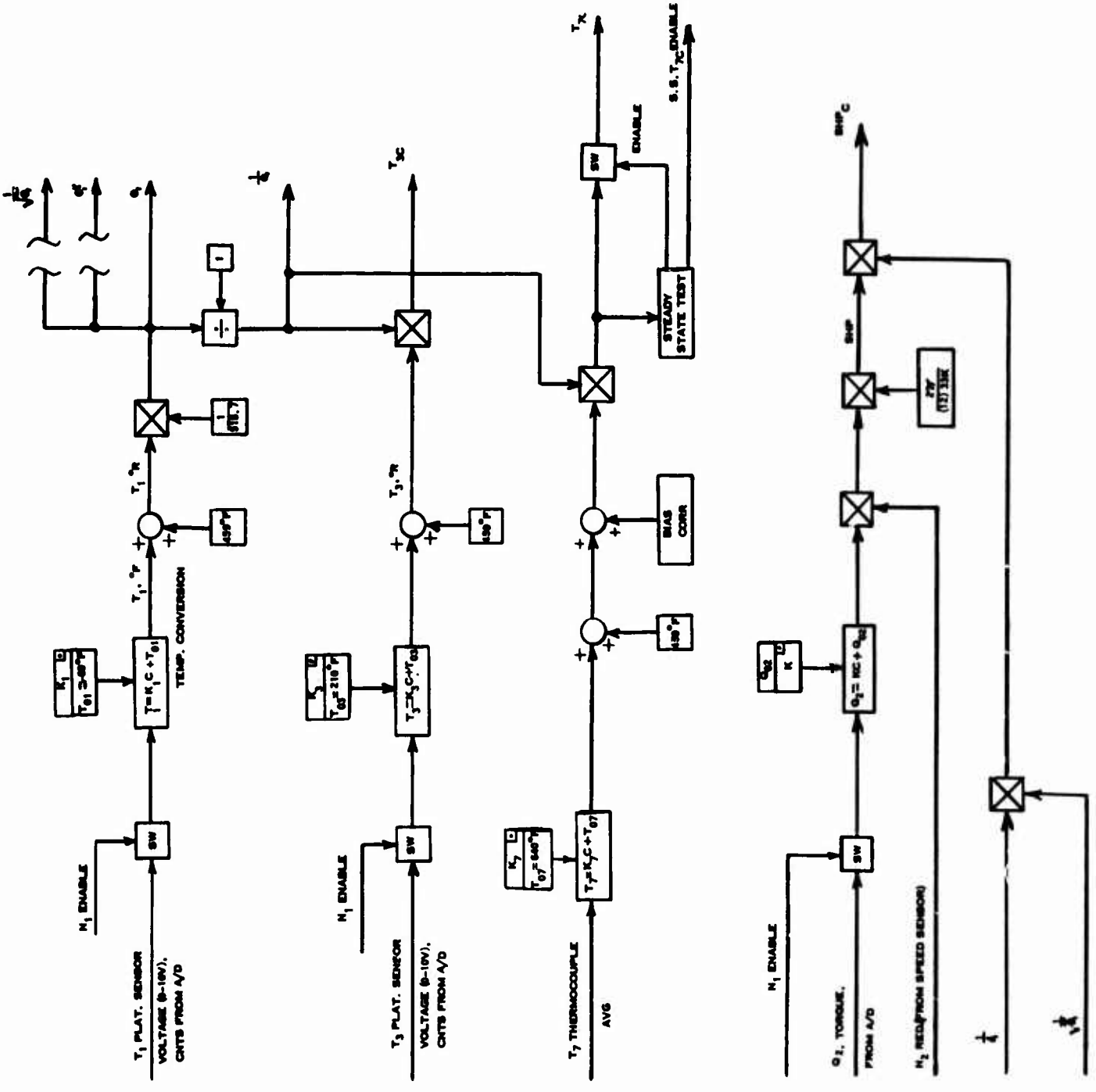

□ DENOTES CALIBRATION DETERMINED CONSTANT

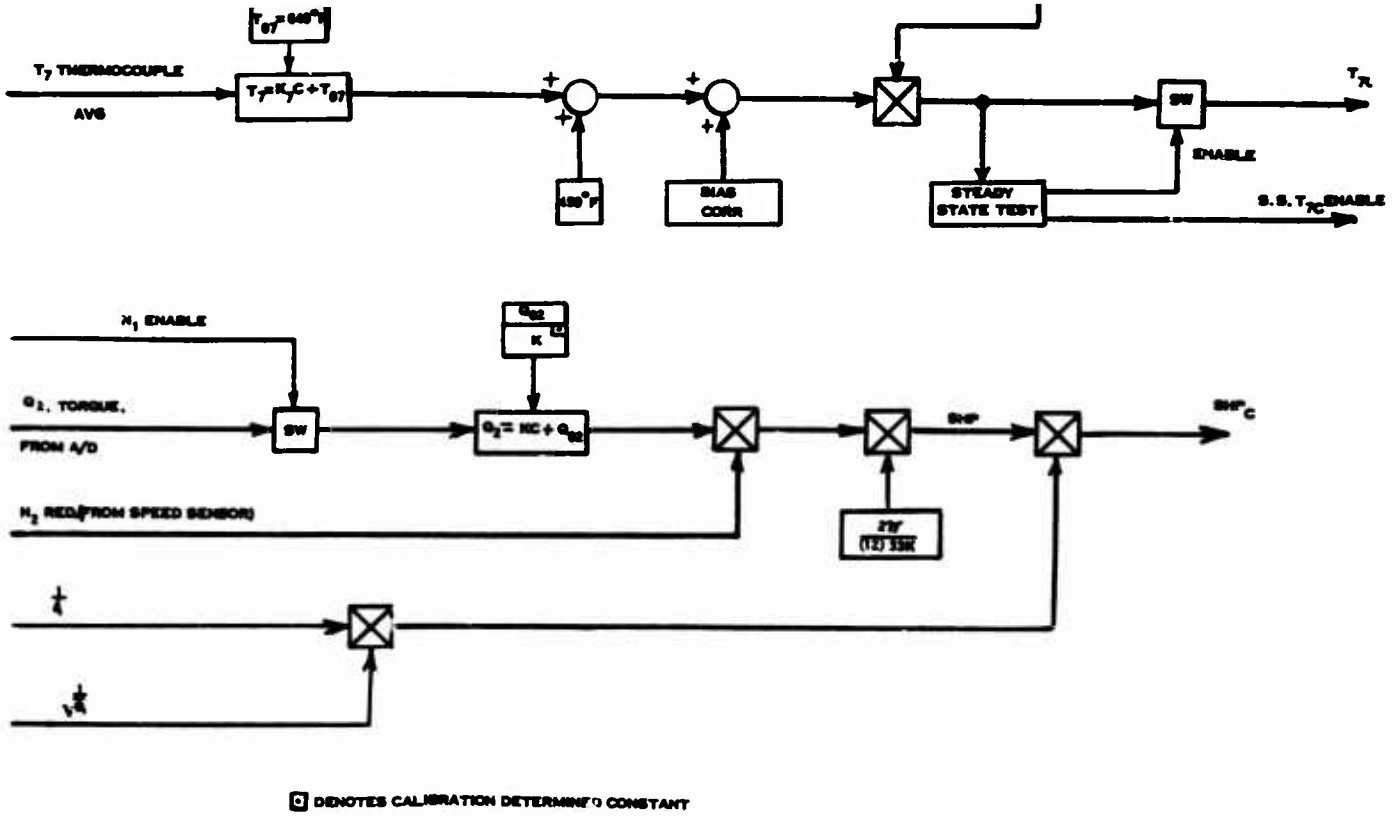

Figure 25. MPA System-Software Block Diagram
Gas Path Analysis Inputs.

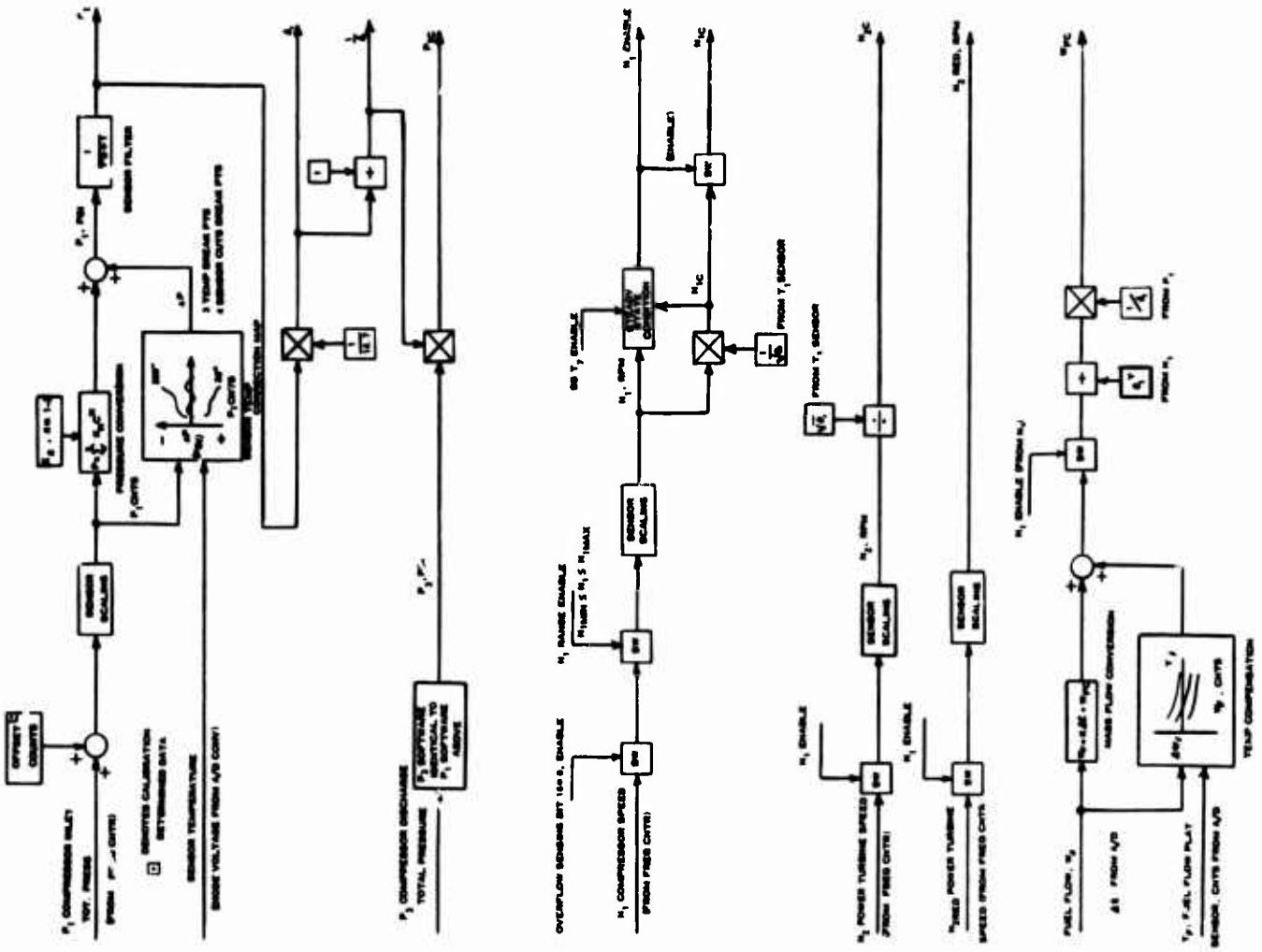

Figure 25. Continued.

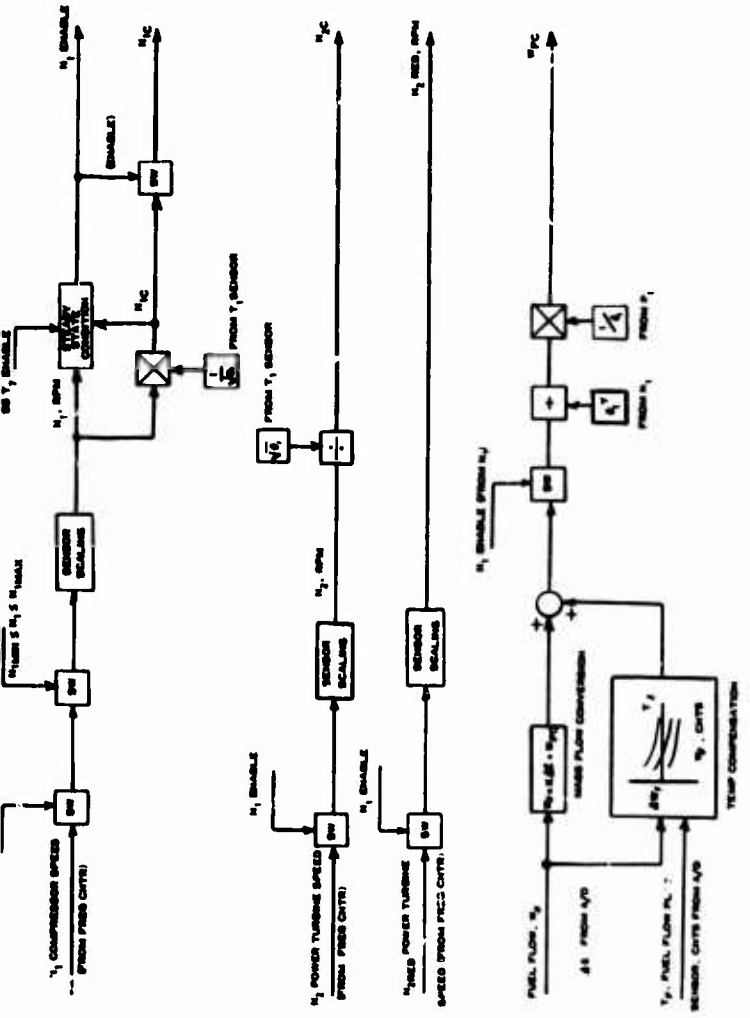

Figure 25. Continued.

A

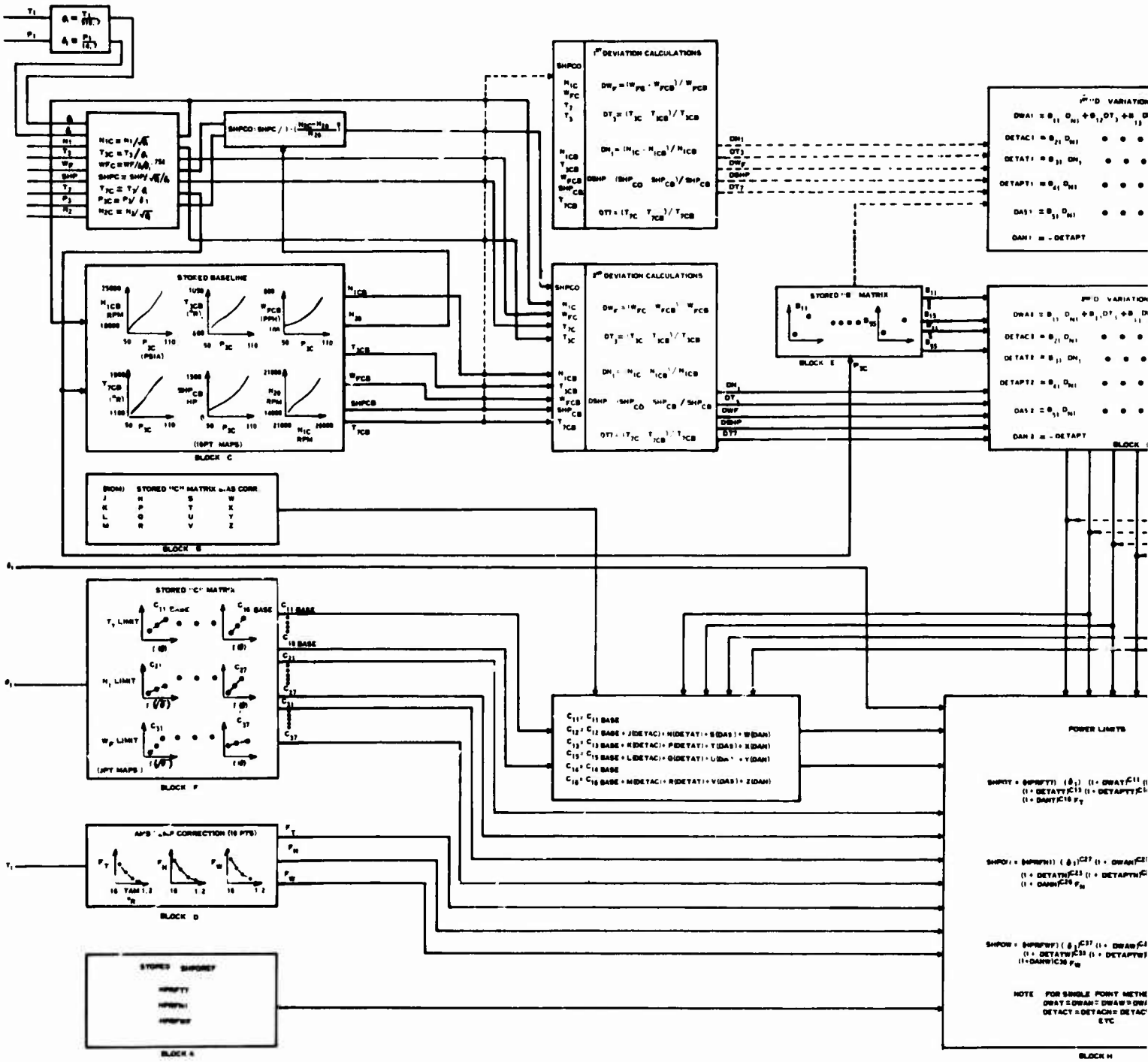

Figure 26. Maximum Power Available Computer Program Block Diagram.

B

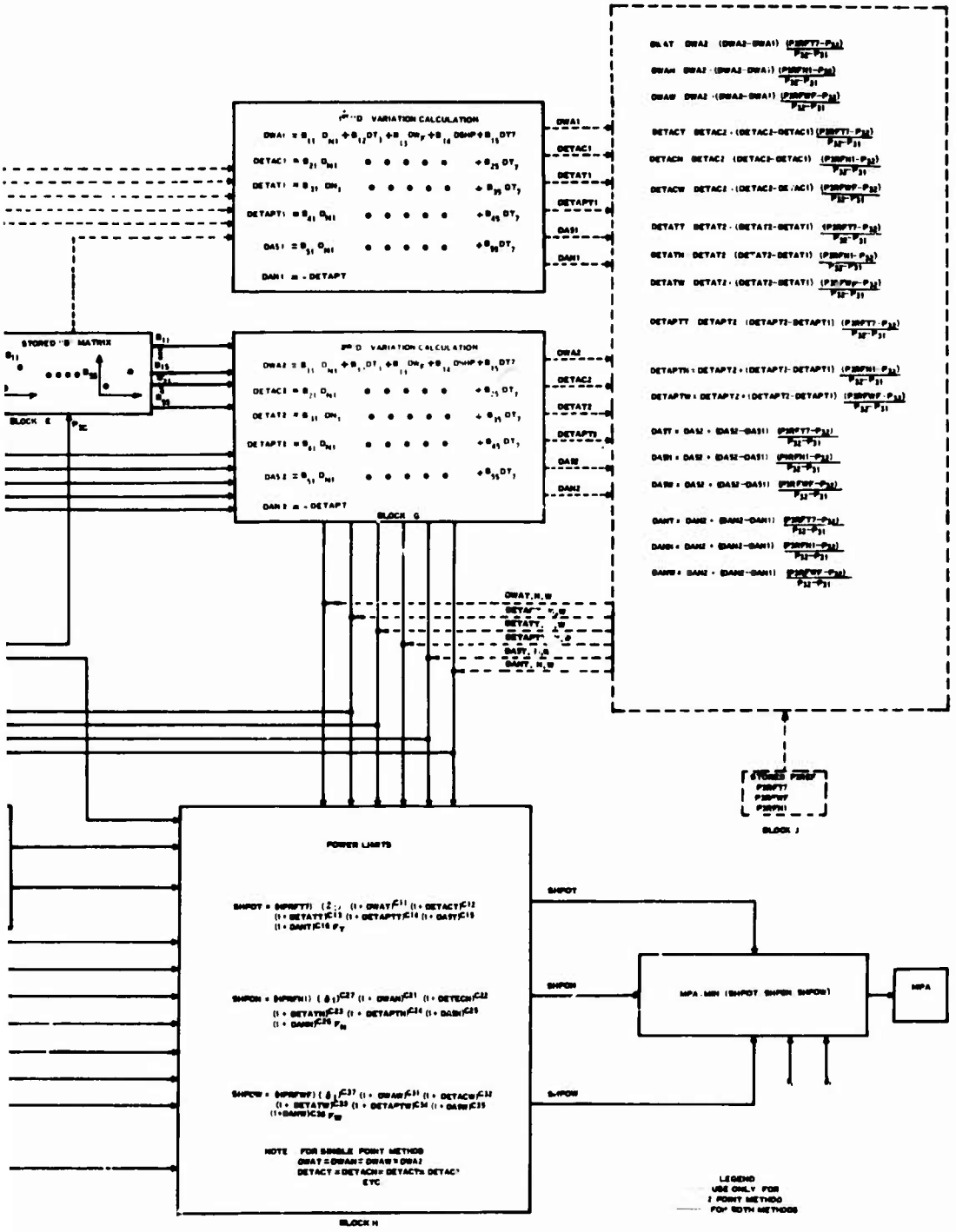

Preceding page blank

Figure 24 summarizes the overall software relationship between the three sets of engine sensor digital input (two measured and one stored frame) to the gas path analyses and the control of the displayed prediction by the I/CU. When a baseline for an engine is not in memory storage, the MPA uses its backup baseline to provide an MPA prediction. The reference or stored frame of data is selected in conjunction with the backup baseline to exercise the complete software program and output a known MPA when in the test mode.

The engine digital inputs to the GPA, illustrated in Figure 24, are derived from the raw engine data after conditioning, scaling, compensation, and correcting to standard day conditions according to the software block diagram illustrated in Figure 25.

Figure 26 illustrates the GPA software leading to the actual MPA prediction. The MPA software is characterized to the generic engine type by the "B" and "C" constant influence materials (Block B, D, E, F) and to an engine through the input of an engine baseline (Block C) and shaft horsepower references (Block A).

Figure 26 also illustrates an alternative software scheme called the "two-point method" as opposed to the "one-point or frame" method described above, which is being considered to improve the MPA prediction accuracy. In this scheme, two frames of engine sensor data separated by at least a 10% power level change are required to obtain an MPA prediction. For the two-point method, the engine is characterized by three inputs: an engine baseline (Block C), a shaft horsepower reference (Block A), and a compressor outlet reference (Block J).

HARDWARE REQUIREMENTS

System and sensor accuracy studies were undertaken to establish the sensor and electronic hardware requirements and to justify the additional hardware for custom compensation of two sensors. In addition, detail studies were also undertaken to establish the memory hardware and system power requirements. This section details the results.

SENSOR ACCURACY/HARDWARE INTERFACE

The normal use of the frequency sensor input interface circuit is to convert the frequency signals into digital signals. Conditioning is provided for the N_1, N_2 and N_2 reduced speed inputs from the magnetic sensors, for the P_1 and P_3 pressure inputs from vibrating cylinder pressure sensors, and for the W_f fuel mass flow input. Speed input N_2 reduced represents the turbine shaft speed measurement from the magnetic speed sensor integral with the torque sensor mounted after the reduction gear used for horsepower calculation.

The frequency input circuit shown in detail in Figure 27 uses the frequency generated from each sensor to gate a fixed frequency clock to a register for a fixed number of sensor frequency periods. As a result, the counts generated are inversely proportional to the shaft speed and pressure input.

The computer clock frequency used in this study is 2 MHz. Accuracy considerations dictate that the number of sensor frequency periods during which the gated computer clock is counted be at least 120, in order to keep resolution inaccuracies small.

Table XXI summarizes the normal sensor granularity and output for the frequency outputs corresponding to the input speed and pressure operating ranges based on a 120 period counter, 2 MHz clock and 60 teeth gear.

As shown in Table XXI, within their operating ranges, both speed and pressure counter outputs will experience, at most, one overflow for a 15-bit counter. For the speed input, at very low input frequencies, where the signal is below the MPA operating range, the counter will overflow many times; to detect this, an overflow signal will be incorporated to warn the processor to disregard the measurement.

For both speed and pressure inputs, the number of counts between maximum and minimum inputs will be less than 2^{15} (32,768) so that a 15-bit counter can be used.

The sampling times shown in the last column of Table XXI represent the longest time required to measure the input, based on the lowest frequency inputs in the operating range and the counter period.

PRESSURE AND SPEED SENSORS

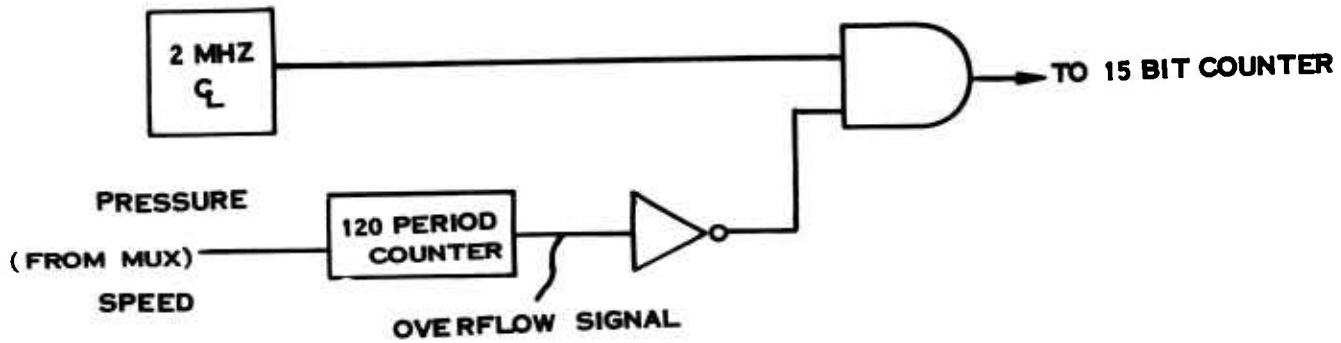

MASS FLOW SENSOR

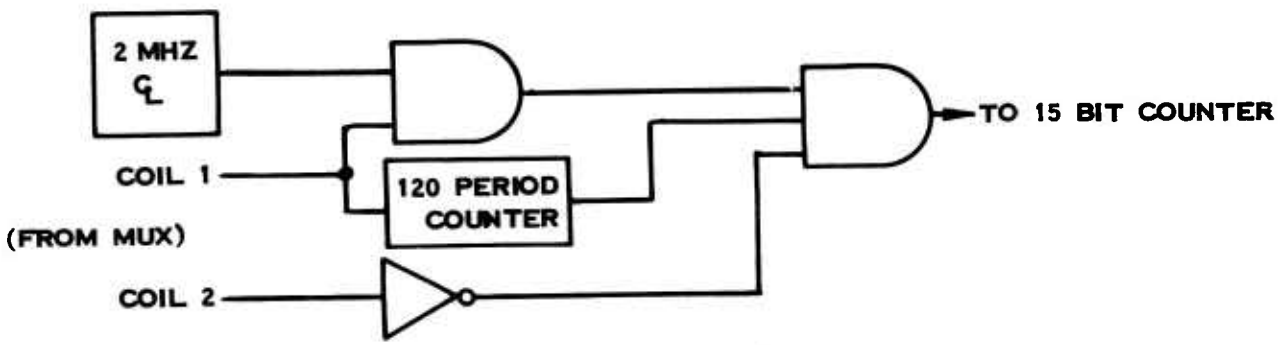

Figure 27. Frequency to Digital Display.

TABLE XXI. SENSOR GRANULARITY AND OUTPUT; MINIMUM SAMPLING TIME

Based on: 2 MHZ clock, 120 period counter

	Granularity (rpm/count)		Counts	Minimum Sampling Time (MSEC)
N_1				
25,000 rpm	2.6		9,600	6
23,000 rpm	1.7		12,000	
N_2				
22,000 rpm	2.01		10,908	9
13,000 rpm	.7		18,460	
N_2 (after gear reduction)				
7,000 rpm	.204		34,284	29
4,200 rpm	.073		57,142	
P_1				
20 psi	.0024	PSIA/COUNT	43,500	27
0 psi	.0016		53,200	
P_3				
0 psi	.013		34,400	17
110 psi	.025		28,600	
250 psi*	.039		24,606	

* Out of MPA operating range.

Table XXII summarizes the magnetic speed sensor and signal conditioning accuracies. The clock is assumed to have an accuracy of 50 PPM. The results are seen to be better than MPA requirements. The errors shown are signal conditioning errors associated with system clock tolerances and counter resolution. Speed errors due to tooth-to-tooth position tolerances and gear eccentricity have been eliminated by selecting a counter period which is an integer multiple of the number of periods in one revolution of shaft rotation.

Table XXIII summarizes the vibrating cylinder pressure transducer accuracy including sensor and signal conditioning interface. The vibrating cylinder pressure sensors are produced at present in 20, 50 and 250 psia ranges. Table XXIII is derived from the 20 psia and 250 psia sensor for the P_1 and P_3 sensor functions respectively.

The frequency input circuit for the mass flow measurement uses the two transmitter pulse to gate the fixed clock frequency to a register for a fixed number of pulse periods. As a result, the counts generated are proportional to the mass flow.

Table XXIV summarizes the expected fuel mass flow sensor and signal conditioning accuracies. The accuracy after custom compensation for fuel temperature effects is also given.

The results of the analysis of the analog sensors and conditioning accuracies are summarized in Tables XXV through XXVII.

Table XXV summarizes the platinum resistance temperature transducer accuracies including sensor probe and signal conditioning interface for the T_1, T_3 and fuel flow temperature compensation sensors. These sensors are replaceable without further calibration.

Table XXVI summarizes the chromel-alumel thermocouple accuracies including sensor, probe, and signal conditioning for the T_7 sensors. The sensor accuracy is obtainable from special grade thermocouple wire.

Table XXVII tabulates the results of an accuracy study of a foil gauge torque meter for the T53 engine. The torque sensor is assumed to measure torque in the driveline on the low speed end of the gear reducer. The required torque sensor is rated at 1200 ft-lb full-scale at 7000 rpm. The results also show the accuracies obtainable by providing for sensor custom calibration.

Need for Custom Compensation

MPA sensors must have high accuracy, stability and reliability. If custom

TABLE XXII. MAGNETIC SPEED SENSORS AND CONDITIONING INTERFACE ACCURACY SUMMARY

Based on: 2 MHZ clock, 50 RPM accuracy, 120 period counter, 60 teeth gear

	LOW LIMIT	RPM	HIGH LIMIT
N_2	13K		22K
Resolution Error	± .35		± 1.05
Clock Errors	± .65		± 1.10
MPA	RSS ± .738 RPM		RSS ± 1.52 RPM
N_2 (reduced)	4.2K		7K
Resolution Error	± .036		± .10
Clock Error	± .200		± .35
	RSS .203 RPM		RSS .36 RPM
N_1	23K		25K
Resolution Error	± 1.10		± 1.25
Clock Error	± 1.15		± 1.25
	RSS ± 1.59 RPM		RSS ± 1.76 RPM

TABLE XXIII. VIBRATING CYLINDER PRESSURE SENSOR AND CONDITIONING INTERFACE ACCURACY

P_3 Sensor

Pressure	1 psia	100 psia	250 psia
a. Clock (50 ppm)	± .022	± .036	± .048
b. Temperature Compensation (2.1°F)	± .000	± .042	± .147
c. Curve Fit (.008%FS)	± .020	± .020	± .020
d. Clock Resolution	± .007	± .010	± .019
	.030	.059	.157
RSS (Interface Errors)			
e. Calibration	± 0013	± 009	± .020
f. Linearity	± .000		
g. Resolution	± .000		
h. Power Supply	± .000		
i. Repeatability (.0001%FS)	± .00025		
j. Long-Term Stability	± .0012		
RSS (Sensor Error)	± .0017	.009	.020
Total Sensor and Interface Accuracy	± .031 psia	± .060 psia	± .158psi

MPA Requirement (50-110 psia) ± .050 (Sensor Only Estimate)

TABLE XXIII. CONTINUED

P_1 Sensor

	0 psia	20 psia
a. Clock (50 ppm)	± .0040	± .005
b. Temperature Compensation (2.1°F)	± .0006	± .003
c. Curve Fit	± .0016	± .0016
d. Clock Resolution	± .0016	± .0016
RSS(INTERFACE ERROR)	± .0046	± .0063
e. Calibration	± .006	± .009
f. Linearity	± .000	± .000
g. Resolution	± .000	± .000
h. Power Supply	± .000	± .000
i. Repeatability (.0001%FS)	± .00002	± .00002
j. Long-Term Repeatability (.006%FS)	± .0012	± .0012
RSS (Sensor)	± .0061	± .0091
Total RSS (Sensor + Interface)	± .0076 psia	± .0110 psia
MPA Requirements (11 to 16 psia) =	± .01 psia (Sensor Only)	

TABLE XXIV. FUEL MASS FLOW METER AND SIGNAL CONDITION ACCURACY

	With Custom Temperature Compensation	No Temperature Compensation
Sensor Static Error Band	.91% point	.91%
Interface		
Clock (50 ppm)	.005% point	.005% point
Clock Resolution	.0016% point ● 800pph .0038% point ● 350pph	.0016% point .0038% point
Temperature Compensation (±40°F)	.0028% point	--
No Temperature Compensation (±60°F) error	--	.42% *
R(SS) Interface	.0069 ● 350pph .0059 ● 800 pph	.420% ● 800pph .420% ● 350pph
Total Sensor and Interface Accuracy	.91% point	1.1% point

* Based on temperature sensitivity of $\frac{.7\%}{100^{o}F}$, and 40°F to 160°F fuel temperature range.

TABLE XXV. PLATINUM RESISTANCE TEMPERATURE SENSOR AND CONDITIONING INTERFACE ACCURACY SUMMARY

Error Source	T_1: - 60°F to 140°F	T_f: (1) +40°F to 160°F	T_3: 210°F to 590°F
Sensor			
1. (2) Interchangeability	± .36°F	± 4.0°F	± .36°F
2. Long-Term Repeatability (.1% of Calibration Range)	± .2°F	± .12°F	± .38°F
3. (3) De-icing Heaters	± .54°F	NA	--
4. (4) Recovery	± .28°F	NA	± .37°F
5. Self-Heating	± .00°F	± 00	± .00°F
RSS (Sensor)	± .74°F	± 4.0°F	± .64°F
Signal Conditioning Interface			
1. A/D error (.09% FS)	± .18°F	± .18°F	± .34°F
2. MUX (.074% FS)	± .15°F	± .15°F	± .28°F
3. Amplifier Drift (.18% FS)	± .36°F	± .36°F	± .69°F
4. Gain Drift (.44% FS)	± .90°F	± .90°F	± 1.7°F
	± .99°F	± .99°F	± 1.9°F
RSS (Sensor and Interface)	± 1.23°F(2)	± 4.10°F	± 2.00°F

NOTES:

1. Fuel Flow Temperature Compensation Sensor
2. Precision Calibration for T_1 and T_3 sensors; not required for T_f
3. After - 1.08°F correction
4. After +.8°F correction

TABLE XXVI, T_7 THERMOCOUPLE ERRORS

		Chromel - Alumel
1.	Sensor Calibration	± 5°F@1800°R ± 2 4°F@1100°R
	Long-Term Drift	± 1.0°F
	RSS	± 5.1°F 1800°R ± 2.6°F 1100°R
2.	Cold Junction (compensation) Accuracy	± 1.0°F
3.	Temp Equilibrium Error (including recovery, conduction and radiation errors)	± 1.8°F
4.	Extension Wires, Plugs, Jacks	± 2.0°F
5.	Signal Conditioning (Amplifier, and A/D)	± 2.4°F
	Total Error	± 6.3°F@1800°R ± 4.5°F@1100°R

TABLE XXVII. TORQUEMETER SENSOR (STRAIN GAUGE TYPE) AND SIGNAL CONDITIONING INTERFACE ACCURACY

	With Inter-changeability	With Custom Calibration*
1. Calibration, Deadweight	± .002%	± .002%
2. Static Error Band	± .2%	± .2%
3. Impedances	± .50%	± .5%
a. Input .5% (Supply)		
b. Output .02% (To Signal Conditioner)		
4. Zero Balance and Gain Error	.00	---
5. Temperature (delta = 200°F)	± .56%	± .56%
a. Zero Shift (.002% FS/°F)		
b. Gain Shift (.002% FS/°F)		
6. Shaft Unit to Unit Repeatability	±2.5%	---
RSS (Sensor)	±2.5% FS	± .78% FS
1. A/D (10 volt)		
a. Drift	± .09%	± .09%
b. Resolution (1/2 count)	± .01%	± .01%
2. MUX	± .07%	± .07%
3. Amplifier		
1. Drift	± .18%	± .18%
2. Gain Drift	± .44%	± .44%
4. Demodulator	± .20%	± .20%
RSS (Signal Cond.)	± .53% FS	± .53% FS
Total RSS	±2.65% FS	± .94% FS

*1) Zero & Gain Control Calibration Reg'd and Deadweight Calibration

NOTE: Signal condition error associated with uncontrolled variables; eg , temperature and drifts are not removed by calibration.

compensation circuits to improve accuracy are required, these preferably should be integral with the sensor unless justified by a significant increase in sensor accuracy and resultant MPA prediction accuracy. Therefore, custom compensation, if required, is justifiable on the latter basis for four of the ten MPA sensors for which the highest sensor accuracies are required: the engine inlet temperature (T_1) sensor, the power turbine torque (Q_2) and turbine inlet temperature (T_7) sensors, and the mass fuel flow sensor (W_f). The remaining sensors require less accuracy improvements as they are minor contributors to MPA prediction error either due to the low sensitivity of the prediction accuracy to their measurement error (i.e., P_1, P_3 and T_3 sensors) or the sensors are practically error-free (i.e., N_1 and N_3).

For MPA, custom compensation of the mass flow and torque transducers must be justified as it can impose more than necessary maintenance work when the sensor must be replaced because of the additional separate hardware required to implement the compensation. The value of custom compensation of the mass flow and torque transducers has been investigated by determining its effects on the MPA prediction accuracy. The results are summarized in Table XXVIII. The accuracy of the mass flow transducer is $\pm 1.1\%$ without custom temperature compensation. Improved accuracy $\pm 0.91\%$ is achievable by utilizing a fuel temperature measurement to compensate for any temperature effect on the sensor. Table XXVIII shows that a significant improvement is obtained in MPA prediction accuracy when on the fuel flow limit by custom compensating the mass flow sensor.

A strain gauge torque sensor accuracy of $\pm 0.94\%$ is achievable by deadweight calibrating of the torque sensor with the EU signal conditioning electronics. The output of a torque sensor can vary by $\pm 2.5\%$ due to shaft-to-shaft variation from mechanical tolerances in manufacturing. It is uneconomical to match them to closer limits. It is, therefore, necessary to calibrate each torque sensor by adjusting the output of the signal amplifier whenever a torque sensor shaft, torque sensor, or EU is replaced in order to maintain its accuracy. As shown in Table XXVIII, a significant MPA prediction inaccuracy is incurred without this form of custom compensation.

MPA Memory Requirements

The MPA memory capacity requirements divided into ROM for program and constants storage, PROM for sensor and sensor compensation data, and baseline data storage are summarized in Table XXIX.

Fifteen chips will provide 1920 16-bit words of memory. Eleven chips shall be ROM chips, and four chips shall be PROM for sensor characteristics and stored baseline for two-engine helicopters.

TABLE XXVIII. EFFECTS OF CUSTOM COMPENSATION ON MPA PREDICTION ACCURACY BASED ON SENSOR MEASUREMENTS AT 50% NRP

Configuration	MPA Prediction Accuracy @ N_1 Limit	@ T_7 Limit	@ W_f Limit
1. Custom Compensated Mass Flow and Torque Meter (Best Sensor Accuracy Configuration)	± 1.94%	± 2.73%	± 2.43%
2. Custom Compensated Torque Meter	± 2.06%	± 2.73%	± 2.92%
3. No Custom Compensated Sensor	± 4.89%	± 4.99%	± 5.22%

TABLE XXIX. MEMORY ESTIMATES FOR MPA

FUNCTION	WORDS ROM	WORDS PROM
1. Subroutines		
a. Map Lookup and Interpolation (univariate and bi-variate)	40	-
b. Pressure Sensor Compensation	60	-
c. Input Interfaces (2 at 30 each)	60	-
d. BCD Output	50	-
2. Built-In Test (includes memory, and lamp check, dummy engine)	100	-
3. Input Logic		
a. Steady-state determination, corrected mass flow conversion	200	-
b. PROM data for sensors and mass flow correction	-	62/engine
4. Multi-Engine Logic (Generalization)	65	-
5. Computer Initialization	25	-
6. Gas Path Analysis		
a. Logic (map lookup and polynominal computation)	200	
b. Data		
1. C matrix	140	
2. C matrix bias	16	
3. Ambient Temperature Correction	27	
4. B matrix	275	
5. Stored Baseline (per engine)		126
6. Stored SHREF (per engine)		3
7. Backup Baseline	126	
Totals	1384 wds	191 wds/ engine
Read/Write Memory		64 wds

Sixty-four words of Scratch Pad Memory (read/write) are required. This is obtainable in four packages.

Power Requirement

Electrical power required to operate the MPAS is obtained from 115 volt, 400 Hz single-phase input to the EU, and 28 VDC for the I/CU.

Total power will not exceed 95 watts (90 watts for EU circuit power and 5 watts for the I/CU display lighting and circuit power). By utilizing solid-state components to the maximum possible extent, the power required by the MPAS has been kept to a minimum.

The MPAS circuits are designed so that all components except the fault lights are energized when the power-on switch is depressed on the I/CU. This action connects power to the EU. To save power, the MPAS units can be de-energized when the power switch is again depressed.

HARDWARE AVAILABILITY

A significant point regarding the availability of MPA sensors to achieve the desired accuracies is the limited range of the measurement required for MPA. Measurements for MPA are required at ground level, static engine conditions between 50% to 100% NRP. This limited range is instrumental in the selection and availability of the MPA sensors.

A second significant aspect affecting sensor selection and availability is the ability of the selected MPA sensors to mechanically integrate with the engine and helicopter. In this respect, sensors can be specified only where the engine and helicopter configuration are defined. Therefore, the selection of sensors reported herein is thus tentative in this respect. The sensors selected are based on their ability to meet MPA accuracy requirements and meet or be capable of being modified to meet military specifications.

Sensors which provide the accuracy delineated in Table XIX are available "off-the-shelf". Table XXX lists various manufacturers who have successfully demonstrated their ability to produce sensors similar to the required items, along with, where available, the sensor model number. Some sensors are standard products which can, with some minor redesign, meet military specifications.

Deadweight calibration provides the most accurate method for calibrating a torque sensor. The torque sensor is deadweight calibrated after installation and during subsequent engine overhaul periods. Between overhaul periods when replacing the EU or the torque sensor, a means of

TABLE XXX. MPA ENGINE INSTRUMENTATION SOURCE LIST

Sensor	Sensor Type	Model	Manufac. Source	Spec.
N_1 - Gas Generator Speed	Pulse Pickup	Series 3010	Electro Corp.	Std.
T_1 - Engine Inlet Temperature	Plat Resist. Single Eleven		Rosemount	MIL
T_3 - Compressor Discharge Total Temperature	Plat. Resistance		Rosemount	MIL
T_7 - Power Turbine Inlet Total Temperature	Thermocouple Probe (Chrom Alumel)		Fenwal HARCO Lab	MIL MIL
P_1 - Engine Inlet Pressure	P_1tot Probes Vibrating Cylinders Transducers			
P_3 - Compressor Discharge Pressure	Pitot Probes Vibrating Cylinders Transducers		Rosemount HSES	MIL STD
W_f - Mass Flow	9-127-16		ELDEC	STD
Q_2 Power Turbine SHP	MCRT 6-02T		Himmelstein	STD

providing accurate routine calibration without the time, effort, and equipment needed for deadweight calibration is required. Present shunt calibration techniques which provide bridge unbalances equivalent to full load torques are not accurate enough for MPA. This technique should be developed for MPA to provide custom calibration for each sensor. The development of the strain gauge calibration circuit which offers promise of highly accurate routine calibration should also be pursued.

The electronic technology proposed for MPA can be provided at the present time by many manufacturers. Much of the technology has been in use on propulsion controls (air inlet and fuel controls) for gas turbine engines. These applications have demonstrated the inherent capability of the electronic component to operate reliably and economically, and within performance specifications when located within a severe environment. As a result, prospects for a successful MPA development appear good.

MPA FEASIBILITY

MPA COST ESTIMATE

It is estimated that the total MPAS hardware (recurring) cost for a twin engine helicopter is $46,000, based on a 100 quantity. This cost is based upon $20,000 for an Electronic Unit, $3,000 for an Indicator/Control Unit, and $13,000 per engine for instrumentation.

WEIGHT

Table XXXI summarizes the MPA system weight estimates. The weight of the EU and I/CU, which contain all of the circuitry necessary to determine and display the MPA of both engines on the aircraft, will not exceed 17 pounds. The weight of engine instrumentation for two engines is approximately 49 pounds, exclusive of cabling weight. Recognizing that much of engine instrumentation used for MPA already exists on helicopters, the weight impact of strictly MPA instrumentation requirement is therefore considerably less than 49 pounds.

Recognizing also the extreme importance of weight on all aircraft, and on helicopters in particular, the weight of the MPAS has been kept to a minimum, consistent with other design and performance requirements. For example, the extensive sensor test and display hardware has been located in a separate maintenance test unit instead of in the EU to minimize weight. Still, some further weight reduction is possible through increased use in circuitry common to both engines, but at the expense of decreased reliability. Also, because of the increased use of circuitry common to both engines, the likelihood of the malfunction of a single component affecting the operation of both engine channels is increased. It is

TABLE XXXI. SYSTEM WEIGHT ESTIMATE
(TWIN ENGINE INSTALLATION)

Quantity per Ship	Component Description	Estimated Weight (lb) per Engine	Weight (lb) per System
1	Electronic Unit		15.0
1	Cockpit Indicator/Control		1.5
1/Engine	HP Transducer *	17.1	34.2
2/Engine	Pitot Probes *	1.8	3.6
3/Engine	Temperature Instrumentation *	3.8	7.6
2/Engine	Speed Transducers *	0.5	1.0
1/Engine	Mass Flow Transducer *	1.3	2.6
	Totals	24.5	65.5

* These weights in reality do not represent an additional weight to the aircraft due to the addition of the MPA system. Many existing sensors could either be utilized or replaced by more accurate sensors. The weight impact on a particular installation would require an analysis of the weights of existing sensors in comparison to replacement sensors (if required) and any additional sensors the MPA System requires.

believed that the circuits as designed utilize the proper degree of circuit commonality, and make the optimum compromise between weight and reliability.

MAINTAINABILITY CONSIDERATIONS

General

Included as major design considerations are the requirements (1) that the MPA hardware be designed and constructed so as to minimize maintenance action during its useful life, and (2) to simplify those maintenance activities that remain. Design features that contribute significantly to minimizing maintenance action are (1) use of solid-state electronic components wherever possible, (2) derating of these components to minimize thermal and electrical stress as much as possible, (3) use of conformal coating on printed circuit boards to minimize effects of atmospheric contaminants, and(4) provide sturdy mechanical construction to withstand vibration environment of helicopter fuselage or flight deck.

Design features that substantially reduce remaining necessary maintenance action are: (1) use of built-in test equipment (BITE) or self-test to virtually eliminate unnecessary removal and maintenance, (2) use of nonhermetically sealed case to reduce access time to circuit components, (3) design all circuit components readily accessible for test or replacement, and (4) use of test points to simplify troubleshooting.

By giving proper consideration to maintenance concepts during the design of the EU, it is possible to minimize total maintenance action, and thereby lower the total cost of ownership of the EU, without significant effects on other design and performance requirements.

BIT

MPA built-in tests (BIT) consist of both continuous and pilot-initiated self-checking of the EU function. Readouts of the BIT results are obtained by means of a fault indicator located on the EU and I/CU and a zeroed I/CU digital display.

The continuous self-checking tests are:

1. Power Supply Check -- The power supply checks itself for regulation and for power resumption following an interruption. Any malfunction results in fault indications on the EU and I/CU. This signal remains on only as long as the power supply fault exists. Power on Reset (POR) resets MPAs to zero.

2. Processor Check -- This test is a short program sequence which uses every instruction, and, therefore, all the arithmetic hardware to perform a fixed sequence of operations. The resulting value at the end of the sequence is compared with the proper stored value, and any discrepancy will show up as EU and I/CU fault light indications and POR resets.

3. Memory Check -- This test adds every word and compares the sum to a stored value. If the two are not identical, the system provides a POR and fault light indication on the EU and I/CU.

4. Range Check -- Each sensor input will be tested with a range test. This test will cover open and shorted input sensors. Out-of-range sensors will initiate an MPA = 0 indication for the engine with an out-of-range sensor and an I/CU fault light indication.

   In addition to the above testing, the pilot, using the mode switch test position, initiates the following tests.

5. Light Test -- The computer briefly commands a lamp test when switched into and out of test to verify visually that all digital light segments, fault lights, and frame lights are operating. Malfunction of the digital lights will require replacement of the I/CU. A complete loss of lighting indicates a power supply malfunction.

6. Program Test -- To supplement BITE for greater reliability, the processor will perform a dummy MPA calculation in the test mode using reference sensor inputs stored in memory. The results are displayed and confirmed visually by the pilot to be a known fixed value.

Table XXXII summarizes the tests, when they are performed, and the action taken when a malfunction is detected. It should be noted that a fault light indication on the I/CU with no malfunction indication on the EU indicates a malfunction of a sensor input to meet range test. A fault light indication on both units indicates a malfunction in the EU.

Maintenance Test Unit (MTU)

A Maintenance Test Unit will provide on-condition maintenance testing of the MPA System. This unit will provide the maintenance activity with the capability of complete system check-out and, if necessary, system calibration. The MTU will provide the test operator with the capability to pin-point system malfunctions to an individual sensor or circuit

TABLE XXXII. BUILT-IN TESTS

TESTS	TEST PERFORMED	Action Taken Due to Test: SYSTEM DISENGAGE MODE	Action Taken Due to Test: I/CU FAULT OUTPUT	Action Taken Due to Test: EU FAULT OUTPUT
1. Range	Continuously with each sensor input	Output of engine MPA set to zero, total MPA equal zero	x	
2. Memory	Each cycle	POR resets output MPA's to zero	x	x
3. Processor	Each cycle	POR reset output MPA's to zero	x	x
4. Power Supply Test	Continuously	POR resets outputs MPA's to zero	x	x
5. Light Test	In Test Mode	None-replace I/CU	None	
6. Program Test	In Test Mode	None	None	

function within the electronic unit. The MTU will also provide the test operator with on-board calibration capability through manual adjustments externally accessible in the electronic unit.

The MTU will be capable of reading each individual sensor signal. The MTU will also be capable of injecting into the electronic control's signal interfaces in range reference sensor inputs (i.e., frequencies, resistance, and voltages) for testing the signal interfaces. These simulated sensor inputs are routed to a test connector on the electronic unit, through the signal cable and into the input circuitry. The processor goes through a normal program and outputs through the test connector to the MTU, the sensor digital data, and the fault light indication discrete. The MTU provides a digital display for each sensor output and fault light indication.

RELIABILITY CONSIDERATIONS

The additions and modifications to the basic helicopter engines associated with MPA must be selected, designed and applied so as not to degrade the reliability of the engines. It is also essential to the credibility of MPA that failure indications be maintained.

To enhance the reliability of the MPA hardware, the following minimum design goals should be used:

1. All MPA electronic components will be rated for continuous operation at +257°F, with an anticipated maximum Electronic Unit ambient temperature of +160°F and a typical maximum internal heat rise of approximately 50°F of a thermal margin of 50°F provided to enhance the reliability of the Electronic Unit. Storage temperature limitations are in excess of +200°F.

   Present state-of-the-art electronics packaging techniques allow continuous avionics operations in ambients in excess of component temperature ratings. However, since this requires elaborate cooling techniques, it is recommended that the MPA electronic unit be mounted in an avionics equipment bay.

2. Further improvement of the reliability of the system may be provided by de-energizing the MPA System after takeoff.

3. All circuit components will be limited in electrical stress to no more than 50% of the rating of the component. Since component malfunction bears direct relationship to temperature and stress levels, this constraint is very effective in increasing the reliability of the MPA hardware.

DIAGNOSTIC CAPABILITY

The MPA system through its use of Gas Path Analysis (GPA) meets the basic requirements for a comprehensive diagnostic system.

GPA for fault isolation provides a powerful tool which, when used in conjunction with the use of known techniques for engine accessory and mechanical component diagnosis, can lead to significant benefits to engine users in terms of reduced maintenance, overhaul and operating costs brought about by timely, exact knowledge of engine status. The technique is applicable for all engine types and in practice is customized to the particular engine installation, instrumentation, and operational history. It is based on relative sensor measurement shifts rather than the absolute measurement and hence is primarily influenced by instrumentation (sensor) repeatability, which is always better than absolute accuracy. It is valid for all multiple combinations of sought-for faults, with isolation to specific modules.

Execution of GPA for diagnostics involves only multiplication and addition to solve the set of linear equations summarized in Table XIX. The GPA diagnostic equation set is identical to the MPA equation set except for the computation of DAN in equation 6 which would require a P_7 power turbine inlet pressure measurement.

Equation set (6) in Table XXXIII defines the six critical engine parameters used to determine whether a significant problem exists in the engine. Table XXXIV summarizes some of the engine problems that can be detected by changes in these six parameters. This table illustrates the general level of diagnostics obtained with GPA. It also illustrates that a more complete and timely diagnostic procedure can be obtained if the results of GPA are reinforced by the results of other diagnostic procedures such as engine bearing lubrication and vibration analysis procedures.

The GPA data requirements for MPA and engine health indication are basically identical. The need for custom baselines for a specific engine for MPA are also needed for diagnostics. This is required since the variations between engines in a new condition are essentially of the same magnitude as the diagnostic limits assigned to each engine variable. As it is not recommended that diagnostic limits be adjustable for specific engines, a custom baseline must be developed for each engine in order to avoid premature engine removal. Proper analysis of any engine demands steady-state engine conditions. The steady-state requirements for MPA are also requirements for the diagnostic measurements.

TABLE XXXIII. GPA EQUATION SET FOR DIAGNOSTICS

I. Refer low-power sensor readings to standard-day conditions.

$$\theta_1 = T1/518.7$$

$$\delta 1 = P_1/14.7$$

$$N_{1C} = N_1/\sqrt{\theta_1}$$

$$N_{2C} = N_2/\sqrt{\theta_1}$$

$$P_{3C} = P_3/\delta_1$$

$$T_{3C} = T_3/\theta_1 \qquad (1)$$

$$W_{fC} = W_f/\delta_1\theta_1 Y$$

$$SHP_C = SHP/\delta_1\sqrt{\theta}_1$$

$$P_{7C} = P_7/\delta_1$$

$$T_{7C} = T_7/\delta_1$$

TABLE XXXIII. CONTINUED

II. Determine baseline values from stored hardware at the same P_{3C} value as in I.

$$N_{1CB} = f_1 (P_{3C})$$

$$N_{2CB} = f_2 (P_{3C})$$

$$T_{3CB} = f_3 (P_{3C})$$

$$W_{fCB} = f_4 (P_{3C}) \qquad (2)$$

$$SHP_{CB} = f_5 (P_{3C})$$

$$P_{7CB} = f_6 (P_{3C})$$

$$T_{7CB} = f_7 (P_{3C})$$

III. Compute optimal corrected SHP from corrected SHP.

$$\text{Correction Factor (CF)} = \left[(N_{2C} - N_{2CB}) / N_{2CB} \right]^2 \qquad (3)$$

$$SHP_{CO} = SHP_C / (1 - CF) \qquad (4)$$

IV. Compute the relative deviation of the measurement data from the stored baseline data.

$$DN1 = (N_{1C} - N_{1CB}) / N_{1CB}$$

$$DT3 = (T_{3C} - T_{3CB}) / T_{3CB}$$

$$DWF = (W_{fC} - W_{f\,CB}) / W_{fCB}$$

$$DSHP = (SHP_{CO} - SHP_{CB}) / SHP_{CB} \qquad (5)$$

$$DT7 = (T_{7C} - T_{7CB}) / T_{7CB}$$

$$DP7 = (P_{7C} - P_{7CB}) / P_{7CB}$$

TABLE XXXIII. CONTINUED

V. Compute the variations in airflow pumping capacity, efficiencies, and geometries from the following matrix equation.

$$\begin{bmatrix} DWA \\ DETAC \\ DETAT \\ DETAPT \\ DA5 \\ DAN \end{bmatrix} = \begin{Bmatrix} (W_{aC} - W_{aCB}) / W_{a_{CB}} \; PC \\ (\eta_C - \eta_{CB}) / \eta_{cb} \\ (\eta_t - \eta_{tB}) / \eta_{tB} \\ (\eta_{pt} - \eta_{ptB}) / \eta_{ptB} \\ (A_5 - A_{5B}) / A_{5B} \\ (A_N - A_{NB}) / A_{NB} \end{Bmatrix} = B \begin{bmatrix} DN1 \\ DT3 \\ DWF \\ DSHP \\ DT7 \\ DP7 \end{bmatrix} \qquad (6)$$

TABLE XXXIV. GPA ENGINE HEALTH INDICATION CAPABILITY

Problem	Indicator
1. Compressor Fouling	Loss in either engine pumping capacity (Wac) and compressor efficiency (η c)
2. Bowed First-Stage (Gas Generator) Nozzle	Increase in high pressure turbine inlet area (A_5) coupled with related high pressure turbine efficiency (η_t) loss
3. Fouled Turbines or Worn Turbine Seals	Loss in both high and low pressure turbine efficiency (η_t and η_{pt})
4. Combustion Hot Spots or Plugged Burner Nozzles	Change in power turbine inlet gas temperature (T_{7C}) profile
5. Missing Blades	
Compressor	Loss in either engine pumping capacity (W_{ac}) and compressor efficiency; differentiable from compressor fouling by vibration measurement
Turbine	Changes in high- and low-pressure turbine inlet areas (A_5, An) and efficiencies (N_t, N_{pt})

The potential source of error in any diagnostic system involves the accuracy of the transducer selected to measure a parameter. The absolute accuracy is not a source of error in diagnostics because the custom baseline is obtained using the same transducer used also for diagnostic measurements. The important error source for diagnostics is long-term repeatability of the transducer. This repeatability is generally much less than the quoted accuracy but is not negligible. It is a sensor requirement, therefore, that the diagnostic limits be much larger than the transducer repeatability (two to four times) in order to prevent premature engine maintenance due to faulty prediction.

Engine diagnostics are not limited to engines operating at maximum conditions only. It may be inferred that a given high power shift will occur if a medium power shift has been encountered.

Diagnostic limits are established for each of the six critical parameters. These limits are determined by examining the degradation that is indicative of required maintenance. They are defined by the engine manufacturer or by testing large numbers of engines. Exceedance at any engine operating power level of any diagnostic limit implies exceedance (when operating at 100% NRP) of one of the following criteria and the need for a complete engine overhaul.

1. Turbine Inlet Temperature Limit
2. Excess SFC
3. Shaft Horsepower Decrease
4. Excess Fuel Flow
5. Gas Generator Speed

Data is required to establish diagnostic limits as described above and also to establish a basis for trending the performance of the various engine components. These trends once established are used to determine how the wear is accumulating or trending, and extrapolated to determine when a serious condition is most likely to occur. The potential for more efficient maintenance can be developed through trending (and prognosis), because the status of critical engine components will be known and slack periods can be used to service those portions which are known to be approaching a maintenance condition.

The first step in GPA diagnostics is to determine if a significant problem exists. This question is answered by comparing the six critical parameters with their associated limits. The parameters and limits are as previously discussed in this section. If these parameters have not exceeded their respective limits, the engine is defined as being in good condition and no immediate action is required. It must be emphasized that flight data is not discarded but is incorporated into the ground based history files for trending and prognosis.

A prognosis limit exceedance in any of the six critical parameters is sufficient to initiate a search of the detailed health logic to isolate the specific faults. This search is capable of isolating a need for cleaning or inspection in addition to replacement and overhaul. Finally, decisions as to the operational status of the engine are investigated. Simple faults such as the need for cleaning or inspection, while demanding preventive maintenance, are not sufficient cause to remove the helicopter from operational status. A combination of faults which indicate that a single component replacement is required will produce a message that the helicopter is marginal and limited to restricted usage. The requirement that at least two of the three major engine components need to be changed is usually sufficient reason to ground the helicopter.

A prognosis limit exceedance in any of the six critical parameters is sufficient to initiate a search of the detailed health logic to isolate the specific faults. This search is capable of isolating a need for cleaning or inspection in addition to replacement and overhaul. Finally, decisions as to the operational status of the engine are investigated. Simple faults such as the need for cleaning or inspection, while demanding preventive maintenance, are not sufficient cause to remove the helicopter from operational status. A combination of faults which indicate that a single component replacement is required will produce a message that the helicopter is marginal and limited to restricted usage. The requirement that at least two of the three major engine components need to be changed is usually sufficient reason to ground the helicopter.

CONCLUSIONS

Conclusions resulting from this study are as follows:

1. The concept of predicting MPA from a helicopter gas turbine engine, while taking into account variations in ambient conditions and engine degradation, is feasible.

2. The MPA can be predicted with an accuracy of ± 2.8% at power levels greater than 50%. Errors associated largely with engine parametric sensors, control power limit errors and the influence of nonstandard day limit the accuracy of the system.

3. Configuration and implementation of the MPA system have been defined, and the system is considered to be feasible. Considerable accuracy improvements are obtained through custom calibration of the turbine inlet temperature and the shaft horsepower sensors; however, further sensor development in these areas would eliminate the need for custom calibration.

4. The use of a continuous update system does not significantly improve system accuracy.

5. An MPA prediction system can be implemented using present-day state-of-the-art digital electronic technology. This system would include an electronic unit for baseline storage and MPA calculations, an Indicator/Control Unit which would display the MPA and the necessary engine sensors.

6. The MPA System (electronics and sensors) providesthe majority of the computational capabilities to implement an engine diagnostic system.

7. The evaluation of the MPA prediction method using actual T53-L13 engine data was inconclusive. The engine data provided was obtained with engine sensors significantly inaccurate with respect to MPA requirements. Secondly, the engine data was available from 60% power level to 100%, excluding the possibility of evaluations below 60% normal rated power. The one-point method had the majority of its predictions within the accuracy limitations of the engine data available; however, improved engine data would provide a basis for a more conclusive analysis. The second method, the two-point method, while demonstrating promise,

was implemented at too late a stage in the program to be fully evaluated. Additional study of the two-point method with improved engine data at power levels of 30% to 100% is required.

8. There was no trend in the MPA prediction accuracy as a function of each engine's life (1200 hours to 4200 hours).

RECOMMENDATIONS

1. Analytical Studies

Analytical studies should be conducted to determine if the one-point or two-point prediction method provides the most accurate MPA computational system. In order to perform this analysis more accurate engine data over power levels from 30% to 100% is required. This data could be acquired under the breadboard testing proposed in Hardware Fabrication.

2. Hardware Fabrication

Concurrent with these analytical studies, an engineering breadboard MPA system should be fabricated. The breadboard system could be used in conjunction with a Lycoming T53, General Electric T64 or a more modern engine design such as a General Electric T700.

Breadboard hardware can be fabricated economically and within a reasonable length of time. Existing state-of-the-art parametric sensors can be used for initial system development.

It is imperative that this MPA breadboard system be utilized to obtain more accurate engine data over power levels from 30% to 100%. The breadboard could then be utilized to evaluate the MPA prediction method. Engine sensors with the best accuracy possible should be utilized; if this is not possible, custom calibration of some sensors, for test cell purposes only, may very well bring all engine sensors within the MPA system sensor accuracy requirements. A long-term engine test is required where (1) several hundred hours will elapse between the baseline acquisition and MPA predictions, and (2) engine parametric sensor data may be obtained at power levels from 30% normal rated power to maximum power; these are essential to the success of an additional phase.

The breadboard hardware could be designed so that only minor modifications are required to allow the use of more accurate sensors, as they become available, and to allow growth from an MPA system to a hover-lift computer system or small diagnostic system.

APPENDIX I

THE MAXIMUM POWER AVAILABLE PREDICTION COMPUTER PROGRAM MANUAL

SUMMARY

This manual describes the usage of the Maximum Power Available Prediction Computer Program in order to allow the evaluation of the prediction method using T53-L13 engine data. This program is based upon an investigation conducted by Hamilton Standard Division of UAC, Windsor Locks, Connecticut, to determine the feasibility of developing a method to predict the maximum power available (MPA) from a helicopter gas turbine engine at full-power conditions. The MPA prediction was to be made with an accuracy goal of at least ±1%, using information obtained from the engine while the engine was operated at a partial-power condition from 50% to 90% of normal rated power. The Lycoming T53-L13 engine, a gas turbine engine presently in use on the Army UH-1 helicopter, was selected for the investigation.

This manual describes the program format and provides a computational flow diagram to assist the user of the computer program to evaluate the MPA prediction method. The program has been written in FORTRAN IV programming language and is compatible with the Fort Eustis IBM 360 system. The program loading instructions (for engine data, B and C Matrix constants, etc.) and output data format (MPA predictions, variation calculations, etc.) are described in detail.

The computer program for the MPA prediction system was developed based on Hamilton Standard's prior experience and knowledge of engine control and diagnostic systems. This method was analyzed to determine the best attainable MPA prediction accuracy and effects on predicted MPA due to all input parameters, the effect of power condition on MPA prediction, and possible alternate MPA prediction methods using various sets of parametric sensors and making various assumptions regarding the relative values of independent engine parameters. The model was further evaluated by the use of actual engine operational test data taken by AVCO Lycoming. The MPA computer program associated with this manual is the result of this evaluation.

The MPA prediction program provides the flexibility to evaluate two prediction methods. The first method consists of taking one frame of engine data, within the baseline range, and using that data to predict the MPA. The second method consists of taking two frames of engine data and extrapolating this data to an MPA prediction. This second method developed at the end of the program provides significantly improved MPA prediction accuracies.

INTRODUCTION

The T53-L13 engine Maximum Power Available (MPA) prediction computer program manual is intended to assist the user in operating the MPA prediction computer program. The MPA prediction program is compatible with both the IBM 360 and the IBM 370 computers. Through the use of this manual and the MPA computer program the MPA of any T53-L13 engine can be predicted. Two program options are available to the user. The first predicts MPA based on one set of sensor measurements; the second predicts MPA based on two sets of sensor measurements. As an added feature the effects of control and sensor inaccuracy at high power on predicted power, as well as the effects of uncertainty in compressor discharge air bleed and shaft power extraction at high power on predicted power, can be obtained. Figure 28 of this manual provides the user with a block diagram of the MPA prediction method to assist in the evaluation of the significance of each parameter on the MPA prediction.

This manual has been developed under contract DAAJ02-73-C-0047 sponsored by the Eustis Directorate, U. S. Army Air Mobility Research and Development Laboratory, Fort Eustis, Virginia.

DISCUSSION

Hamilton Standard has developed a computer algorithm for predicting maximum power available from a free turbine engine based on measurements taken at reduced engine power. This activity was sponsored by Eustis Directorate, U. S. Army Air Mobility Research and Development Laboratory, Fort Eustis, Virginia under contract DAAJ02-72-C-0003 (USAAMRDL Technical Report 72-58). A detailed description of the operation of this computer algorithm is included in the reports written under this contract. A block diagram of this computer algorithm is provided in Figure 28 to assist the user in following the MPA computer prediction program. Various function blocks in Figure 28 have block designations and are referred to in the MPA computer deck description.

The MPA prediction program computer deck was developed to analyze a single-spool, free turbine engine. Numerical data provided is specifically for the Lycoming T53-L13 engine. Printout format is specifically for set IV sensors (T_1, P_1, N_1, N_2, P_3, T_3, W_f, SHP, T_7 and assume $\partial A_N / AN = \partial \eta_{PT} / \eta_{PT}$). In addition to calculating the MPA, the computer program has the flexibility to be utilized to determine the effects of additional sources of error in the MPA prediction accuracy such as bleed air (W_{BL}) and the sensitivity of SHP to engine airflow (SHP/WA).

The model is based upon the assumption that maximum power is limited by one of three limits: a gas generator speed limit, a gas generator turbine discharge temperature limit, or a metered fuel flow limit in the engine control. The speed limit is obtained from a droop type control with a droop slope given by:

$$\frac{\partial W_f / \delta_1}{W_f / \delta_1} \Big/ \frac{\partial N_1 / \sqrt{\theta}_1}{N_1 / \sqrt{\theta}_1} = -6.5$$

A

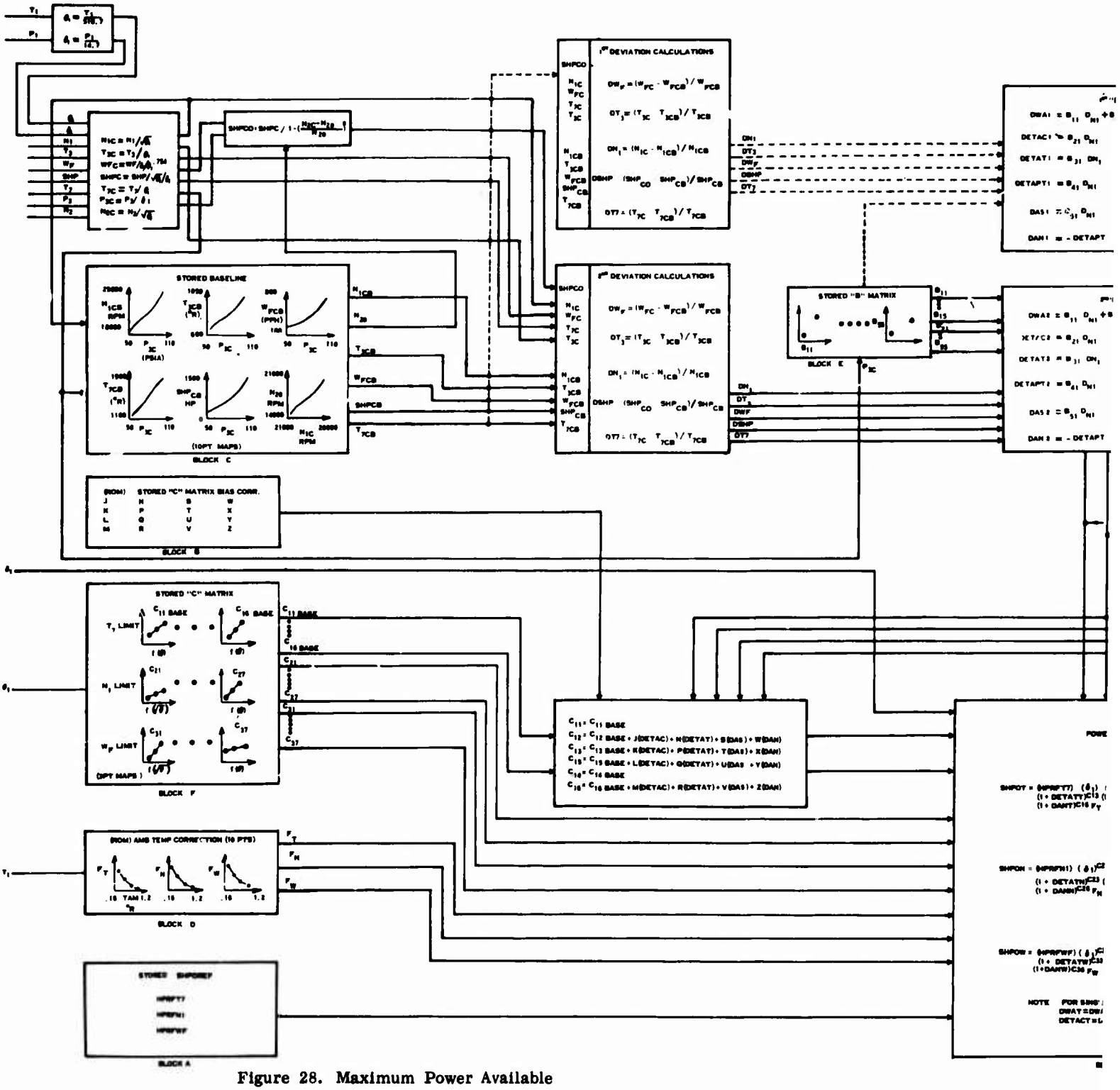

Figure 28. Maximum Power Available Computer Program.

B

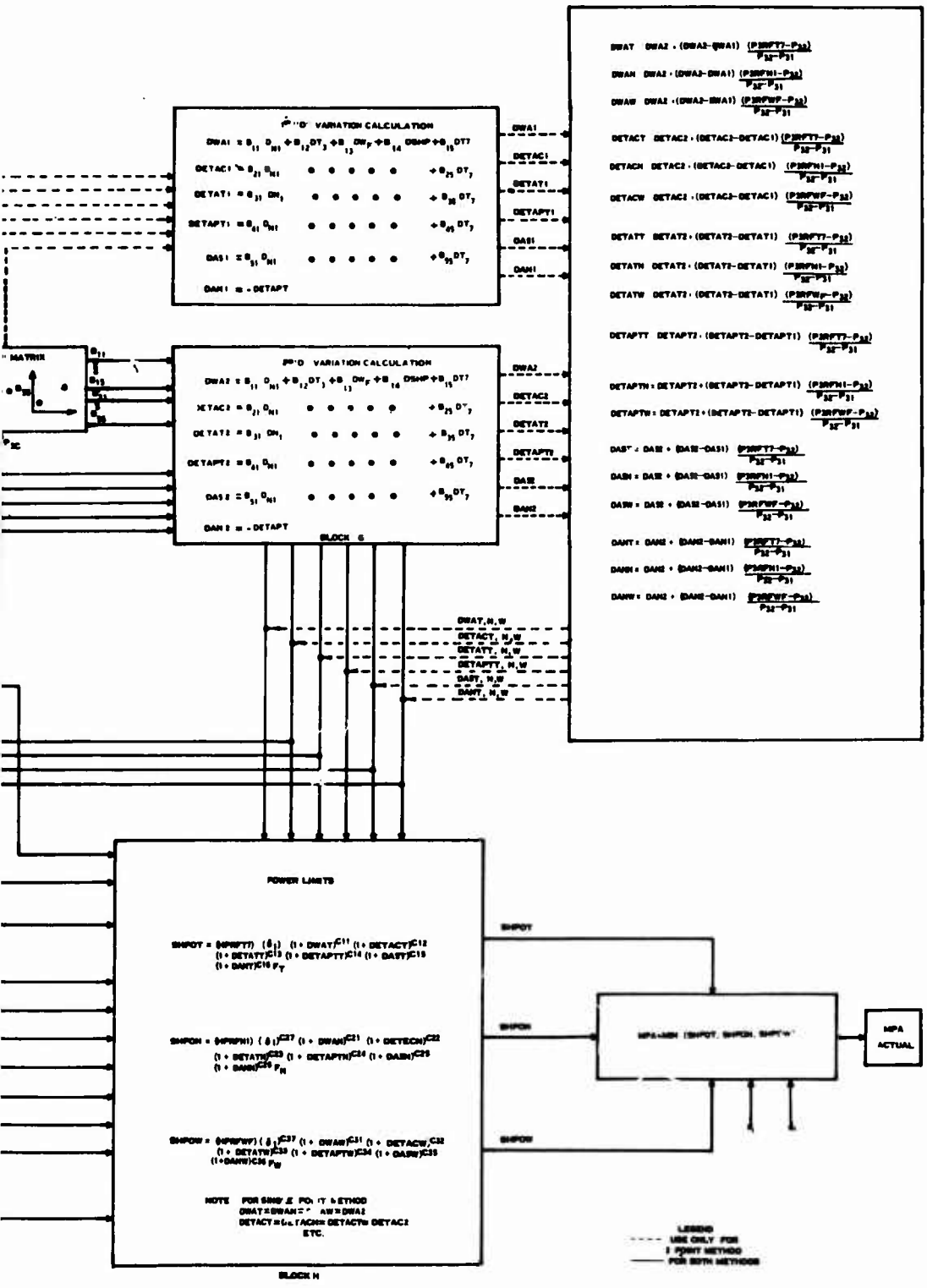

Preceding page blank

GENERAL DESCRIPTION

The user of this manual must provide T53-L13 engine data, maximum horsepower baseline references and compressor discharge pressure at the maximum horsepower baseline references to perform the MPA prediction. Engine data is loaded into the program representing two different periods of time in the history of the engine. The data from the first period provides the engine baseline characteristics. The second set of data is compared to the baseline data by the program to develop the degree of degradation represented and to compute the MPA. The engine baseline data must be loaded into the program at discrete power level points that encompass the range of power levels to be evaluated. The second set of data is a discrete frame (s) of data representing one (two) engine operating condition(s). Two requirements of this data are:

1. In corrected parameter form the data must be within the range of the baseline data.

2. No engine changes affecting engine performance may have been incorporated since the baselines were obtained.

The prediction program allows computation of the MPA at power levels within the range of the baseline data.

The initial set of data locations (1-16) are for program instructions and run definitions. Data locations 21-36 contain C matrix bias corrections used only on the T_7 limit computation. This data is provided in the sample program with the recommended values.

- Data locations 51 through 110 are used to load the engine baseline data. This baseline data must encompass all the power levels to be evaluated as well as the 100% NRP level. While the sample program contains a set of engine baseline data, the user must load this data for each engine to be evaluated.

- Locations 121 through 140 contain the stored N_2 optimum vs. N_1 curve which is fixed data and provided with the sample program. These values should not be changed.

- Data locations 141 through 180 contain the ambient temperature correction factors which are fixed constants and provided with the sample program. These values also should not be changed.

- Data locations 701 through 880 contain the C matrices for each of the three fuel control governing limits (N_1, T_7 and W_f). Locations 701 through 760 contain the C matrix values for $N_1/\sqrt{\theta_1}$ = 100% (701 - 720 N_1 limit, 721 - 740 T_7 limit and 741 - 760 W_f limit). Locations 761 through 820 contain the C matrix for $N_1/\sqrt{\theta_1}$ = 112%

and locations 821 through 880 contain the C matrix for $N_1/\sqrt{\theta_1}$ = 88%. Terms in these matrices not identified as C matrix terms are additional terms not required for the MPA calculation. These additional terms may be used primarily for determining the effects of sensor and fuel control accuracies on the MPA prediction.

- Data locations 1001 through 1100 are where the engine data from which the MPA is to be predicted is loaded. The data for each condition is grouped in 20 locations (e.g., 1001 through 1020, next condition 1021 through 1040). The following uncorrected (not referred) actual engine data is required for an MPA prediction:

  N_1 , T_3 , W_f , SHP, T_7, W_{BL} *, SPE*, P_3 , N_2 , θ_1 (T_1 /519°R) and δ_1 (P_1 / 14.7PS1A).

  Terms DNCSET, DNCSEN, DT7SET, DT7SEN, DTIC, DPIC, DWFC and PIPAM are all optional terms which normally should be loaded as zeros, except PIPAM which should be loaded as unity. These optional terms were used primarily to evaluate the sensor and fuel control accuracies.

  *Not needed for engine test cell data.

The output data is presented in nine lines for the method with one set of sensor measurements or eleven lines with two sets.

- Lines 1 and 2 are the actual engine input frame data.
- Line 3 contains the corrected engine input data.
- Line 4 contains the corrected baseline data.
- Line 5 (5, 6 and 7) contains the calculated engine degradations such as the change in engine pumping capacity DWA.
- Lines 6, 7, and 8 (8, 9 and 10) contain the horsepower multiplication factors for the speed (N_1), temperature (T_7), and fuel flow (W_f) limits. Each multiplication factor is obtained by raising the appropriate degradation factor to a C matrix exponent.
- Line 9 (11) contains the corrected and uncorrected values of MPA for each limit as well as the MPA prediction.

Data Input

Card Format and Program Instructions

The computer cards necessary to run the MPA deck are described as follows:

The first card is a title card which documents the case to be run. All 80 card columns can be used for the title. Data cards are entered after the title card using the following format:

cc	1	2-12	13-24	25-36	37-48	49-60	61-72
	n	data loc	data	data	data	data	data

where:

cc = card column number

n = number of pieces of data input on this card

data loc = number to indicate where data storage starts

data = actual data (5 per card maximum)

Data loc and data are fixed point numbers whereas n is an integer (0, 1, 2, 3, 4 or 5). The fixed point numbers may be located anywhere within the assigned card columns. After the last data card is read in, further reading is inhibited by a card containing n = 0 and data loc = -1. If another case is to be run, this 0-1. card is followed by another title card, data cards, 0-1. card, etc., until all cases are defined. The run is terminated by a blank card replacing the next case title card. Any data locations not specified in case 1 will have a value of 0 in case 1. Only data that changes need be defined in subsequent cases.

Data Locations

The data to be loaded is defined as follows:

Instructions

Data Location	Symbol	Definition
1.	RITEF	If a number >0. is loaded, the baseline functions will be printed out.
2.	RITEB	If a number >0. is loaded, the "B" coefficient matrices will be printed out.
3.	RITEC	If a number >0. is loaded, the "C" coefficient matrices will be printed out.
4.	RITED	If a number >0. is loaded, the frame* data will be printed out.
5.	ZNBJ	Number of rows defining the "B" matrix (10 maximum)
6.	ZNBI	Number of columns defining the "B" matrix (10 maximum)
7.	ZNF	Number of frames of data loaded for this case (5 maximum)
8.	HPRFN1	Horsepower baseline reference for the N_1 limit (Block A, Figure 1)
9.	HPRFT7	Horsepower baseline reference for the T_7 limit (Block A, Figure 1)
10.	HPRFWF	Horsepower baseline reference for the W_f limit (Block A, Figure 1)
11.	P3RFN1	Value of P_3 at which baseline engine encounters N_1 limit
12.	P3RFT7	Value of P_3 at which baseline engine encounters T_7 limit

*A frame of data is made up of the values for the measurements N_1, T_3, W_f, SHP, T_7, P_3, N_2, T_1, and P_1

Data Location	Symbol	Definition
13.	P3RFWF	Value of P_3 at which baseline engine encounters W_f limit
14.	EXTRAP	= 1. means single measurement with no extrapolation = 2. means dual measurement with extrapolation
15.	ZNP1 **	First measurement set used with dual-measurement MPA
16.	ZNP2	Second measurement set used with dual-measurement MPA

** If all 5 frames of measurement data are loaded as required in order of decreasing power, e. g., 90, 80, 70, 60 and 50% powers, for a dual measurement at 60 and 80% power, EXTRAP is set equal to 2 and ZNP1 and ZNP2 must be loaded as 2 and 4 respectively. For a dual measurement at 60 and 70% power, ZNP1 is set equal to 3.

Derivation of HP Reference (HPRFT7, etc.) and P3 Reference (P3RFT7, etc.)

The three control limits from which the HP and P3 references are determined are:

$$N_{1C} = 25400 \text{ rpm}$$

$$T_{7C} = 1840^{\circ}R$$

$$W_{FC} = 820 \text{ pph}$$

These values are defined to be the corrected control limits of the T53-L13 engine at 100% normal rated power.

Using the W_{FC} limit of 820PPH and the T_{7C} limit of 1840°R, the P3 and HP reference values at each limit are determined for an engine from its baseline data. On a plot of W_{FC} versus N_{1C} from the engine's baseline data, the engine droop characteristic

$$\frac{\partial W_F / \delta_1}{W_F / \delta_1} \div \frac{\partial N_1 / \sqrt{\theta_1}}{N_1 / \sqrt{\theta_1}} = -6.5$$

is plotted through the N_{1C} = 25,400 RPM and W_{FC} = 820 PPH point. At the intersection of the droop characteristic and the engine's steady-state W_{FC} vs. N_{1C} characteristic, a value for an engine's N_1 limit is determined. For the engine's N_1 limit, reference values of P_3 and HP are determined from the baseline data of the engine.

These control limits were derived by Hamilton Standard during its evaluation of the MPA prediction method using engine data procured from AVCO Lycoming. The limits were determined by averaging the recorded values of each parameter at the 100% normal rated power point for a sample lot of ten engines. These control limits are the recommended values to be used regardless of the number of engines to be evaluated.

C Matrix Bias Corrections

Data Locations 21 - 36 are loaded with the stored "C" matrix bias corrections (Block B Figure 28).

Data Location	Symbol	Definition
21	J	Variation in T_7 "C" coefficient C12 base due to Δ ETA-C
22	N	Variation in T_7 "C" coefficient C12 base due to Δ ETA-T
23	S	Variation in T_7 "C" coefficient C12 base due to Δ A5
24	W	Variation in T_7 "C" coefficient C12 base due to Δ AN
25	K	Variation in T_7 "C" coefficient C13 base due to Δ ETA-C
26	P	Variation in T_7 "C" coefficient C13 base due to Δ ETA-T
27	T	Variation in T_7 "C" coefficient C13 base due to Δ A5
28	X	Variation in T_7 "C" coefficient C13 base due to Δ AN
29	L	Variation in T_7 "C" coefficient C15 base due to Δ ETA-C
30	Q	Variation in T_7 "C" coefficient C15 base due to Δ ETA-T
31	U	Variation in T_7 "C" coefficient C15 base due to Δ A5
32	Y	Variation in T_7 "C" coefficient C15 base due to Δ AN
33	M	Variation in T_7 "C" coefficient C16 base due to Δ ETA-C
34	R	Variation in T_7 "C" coefficient C16 base due to Δ ETA-T
35	V	Variation in T_7 "C" coefficient C16 base due to Δ A5
36	Z	Variation in T_7 "C" coefficient C16 base due to Δ AN

Baseline Data

Baseline data are loaded starting with data location 51 and ending with data location 110 (Block C Figure 28)

Data Locations	Data Loaded
51-60	Increasing values of $P_3/\delta 1$ (10 max)
61-70	Corresponding values of $N_1 / \sqrt{\theta}_1$
71-80	Corresponding values of T_3 / θ_1
81-90	Corresponding values of $W_f / \delta_1 \theta_1$
91-100	Corresponding values of $HPPT/\delta_1\sqrt{\theta}_1$
101-110	Corresponding values of T_7 / θ_1

Optimum N_2

Optimum power turbine speed versus gas producer speed is loaded into data locations 121 through 140 (Block C Figure 28).

Data Locations	Data Loaded
121-130	Increasing values of N_1 (10 max)
131-140	Corresponding values of N_2 optimum

F Correction

Data locations 141 through 180 are loaded with horsepower "F" correction data for N_1, T_7, and W_f limits as a function of ambient temperature ratio θ_1 (Block D Figure 28).

Data Locations	Data Loaded
141-150	Increasing values of θ_1 (10 max)
151-160	Corresponding values of N_1 limit HP correction factor
161-170	Corresponding values of T_7 limit HP correction factor
171-180	Corresponding values of W_f limit HP correction factor

B Matrix

Five values of P_3/δ_1 at which corresponding values of the "B" matrix are obtained are loaded into data locations 196 through 200. Starting in data locations 201, 301, 401, 501 and 601 are loaded the "B" matrix values obtained at the values of P_3/δ_1 loaded into data locations 196 through 200, respectively (Block E). The following is the format of the "B" matrix for use with set IV sensors including two rows used only for error analysis and not for MPA prediction.

GAM1	ETA-C	ETA-T	ETA-PT	A5	AN	
201 (B11)	202 (B21)	203	204	205	206	$N_1 / \sqrt{\theta_1}$
211 (B12)	212	213	214	215	216	T / θ_1
221	222	223	224	225	226	$W_f/\delta_1 \theta_1$
231	232	233	234	235	236	$HP/\delta_1\sqrt{\theta_1}$
241	242	243	244	245	246	T_7/θ_1
251	252	253	254	255	256	WABL *
261	262	263	264	265	266	SHP/WA*

*This portion of the matrix is not required for the MPA prediction.

According to the assumption used with set IV sensors, i. e., $\partial A_N / A_N = - \partial \eta_{PT} / \eta_{PT}$, the values of column A_N are equal to the negative of the values of column ETA-PT.

C Matrix

Starting in data locations 701, 761, and 821 are loaded three "C" matrices obtained at values of $N_1/\sqrt{\theta}_1$ of 100%, 112% and 88% respectively (Block F Figure 28). The following is the format of the "C" matrix:

N_1 GOV

GAM-1	ETA-C	ETA-T	ETA-PT	A5
701.(C21)	702.(C22)	703.(C23)	704(C24)	705. (C25)
AN	WABL	0	PAM	P1/PAM
706.(C26)	707.	708.	709(C27)	710.
DWFC	DTIC	DNC2-DNC1	SHP/WA	
711.	712.	713.	714.	

T_7 LIM

GAM-1	ETA-C	ETA-T	ETA-PT	A5
721.(C11)	722.(C12)	723.(C13)	724.(C14)	725.(C15)
AN	WABL	0.	PAM	P1/PAM
726.(C16)	727.	728.	729.(C17)	730.
T_7 Set + Sen		SHP/WA		
731.		732.		

W_f LIM

GAM-1	ETA-C	ETA-T	ETA-P7	A5
741.(C31)	742.(C32)	743(C33)	744.(C34)	745.(C35)
AN	WABL	0.	PAM	DPIC
746.(C36)	747	748	749.(C37)	750
DWFC	SHP/WA			
751	752			

Input Frame Data

The input frame data representing measured engine data taken at a time later than the baseline data is loaded into data locations 1001 through 1100 in sequences of 20 data locations. The first data frame is described as follows:

Data Location	Symbol	Definition
1001	N_1	Actual measured N_1 - rpm
1002	T_3	Actual measured T_3 - ^oR
1003	W_f	Actual measured W_f - pph
1004	SHP	Actual measured SHP - hp
1005	T_7	Actual measured T_7 - ^oR
1006	-WBL	Actual measured bleed air - pps
1007	SPE	Actual measured shaft power extraction per pound per second engine airflow - hp/pps
1008	--	Not Used
1009	P_3	Actual measured P_3 - psia
1010	N_2	Actual measured N_2 - rpm
1011	THETA = $\frac{T1}{519^oR}$	Correction to standard day temperature (T = 59^{o}F) - ratio
1012	DELTA = $\frac{P1}{14.7\ psia}$	Correction to standard day pressure - ratio
1013	DNCSET	Fractional error in N_1 set speed to determine effect on predicted horsepower when on N_1 limit
1014	DNCSEN	Fractional error in N_1 sensed speed to determine effect on predicted horsepower when on N_1 limit
1015	DT7SET	Fractional error in T_7 set temperature to determine effect on predicted horsepower when on T_7 limit
1016	DT7SEN	Fractional error in T_7 sensed temperature to determine effect on predicted horsepower when on T_7 limit

Data Location	Symbol	Definition
1017	DTIC	Fractional error in T_1 compressor inlet temperature to determine the effect on predicted horsepower when on N_1 limit
1018	DPIC	Fractional error in P_1 compressor inlet pressure to determine the effect on predicted horsepower when on W_f limit
1019	DWFC	Fractional error in W_f engine fuel flow to determine the effect on predicted horsepower when on N_1 and W_f limits
1020	PIPAM	Ratio of P_1 to P ambient pressures - ratio (under static conditions = 1)

This completes the definition of the input data.

Data Output

The output data from the MPA prediction program has been selected to permit evaluation of the prediction results. It consists of the data input, corrected data input, the "D" calculations at the 3 limits and is described as follows:

Lines 1 & 2 - AU Parameters

These parameters are actual engine input data and are identical to the corresponding input frame data described in the previous section.

Line 3 - AC Parameters

These parameters are corrected engine input data and are the values of the input frame data after being corrected to standard day conditions.

Line 4 - AB Parameters

These parameters are corrected baseline data and are the values of N_1, T_3, W_f, etc., obtained from the stored baselines at a value of P_3 = PS3C.

Line 5 (5, 6 and 7) AA Parameters

Degradation Terms - Block G

Symbol	Definition
DWA	Change in engine pumping capacity between current measurements and baseline measurements.
DETAC	Change in compressor efficiency between current measurements and baseline measurements.
DETAT	Change in turbine efficiency between current measurements and baseline measurements.
DEPT	Change in power turbine efficiency between current measurements and baseline measurements.
DA5	Change in gas generator turbine inlet nozzle effective area between current measurements and baseline measurements.
DAN	Change in power turbine inlet nozzle effective area between current measurements and baseline measurements.

DWAN, DWAT, DWAW, etc., for degradations using the two-point method for the speed (N), temperature (T), or fuel (W) limits respectively.

Line 6 (8) HN Parameters

Multiplication Factors when on N_1 Speed Limit - Block H

Symbol	Definition
$(1 + DWA)^{C21}$	Horsepower multiplication factor when on speed limit due to a change in engine pumping capacity.
$(1 + DETAC)^{C22}$	Horsepower multiplication factor when on speed limit due to a change in compressor efficiency.
$(1 + DETAT)^{C23}$	Horesepower multiplication factor when on speed limit due to a change in turbine efficiency.
$(1 + DEPT)^{C24}$	Horesepower multiplication factor when on speed limit due to a change in power turbine efficiency.
$(1 + DA5)^{C25}$	Horsepower multiplication factor when on speed limit due to a change in gas generator turbine inlet nozzle effective area.
$(1 + DAN)^{C26}$	Horsepower multiplication factor when on speed limit due to a change in power turbine inlet nozzle effective area.

Symbol	Definition
-WBL	Horsepower multiplication factor when on speed limit due to bleed air flow uncertainty.
$(DELTA)^{C27}$	Horsepower multiplication factor when on speed limit due to nonstandard day pressure.
PIPAM	Horsepower multiplication factor when on speed limit due to P1 not being equal to P ambient.
DWFC	Horsepower multiplication factor when on speed limit due to error in fuel flow.
DTIC	Horsepower multiplication factor when on speed limit due to error in compressor inlet temperature.
DNSET/N	Horesepower multiplication factor when on speed limit due to errors in gas generator set and sensed speed measurements.
SPE	Horsepower multiplication factor when on speed limit due to shaft power extraction uncertainty.
$f_N = f(THETA)$	Horsepower multiplication factor when on speed limit due to "C" variations with nonstandard day temperature.

Line 7 (9) HT Parameters

Multiplication Factors When on T_7 Temperature Limit - Block H

Symbol	Definition
$(1 + DWA)^{C11}$	Horsepower multiplication factor when on temperature limit due to a change in engine pumping capacity.
$(1 + DETAC)^{C12}$	Horsepower multiplication factor when on temperature limit due to a change in compressor efficiency.
$(1 + DETAT)^{C13}$	Horsepower multiplication factor when on temperature limit due to a change in turbine efficiency.
$(1 + DEPT)^{C14}$	Horsepower multiplication factor when on temperature limit due to a change in power turbine efficiency.

Symbol	Definition
$(1 + DA5)^{C15}$	Horsepower multiplication factor when on temperature limit due to a change in gas generator turbine inlet nozzle effective area.
$(1 + DAN)^{C16}$	Horsepower multiplication factor when on temperature limit due to a change in power turbine inlet nozzle effective area.
-WBL	Horsepower multiplication factor when on temperature limit due to bleed airflow uncertainty.
$(DELTA)^{C17}$	Horsepower multiplication factor when on temperature limit due to nonstandard day pressure.
PIPAM	Horsepower multiplication factor when on temperature limit due to P_1 not being equal to P ambient.
DTSET/N	Horsepower multiplication factor when on temperature limit due to errors in turbine inlet set and sensed temperature measurements.
SPE	Horsepower multiplication factor when on temperature limit due to shaft power extraction uncertainty.
$f_T = f$ (THETA)	Horsepower multiplication factor when on temperature limit due to "C" variations with non-standard day temperature.

Line 8 (10) HW Parameters

Multiplication Factors When On Fuel Flow Limit - Block H

Symbol	Definition
$(1 + DWA)^{C31}$	Horsepower multiplication factor when on fuel flow limit due to a change in engine pumping capacity.
$(1 + DETAC)^{C32}$	Horsepower multiplication factor when on fuel flow limit due to a change in compressor efficiency.
$(1 + DETAT)^{C33}$	Horsepower multiplication factor when on fuel flow limit due to a change in turbine efficiency.

Symbol	Definition
$(1 + DEPT)^{C34}$	Horsepower multiplication factor when on fuel flow limit due to a change in power turbine efficiency.
$(1 + DA5)^{C35}$	Horsepower multiplication factor when on fuel flow limit due to a change in turbine inlet nozzle effective area.
$(1 + DAN)^{C36}$	Horsepower multiplication factor when on fuel flow limit due to a change in exhaust nozzle effective area.
-WBL	Horsepower multiplication factor when on fuel flow limit due to bleed airflow uncertainty.
$(DELTA)^{C37}$	Horsepower multiplication factor when on fuel flow limit due to nonstandard day pressure.
DPIC	Horsepower multiplication factor when on fuel flow limit due to error in compressor inlet pressure.
DWFC	Horsepower multiplication factor when on fuel flow limit due to error in fuel flow.
SPE	Horsepower multiplication factor when on fuel flow limit due to shaft power extraction uncertainty.
fW = f (THETA)	Horsepower multiplication factor when on fuel flow limit due to "C" variations with non-standard day temperature.

Line 9 (11) - AE Parameters

Symbol	Definition
SHPØNC	Predicted value of maximum corrected horsepower if on N_1 speed limit.
SHPØTC	Predicted value of maximum corrected horsepower if on T_7 temperature limit.
SHPØWC	Predicted value of maximum corrected horsepower if on W_f fuel flow limit.
SHPMXC	Minimum value of three predicted maximum corrected horsepowers, SHPØNC, SHPØTC, and SHPØWC.
SHPØNU	Predicted value of maximum uncorrected horsepower if on N_1 speed limit.
SHPØTU	Predicted value of maximum uncorrected horsepower if on T_7 temperature limit.
SHPØWU	Predicted value of maximum uncorrected horsepower if on W_f fuel flow limit.
SHPMXU	Minimum value of three predicted maximum uncorrected horsepowers, SHPØNU, SHPØTU, and SHPØWU.

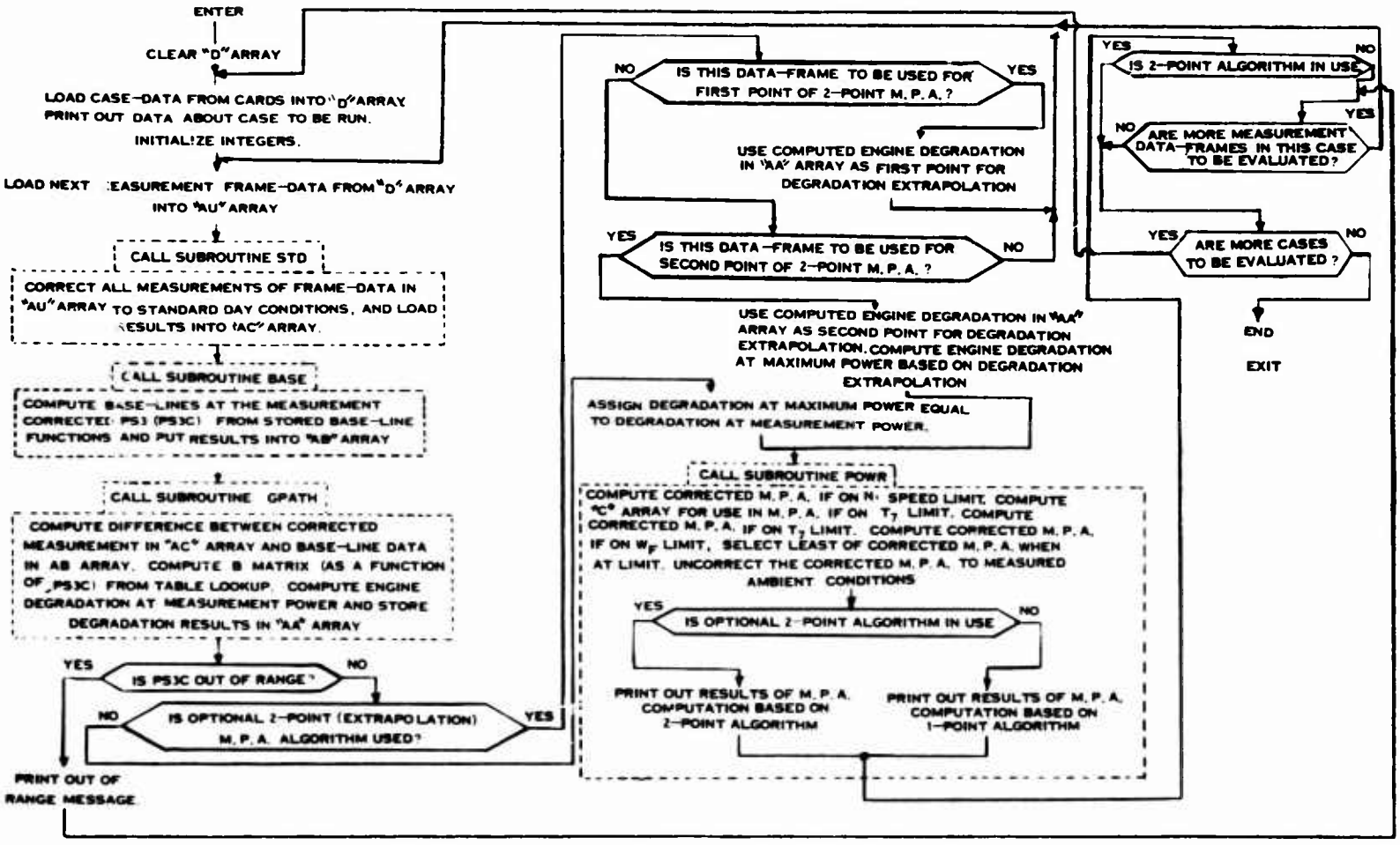

Figure 29. Computer Deck Flow Chart.

APPENDIX II

RECOMMENDED AND SAMPLE INPUT DATA

All data with asterisks are the recommended values of the data. All data without asterisks are sample data and may be changed at the option of the user.

PROGRAM CONTROL DATA

RITEF	RITEB	RITEC	RITED	ZNBJ
1.00000	1.00000	1.00000	1.00000	7.00000
ZNBI	**ZNF**	**HPRFN1**	**HPRFT7**	**HPRFWF**
6.00000	4.00000	1461.00000	1425.00000	1447.00000

OPTIMUM POWER TURBINE SPEED VS. GAS PRODUCER SPEED*

N1	21500.0000	22320.0000	22900.0000	23200.0000	23560.0000
N2	14150.0000	15810.0000	16820.0000	17400.0000	17950.0000
N1	24120.0000	24700.0000	25400.0000	25700.0000	26000.0000
N2	18690.0000	19380.0000	20150.0000	20500.0000	20820.0000

HP CORRECTION ON SPEED, TEMP., AND FUEL FLOW LIMITS AS A FUNCTION OF THETA*

THETA	0.7600	0.8800	0.9200	0.9600	1.0000
N1	1.6450	1.3000	1.1940	1.0980	1.0000
T7	1.9250	1.4500	1.2950	1.1420	1.0000
Wf	1.1010	1.0510	1.0330	1.0170	1.0000
THETA	1.0400	1.0800	1.1200	1.1600	1.2000
N1	0.9115	0.8250	0.7450	0.6700	0.5970
T7	0.8660	0.7480	0.6370	0.5375	0.4500
Wf	0.9830	0.9690	0.9540	0.9410	0.9275

P3'S AT WHICH "B" COEFFICIENTS ARE EVALUATED*

81.80730	89.46799	93.82899	98.15099	105.60480

"B" COEFFICIENTS*

P3C = 81.80730

	GAM-1	ETA-C	ETA-T	ETA-PT	A5
N1	-3.7839975	0.0100000	0.0	0.0000010	-0.0000010
T3	0.1034549	-2.2294254	1.8145847	-0.1012180	0.3416179
Wf	0.9999990	0.0	0.0903710	-0.9783919	1.0695543
HP	0.0000010	0.0	0.3691469	0.4192380	0.0212310
T7	-1.7395105	0.0	-1.3212709	0.9322910	-1.4737644
WABL	-0.6161720	0.0	-0.7602479	-0.3755330	0.3222089
SHP/WA	-0.0022180	0.0	0.0043920	0.0021700	-0.0018620

AN = - (ETA-PT)

P3C = 89.46799

	GAM-1	ETA-C	ETA-T	ETA-PT	A5
N1	-3.4327984	0.0740010	-0.0000010	0.0	-0.0000010
T3	0.1054590	-2.1489553	1.7425718	-0.1029119	0.3397980
Wf	1.0000000	0.0	0.0901560	-0.9758590	1.0685482
HP	0.0	0.0	0.3999259	0.4491570	0.0227790
T7	-1.7032394	0.0	-1.3340130	0.8734739	-1.4341354
WABL	-0.6167530	0.0	-0.7571000	-0.3739940	0.3194330
SHP/WA	-0.0020320	0.0	0.0040140	0.0019830	-0.0016940

AN = - (ETA - PT)

P3C = 93.82899

	GAM-1	ETA-C	ETA-T	ETA-PT	A5
N1	-3.2311974	0.1060010	-0.0000010	0.0000030	-0.0000020
T3	0.1060950	-2.1084414	1.7064734	-0.1034240	0.3383980
Wf	1.0000010	0.0	0.0897410	-0.9748400	1.0679703
HP	0.0	0.0	0.4163049	0.4645270	0.0235970

P3C = 93.82899 Continued

	GAM-1	ETA-C	ETA-T	ETA-PT	A5
T7	-1.6829185	0.0	-1.3394775	0.8423960	-1.4120998
WABL	-0.6173360	0.0	-0.7556600	-0.3730350	0.3176700
SHP/WA	-0.0019370	0.0	0.0038250	0.0018880	-0.0016080

AN = - (ETA-PT)

P3C = 98.15099

	GAM-1	ETA -C	ETA-T	ETA-PT	A5
N1	-3.0331984	0.1420010	-0.0000010	0.0000020	-0.0000020
T3	0.1064840	-2.0714359	1.6737185	-0.1036810	0.3368400
Wf	1.0000000	0.0	0.0896490	-0.9736750	1.0674229
HP	-0.0000010	0.0	0.4327130	0.4803530	0.0244230
T7	-1.6638021	0.0	-1.3456974	0.8120950	-1.3913364
WABL	-0.6181250	0.0	-0.7542950	-0.3718220	0.3157740
SHP/WA	-0.0018490	0.0	0.0036510	0.0018000	-0.0015290

AN = - (ETA-PT)

P3C = 105.60480

	GAM-1	ETA-C	ETA-T	ETA-PT	A5
N1	-2.7055998	0.2260000	-0.0000010	0.0000010	-0.0000020
T3	0.1059189	-2.0129433	1.6222525	-0.1028320	0.3330160
Wf	0.9999990	0.0	0.0905409	-0.9708880	1.0665560
HP	-0.0000010	0.0	0.4579950	0.5054580	0.0256860
T7	-1.6329594	0.0	-1.3561230	0.7626310	-1.3577118
WABL	-0.6196940	0.0	-0.7518010	-0.3692330	0.3124070
SHP/WA	-0.0017120	0.0	0.0033840	0.0016620	-0.0014060

AN = - (ETA-PT)

C COEFFICIENTS*

N1 GOV (88% N1)

GAM-1	ETA-C	ETA-T	ETA-PT	A5
1.2495041	-0.5779859	-0.7957470	1.0046921	0.8254949
AN	**WABL**			**P1/PAM**
-1.6928616	0.9144550	0.0	1.0000000	1.2017241
DWFC	**DTIC**	**DAC2-DNC1**	**SHP/WA**	
0.5639859	-0.7625080	3.6659079	0.0015550	

T7 LIM (88% N1)

GAM-1	ETA-C	ETA-T	ETA-PT	A5
0.1965269	2.9437799	3.9158773	1.0064087	-1.8133783
AN	**WABL**			**P1/PAM**
2.4317856	3.1110544	0.0	1.0000000	1.1711607
T7SET + SEN	**SHP/WA**			
4.2446394	-0.0135260	0.0	0.0	0.0

WF LIM (88% N1)

GAM-1	ETA-C	ETA-T	ETA-PT	A5
0.0506360	0.7584479	1.1180286	1.0053825	-0.5686229
AN	**WABL**		**PAM**	**DPIC**
0.0338840	1.4365196	0.0	-0.9040800	-0.4382700
DWFC	**SHP/WA**			
1.4658117	-0.0064320	0.0	0.0	0.0

N1 GOV (100% N1)

GAM-1	ETA-C	ETA-T	ETA-PT	A5
1.3189383	-0.7739960	-1.0606155	1.0063133	0.8125390
AN	WABL			P1/PAM
-1.5999908	0.7307850	0.0	1.0000000	1.0857496
DWFC	DTIC	DNC2-DNC1	SHP/WA	
0.4270549	-0.5773780	2.7758551	0.0020500	0.0

T7LIM (100% N1)

GAM-1	ETA-C	ETA-T	ETA-PT	A5
0.4840890	1.8165712	2.4464483	1.0076447	-1.1191549
AN	WABL			P1/PAM
1.5064964	2.2823324	0.0	1.0000000	0.9836790
T7SET + SEN	SHP/WA			
3.0191298	-0.0062680	0.0	0.0	0.0

WF LIM (100% N1)

GAM-1	ETA-C	ETA-T	ETA-PT	A5
0.1115950	0.4187620	0.6646480	1.0069647	-0.3491220
AN	WABL		PAM	DPIC
-0.0824389	1.0623169	0.0	-0.6220530	-0.3733550
DWFC	SHP/WA			
1.2486992	-0.0033140	0.0	0.0	0.0

N1 GOV (112% N1)

GAM-1	ETA-C	ETA-T	ETA-PT	A5
1.2307758	-0.4779930	-0.6602899	1.0039988	0.8061080

N1 GOV (112% N1) Continued

AN	WABL			P1/PAM
-1.7334976	1.0257969	0.0	1.0000000	1.2498236
DWFC	DTIC	DNC2-DNC1	SHP/WA	
0.6375320	-0.8619429	4.1439610	0.0010620	0.0

T7 LIM (112% N1)

GAM-1	ETA-C	ETA-T	ETA-PT	A5
0.0948040	3.5098314	4.6423244	1.0059395	-2.1661224
AN	WABL			P1/PAM
2.8532095	3.5697680	0.0	1.0000000	1.3435984
T7 SMT + SEN	SHP/WA			
4.8675985	-0.0179970	0.0	0.0	0.0

WF LIM (112% N1)

GAM-1	ETA-C	ETA-T	ETA-PT	A5
0.0252700	0.9355180	1.3484869	1.0047255	-0.6824250
AN	WABL		PAM	DPIC
-0.0143300	1.6336269	0.0	-1.0477934	-0.4713489
DWFC	SHP/WA			
1.5764465	-0.0083300	0.0	0.0	0.0

C MATRIX BIAS CORRECTIONS*

J = -4.48	N = -5.91	S = 3.01	W = -3.91
K = -5.93	P = -7.07	T = 3.66	X = -4.89
L = 2.99	Q = 3.59	U = -5.17	Y = 5.74
M = -3.52	R = -4.33	V = 5.53	Z = -6.55

LIST OF SYMBOLS

A/D	Analog to Digital
A_N	Power turbine inlet nozzle effective area, $in.^2$
A_5	Gas generator turbine inlet nozzle effective area, $in.^2$
$B_{(bij)}$	Matrix relating relative variations in engine airflow pumping capacity, component efficiencies, and geometries to measured relative variations in engine parameters sensed at low power at a constant value of P_3/δ_1
BCD	Binary Coded Decimal
BITE	Built-in test
$C_{(Cij)}$	Matrix relating the relative variations in maximum power at each control limit to the computed relative variations in engine pumping capacity, component efficiencies and geometries
CF	Nonoptimal N_2 correction factor
DAN	Computed relative change in A_N
DA5	Computed relative change in A_5
δ_1	Relative compressor inlet absolute pressure ($= P_1/14.7$)
DETAC	Computed relative change in n_c
DETAPT	Computed relative change in n_{pt}
DETAT	Computed relative change in n_t
DN1	Measured relative change in $N_1 / \sqrt{\theta_1}$ at constant P_3/δ_1
DP7	Measured relative change in P_7/δ_1 at constant P_3/δ_1
DSHP	Measured relative change in $SHP / \delta_1 \sqrt{\theta_1}$ at constant P_3/δ_1

DT3	Measured relative change in T_3/θ_1 at constant P_3/δ_1
DT7	Measured relative change in T_7/θ_1 at constant P_3/δ_1
DT9	Measured relative change in T_9/θ_1 at constant P_3/δ_1
DWA	Computed relative change in $W_a\sqrt{\theta_1}/\delta_1$
DWF	Measured relative change in $W_f/\delta_1\theta_1^{.8}$ at constant P_3/δ_1
η_c	Compressor efficiency
η_{pt}	Power turbine efficiency
η_t	Gas generator turbine efficiency
EU	Electronic Unit
f_N	Ambient temperature correction factor in computing maximum horsepower at N_1 limit
f_T	Ambient temperature correction factor in computing maximum horsepower at T_7 limit
f_W	Ambient temperature correction factor in computing maximum horsepower at W_f limit
GPA	Gas Path Analysis
I/CU	Indicator/Control Unit
MPA	Maximum Power Available, hp
MPAS	Maximum Power Available System
MTU	Maintenance Test Unit
N_1	Gas generator turbine rotational speed, rpm
N_2	Free power turbine rotational speed, rpm

P_{AM}	Ambient pressure, psia
P_1	Compressor inlet total pressure, psia
P_3	Compressor discharge pressure, psia
P_7	Power turbine inlet pressure, psia
PPM	Parts Per Million
PROM	Programmable Read Only Memory
ROM	Read Only Memory
SHP	Power turbine shaft horsepower, hp
SHP_{CO}	Optimal power turbine horsepower referred to sea-level standard-day conditions, hp
SHPON	Predicted maximum power at N_1 limit, hp
SHPOT	Predicted maximum power at T_7 limit, hp
SHPOW	Predicted maximum power at W_f limit, hp
SHP_{REF}	Sea-level standard-day value of horsepower at each control limit, hp
SPE/W_a	Shaft power extraction/ (lb/sec of compressor airflow), hp/(lb/sec)
T_{AM}	Ambient temperature, ^{o}R
T_1	Compressor inlet total temperature, ^{o}R
T_3	Compressor discharge total temperature, ^{o}R
T_7	Power turbine inlet total temperature, ^{o}R
T_9	Power turbine discharge total temperature, ^{o}R
θ_1	Relative compressor inlet absolute temperature ($= T_1/518.7$)
W_{BL}	Compressor discharge bleed air as a percentage of total compressor airflow

W_f	Engine fuel flow, pph

SUBSCRIPT

B	Designates corrected baseline values
C	Designates quantities referred to sea-level, standard-day conditions

Several abbreviations and program instructional terms which have no universal engineering significance and are peculiar to the computer program manual only and have been defined in detail within the text have been omitted from this list to avoid redundancy.

U.S. GOVERNMENT PRINTING OFFICE 1974 636 156/34